CZECH TECHNICAL UNIVERSITY IN PRAGUE
FACULTY OF MECHANICAL ENGINEERING

PhD Thesis

Design and analysis of energy efficient indoor-climate control methods for historic buildings

Mechanical engineering
Control and systems engineering

Magnus Wessberg

Supervisors:

Prof. Tomáš Vyhlídal, CTU in Prague

Prof. Tor Broström, Uppsala University

2018

Declaration

I declare that the information provided in this document is true. The text that is related to the already published material is properly cited, including references to the original sources. All the materials used in this text are related to the author's work as the main contributor or co-author.

Date ……………….. Signature ……………………

Abstrakt

Z výzkumného a implementačního hlediska je monitorování kvality a efektivní řízení vnitřního prostředí v historických objektech zajímavým problémem, s netriviálním řešením. Při stanovení charakteristik prostředí je nutné jednak zajistit akceptovatelný komfort pro návštěvníky a zejména pak zajistit jeho vhodnost z pohledu ochrany interiéru budovy a vystavených objektů památkové péče. Následným problémem je technická implementace systému úpravy vnitřního prostředí s ohledem na jeho neinvazivnost a šetrnost vůči interiéru historické budovy. Důležitým faktorem je též častý požadavek na nízké pořizovací náklady a nízkou energetickou náročnost. Z pohledu památkové péče, je klíčovým sledovaným parametrem relativní vlhkost vzduchu v interiéru. Kromě monitorování a řízení dosažených extremálních hodnot, je nutné sledovat též variabilitu relativní vlhkosti v krátkodobém časovém měřítku. I přes zvýšenou pozornost věnovanou návrhu metod řízení relativní vlhkosti v historických budovách a jejich technické implementaci, lze stále najít řadu otevřených problémů, a to zejména právě vzhledem k šetrnosti a energetické náročnosti daných řešení.

Tato práce je zaměřena na analýzu vybraných metod řízení prostředí v historických budovách, a to jak z pohledu stanovené metodiky, tak i z pohledu technické implementace. První analyzovanou metodou je krátkodobé vytápění historických objektů, typicky aplikované u příležitostně využívaných kostelů před církevními obřady. Nejprve je navržen aproximativní hygro-termální model dané třídy objektů, kde typickým faktorem je masivní konstrukce budovy s vysokou tepelnou kapacitou. V dalším kroku je stanoven postup parametrizace modelu na základě neměřených průběhů teploty a relativní vlhkosti v odezvě na skokovou změnu tepelného výkonu otopného systému. Hlavním výsledkem je poté návrh algoritmu pro postupné zvyšování tepelného výkonu tak, aby byl eliminován nebezpečně rychlý pokles relativní vlhkosti. Daná metodika je validována na měřených datech a simulačních modelech třech kostelů nacházejících se na ostrově Gotland, ve Švédsku.

U nevytápěných historických objektů lze často pozorovat zvýšené hodnoty relativní vlhkosti, které mohou vést k nežádoucímu růstu plísní v jejich interiérech. Jednou z energeticky šetrných metod, kterou lze dané riziko snížit, je tzv. adaptivní ventilace. Tato metoda byla zejména v posledních letech analyzována jak z pohledu algoritmizace, tak i technické implementace. Závěry provedených studií jsou ale nejednoznačné, v některých případech i protichůdné. Důkladná analýza této metody formuje druhý řešený problém disertační práce. Kromě teoretických aspektů, spočívajících zejména v aplikaci pokročilého zpracování dat pomocí kritérií mapujících riziko růstu plísní a riziko mechanického poškození vystavených objektů hygroskopického charakteru, jsou analyzovány implementační aspekty této metody a to včetně validace na historických budovách. Z provedené analýzy vyplývá efektivnost adaptivní ventilace ve významném snížení rizika vzniku plísní. Bohužel, při dlouhodobém provozu je možné indikovat nezanedbatelné časové intervaly, kdy vlivem nevhodných podmínek venkovního prostředí není možné kvalitu vnitřního prostředí řízenou ventilací zlepšit. V těchto intervalech je vhodné využít alternativních metod redukce relativní vlhkosti, např. pomocí sorpčních odvlhčovačů. Z analýzy naměřených dat též vyplývá, že adaptivní ventilace vede ke zvýšení variability relativní vlhkosti, čímž se zvyšuje riziko poškození vystavených objektů hygroskopické povahy následkem zvýšení sorpčně-pevnostních gradientů. Následně je v práci provedeno vyhodnocení tříletého experimentu na barokním zámku Skokloster ve Švédsku, s cílem porovnat tři různé metody úpravy vnitřního prostředí, jmenovitě – i) sorpční odvlhčování, ii) vlhkostně řízené vytápění, a iii) adaptivní ventilaci – a to vzhledem k schopnosti zamezení vzniku plísní, udržení stability prostředí a energetické efektivnosti. Z výsledků analýzy vyplývá, že pro daný typ interiérů nacházejících se ve vrchních patrech objektu, s absencí vnitřních zdrojů vlhkosti, je nejvhodnější aplikovat odvlhčování pomocí sorpčních odvlhčovačů. Analýza též poukazuje na důležitost zajištění vzduchotěsnosti jako primárního opatření pro zachování bezpečného prostředí dané třídy historických interiérů.

Abstract

Indoor climate in historic buildings pose both practical and scientific challenges. There are two fundamental challenges that must be addressed. The first challenge is establishing a proper indoor climate with respect to both human comfort and, above all, conservation of the building itself and its interior including artworks and furniture. The second challenge is achieving the desired indoor climate in a non-invasive, sustainable, and energy efficient way. With a focus on preservation, relative humidity is the most important parameter. Not only the level but also the change rate of relative humidity is of importance. Although the methods and technical equipment for humidity control in historic buildings have been widely investigated, a number of problems need further investigation, including efficiency and safety.

This thesis explores the link between technical implementation and target ranges for indoor climate, including control strategies and algorithms that take into account cost effectiveness, energy efficiency, and sustainability. The first addressed method is intermittent heating of massive historic buildings. To control the change rate of relative humidity at a heat-up event, a simplified model is presented for heat and moisture transfer during the heat-up period. In addition, a method is presented and validated to derive the hygrothermal parameters and the time constant of the building from measurements measured at a step response test. Finally, the study considers a feedforward control algorithm that uses the model to predict and control the change rate of relative humidity during the heat-up procedure. The method has been validated on measurements and models of three churches on the island of Gotland, Sweden.

Unheated historic buildings often face problem with high humidity levels that can lead to increased risk of mould growth. One of the energy efficient methods that can decrease the mould growth risk is adaptive ventilation. Adaptive ventilation was designed to be a low energy and low impact option, but needs validation and further development. The main questions are if the measure is sufficient to limit the risk for mould growth, how it influences the stability in relative humidity, and if it is an energy efficient measure. These aspects are widely addressed in the thesis. A great deal of attention is paid to installation aspects of the case study objects and subsequent thorough data analysis. The performed research shows that adaptive ventilation essentially lowers the number of hours of risk for mould growth on a yearly basis, but there is still an increased risk for some short periods when adaptive ventilation is not a sufficient measure. The performed study also indicates that the adaptive ventilation measure is likely to increase risk of mechanical damage to objects due to increased variability of relative humidity fluctuations. Finally, in a three year study of Skokloster Castle, three climate control measures are compared: dehumidification, conservation heating, and adaptive ventilation. This comparison includes efficiency to prevent risk for mould growth, indoor climate stability, and energy efficiency. The study shows that dehumidifying had the best result regarding all three criteria for rooms located in the upper floors, which typically lack internal moisture sources. However, rather than a method to eliminate the risky levels of relative humidity, the air-tightness of the interiors was revealed as the prime mitigation measure for the given interior class.

Acknowledgements

I gratefully acknowledge the support from the Swedish Energy Agency's research program for energy efficiency in cultural heritage buildings (*Spara och Bevara*). The work was also supported by European Commission funding under the of the 7th FP EU project Climate for Culture No. 226973 and by the Grant Agency of the Czech Technical University in Prague, project No. SGS17/176/OHK2/3T/12.

I would like to thank my supervisor at CTU in Prague, Professor Tomáš Vyhlídal, for all the invaluable help and positive support during my Ph.D. studies. Professor Vyhlídal has really guided me to new ways of thinking about indoor climate control.

I would like to thank my supervisor at Uppsala University, Professor Tor Broström, for all his help and support during the process and his always encouraging attitude and inspiring discussions during my PhD studies.

Also I would like to thank my wife, Pernilla, who has supported me and our family throughout the process of writing this thesis. This would not have been possible without you.

Contents

1 Introduction

Indoor climate in historic buildings such as museums, castles, and churches pose both a practical and a scientific challenge. There are two fundamental challenges that must be addressed [52]:

1. What is the proper indoor climate with respect to human comfort and conservation of the building itself and its interiors such as artwork and furniture?
2. How do we achieve the desired indoor climate in a sustainable way?

In conservation science, much attention has been paid to defining climate-induced risks and, as a consequence, safe ranges for temperature and relative humidity (RH). Heating and humidity control equipment used in historic buildings are also well researched. This thesis aims to further explore the link between technical equipment and target ranges for indoor climate. That is, control strategies and algorithms based on the hypothesis that smarter and more effective control of the indoor climate using specific characteristics of the building in question can be cost effective ways to achieve a sustainable indoor climate.

Heating practices in historic buildings have varied over the centuries. Monumental buildings such as churches, castles, and manor houses were kept cold when not being used. If used during the winter, only part of the building was heated, usually by stoves and open fireplaces. More recently, central heating systems such as electric radiators and hydronic systems have been installed, making it possible to control the climate both for comfort and for conservation [24]. However, for economic reasons many historic buildings are still intermittently heated and kept cold when not used. As a complement to intermittent heating, some buildings have simple climate control measures such as dehumidification or background heating at low temperatures.

Insufficient climate control will result not only in unfavourable indoor climate for both the building and its historical artefacts but also in unnecessarily high energy use. The energy cost associated with climate control is a major problem as it might prevent owners of historic buildings from using proper climate control, leaving the building to disrepair.

According to the Intergovernmental Panel on Climate Change (IPCC), climate has warmed since the 1950s and most probably it will be warmer in the future [76]. As the climate becomes warmer, humidity and precipitation will most likely increase. A warmer and more humid climate will lead to higher risk of damage to historic buildings as well as artefacts and objects. To manage the cultural heritage in a sustainable way, it is important to predict how the future climate will influence the indoor climate so necessary proactive activities can be performed.

The European project Climate for Culture (CfC)[1] [77, 86, 87] aimed to develop effective and efficient strategies for indoor climate control to preserve cultural heritage. The project combines high resolution models for the future climate scenario in Europe with building simulation software used to predict the future indoor climate. By studying the outcome of these simulations, damage risks for different regions in Europe can be identified. The project goes further and develops damage/risk assessments tools based on damage functions. For a definition of damage function, see section 1.1.1. In connection to the future challenges of climate change, the project also focuses on energy efficient climate control. The present thesis, originating in the Climate for Culture project, aims to further develop a model for climate control of historic buildings.

1.1 Climate requirements for conservation

From a conservation perspective, the indoor climate in a historic building is mainly determined by air temperature and humidity. Common climate-related problems in occasionally used historic buildings include corrosion and biodegradation as the result of high RH and damage to the mechanical workings of the building and objects. In addition, large variations in temperature and RH can result in salt efflorescence on masonry walls. Major risk factors and climate target ranges are presented below.

1.1.1 Damage functions

Generally, a damage function transforms some sort of input data to a quantified damage risk. Damage function is defined as 'a quantitative expression of cause and effect relationships between environmental factors and material change' [88]. In climate control for conservation, damage functions are used to assess the risk for microclimate conditions, such as temperature and RH, for cultural heritage objects, and the output, for example, is quantified damage risk for mechanical degradation, chemical degradation, or biological degradation [91]. The damage function is usually expressed as a formula or a dose-response relationship but can also be in the form of a graph or a table [88].

1.1.2 Moisture content

Moisture content in hygroscopic materials is determined by ambient air RH and temperature. The equilibrium moisture content (EMC) – i.e., the moisture content when the material neither absorbs nor releases moisture – in relation to RH is described by sorption isotherms empirically-derived for different materials at a given temperature [94] (Figure 1.1). The sorption isotherms depend on the material and how the material is structured, but common to all is that EMC depends predominantly on RH and temperature (Figure 1.1). From the preservation point of view, which will be discussed in more detail later, it is recommended to keep the moisture content constant or at least within a limited range [12]. These recommendations are motivated by the association of the EMC variation with mechanical damage [13]. Control methods concerning the EMC ramifications will be further discussed in the following text.

[1] https://www.climateforculture.eu/

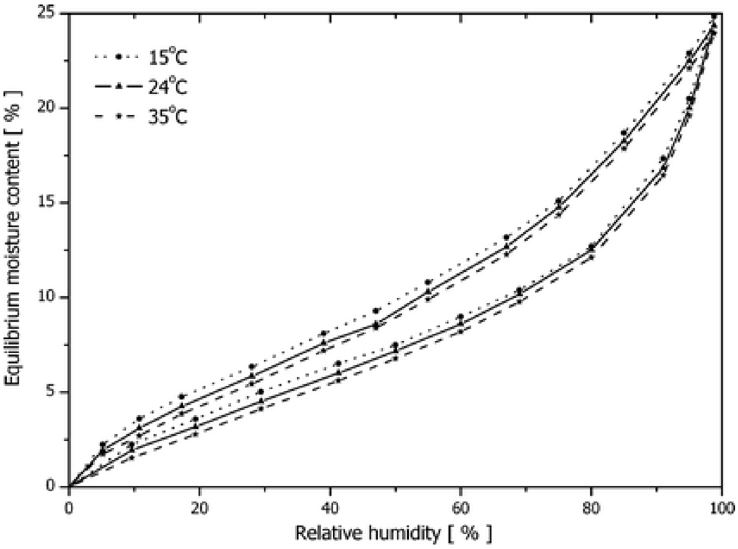

Figure 1.1. Sorption isotherms of lime wood for several temperatures. The lower for adsorption, the upper for desorption [14].

1.1.3 Mechanical degradation of wood

Due to absorption and desorption of moisture, hygroscopic objects will swell and shrink as the EMC changes with changes in RH of the ambient air [15]. Dimensional change is also due to temperature change, but dimensional changes due to humidity are generally much larger [14]. Although a restrained object exposed to fluctuating temperature or RH can´t swell or shrink, but will experience stress instead [12, 16]. Fast changing RH causes gradients in moisture content as the parts closer to the surface respond faster to humidity changes than deeper parts. These moisture gradients lead to increased stress levels that in turn can result in cracks in the outer wood. The outer part will be strained by tension while the inner part will be strained by compression. These increased stress levels in combination with the weak tangential strength can result in radial cracks [16, 17].

Slow changes in RH are considered less harmful to wood as the moisture gradients are smaller. Rapid and slow changes are relative concepts as they depend on the object’s material, composition, and size. In a study of RH variations on a wooden cylinder with a diameter of 13 cm it was found that the initial level of RH and the amplitude of RH variation are important. A RH variation of 10% is regarded as safe only if the variation’s initial value is between 30% and 70%. Outside this range, the object will experience irreversible strain levels. RH variations of 40% could cause direct failure if the initial value is above 90%. In these simulations, the variation of RH was performed over a few seconds, a condition rarely found in historic buildings. However, in simulations where the RH changes over 24 hours, the risk for irreversible strain is lower and the safe range of variations increases to approximately 20%. This result is in good agreement with the old conservator’s wisdom that a large change in RH can be harmless if objects are given enough time to adapt [14].

One of the most sensitive types of objects include painted wood objects, which are composed of several layers of materials with different hygroscopic properties that move differently when absorbing or releasing moisture [18, 19, 20]. Historic buildings, especially churches, have a number of objects of this type – e.g., the altarpiece, the pulpit, painted pews, and parts of the organ [21]. In a case study of how real objects respond to variations in climate, Bratasz and Kozlowski examined how climate variation affected an altar piece in an Italian Church. Using laser triangulation, they determined the relationship between the indoor climate and movements of wooden details in the altar piece. They found a strong connection between large fluctuations in RH and dimensional change of wooden objects when the church was heated intermittently. During an intermittent heating event, one small wooden part of the altarpiece was exposed to stress levels that increased the risk for cracks [22].

The European standard EN 15757 – specifications for temperature and relative humidity to limit climate-induced mechanical damage in organic hygroscopic materials [23] – does not specify the indoor climate in numbers but rather provides a method to determine allowable variations based on recent climate. The method is based on the hypothesis that an object with hygroscopic materials that has been in a specific climate for a significant time has been acclimatised to this climate. That is, the hypothesis assumes the possible damage to the object such as cracks and straining has already occurred, which makes the object more adaptable to future indoor climate changes compared to the climate that generally is accepted as good for preservation. The standard also states that these more flexible specifications can lead to the use of simpler climate control equipment that in turn leads to reduced costs for both investments and energy.

To determine the target range for RH, the standard proposes that climate monitoring should be performed for at least one year. In addition, 15+15 days of measurements are necessary when calculating the 30-day running average over a full year. Then, 30-days central running average over the full year is calculated as follows:

$$\bar{\varphi}_{30}(t) = \frac{1}{T}\int_{-T/2}^{T/2} \varphi(t)\, dt, \tag{1}$$

where T is 30 days. The 30-days running average can be seen as a running monthly average. Short-term fluctuations are calculated in the same way as the standard deviation except for using of the difference between a RH sample and the 30-day running average instead of the normal average of the full year:

$$SD30 = \sqrt{\frac{1}{T_s}\int_0^{T_s}\left(\varphi(t)-\bar{\varphi}_{30}(t)\right)^2 dt}, \tag{2}$$

where T_s is the whole investigated period. The target range for the future climate is then between the 7th and the 93rd percentile of the fluctuations, which corresponds to 1.5 SD30 if the fluctuations are considered to be Gaussian distributed. This means that 14% of the largest fluctuations are removed. If the 7th and the 93rd are less than 10% RH from the running average level, the target range is ±10% RH. Figure 1.2 provides an example of this using data from a measuring campaign in a historic farmhouse. The fluctuations are rather small and the target range according to 7th to 93rd percentile is ± 3.3% RH from the running average, which according to the standard is regarded as unnecessarily small. The target range for future climate in this building is therefore set to ±10% RH.

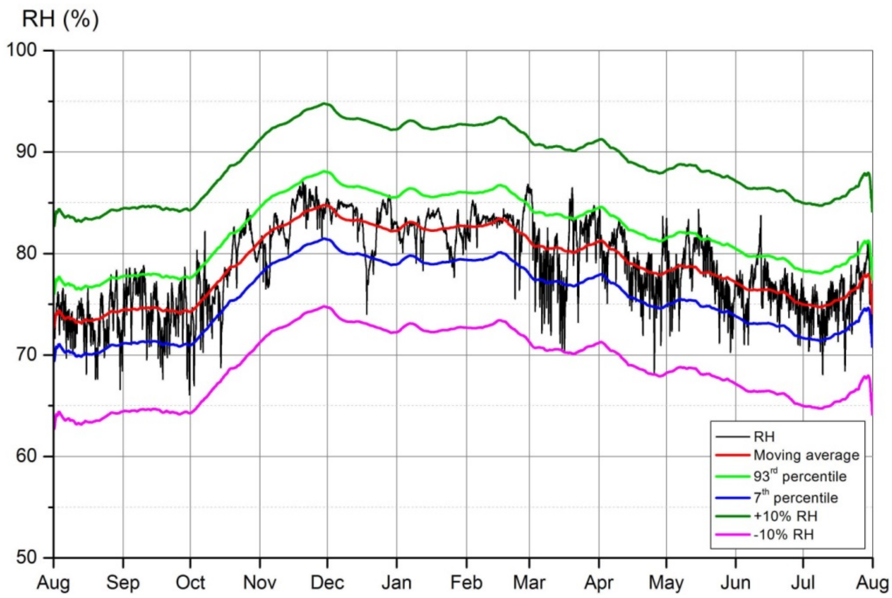

Figure 1.2. One year of climate data from a farm house.

1.1.4 Mould risk

A common problem in historic buildings is mould growth. Mould spores are always present in buildings [25, 26], and germination and growth rate depends on temperature, humidity, and nutrition [27].

Mould goes through four life stages (Figure 2.2, left): spore, germination, hyphal growth, and reproduction [27]. Mould degrades biological materials to some extent by, for example, infesting and discolouring surfaces of objects, but the primary danger with mould growth in buildings is the production of pathogens – e.g., mycotoxins or other microbial volatile organic agents – that can cause illness or unpleasant odours [26, 28].

Surface humidity is quantified in water activity (a_w), which is defined as the ratio of the partial pressure of water vapour on the surface and the partial pressure of water, both given at the same temperature. The water activity is expressed in a fraction ranging from 0 to 1. If the surface is in equilibrium with the ambient air, the water activity is the same as RH divided by 100 [29], which often is the case in a historic building.

Several mould growth predictions models have been presented – e.g., the VVT model on wood [30], time of wetness [25], and mould growth indices [31].

A commonly used model to predict mould growth is the isopleth system, where an isoline in a RH-temperature diagram shows the combination of temperature and RH representing climatic conditions for the same rate of mould growth [32, 33]. The lowest isopleth for mould, LIM, is an isoline that represents the lowest RH level at different temperatures required for mould growth on a specified substrate [28]. That is, the area above the LIM represents a favourable and the area below the LIM represents a non-favourable climate for mould growth. Figure 1.3 (right) shows the LIM for substrate category I, building materials produced from biological raw material such as gypsum board and wall paper [34]. In the work that follows, the LIM I isopleth is used as the damage function for evaluation of indoor climate for mould risk.

Traditionally, climate control aimed to eliminate mould growth has been based only on a safe range for RH. As can be seen from Figure 1.3, this is either a risky approach or gives an unnecessarily large safety margin, which often is costly.

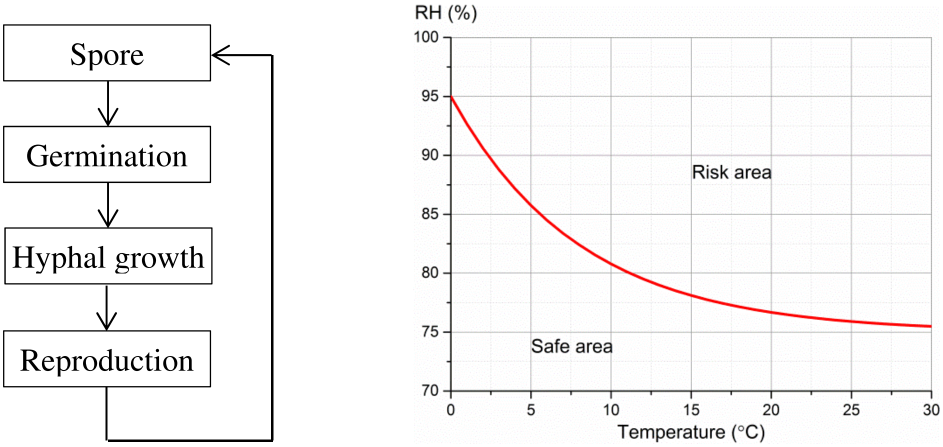

Figure 1.3. Left – mould growth stages. Right – Lowest Isopleth for Mould (LIM I) according to Sedlbauer [28].

1.2 Climate control for comfort

Thermal comfort for people depends mainly on temperature and air movements and to a lesser extent on RH. Physical activity, clothing, and duration of exposure will determine comfort ranges for each person [35].

This section describes low energy climate control methods often used in occasionally used historic buildings to achieve thermal comfort.

1.2.1 Intermittent heating of a massive building

Traditionally, historic buildings have been heated intermittently with open fireplaces or stoves [36]. Even with the introduction of new heating sources, intermittent heating is still very common in historic buildings [37]. Intermittent heating relies on the rapid heating of a building before the building is to be used. In between periods of use, the building is kept cold or heated using only background heating. Compared to continuous heating, intermittent heating requires larger heating power [37]. Although intermittent heating is energy efficient, fast changes in temperature and RH may be harmful to some objects and materials.

In historic buildings with massive walls, thermal inertia is the dominant factor in the heat balance of the building. Because most of the supplied energy is used to heat the wall, the ceiling, and the floor, steady state models are not applicable for intermittent heating [38]. As a result, the indoor air temperature is largely influenced by the wall surface temperature.

Studies of intermittent heating in massive monumental buildings have been ongoing since the end of the 19th century when heating systems started to be installed in such buildings. In 1922, the Swedish state-owned energy company, *Vattenfall*, began to be interested in electrical heating in churches. Engineer Frits Jacobsson conducted theoretical and practical studies for the design of heating systems [39]. In 1930, Krischer presented a model that was similar to the one that Jacobson had proposed. In 1936, Henning extended Jacobsson's work by including heat losses from transmission and infiltration [40], an approach also used by Krisher and Kast in 1957 [41]. However, these extended solutions were not practical, so Jacobsson's and Krischer's initial (and simpler) solutions were adopted. Pfeil gives an overview of church heating models from Fisher in 1890 to Krischer and Kast in 1957 [42]. Broström used Jacobsson's model to develop a method that determined hygrothermal properties of a stone church [38]. Broström found that heating a massive stone church with a constant heat flux, the increase in temperature during a heat-up event is proportional to the square root of time.

The fundamental theory for intermittent heating of massive buildings is thus well known and has been used to calculate heat up time in relation to the required installed power for intermittent heating systems [39]. However, no existing theories or models have been used to actually control a heat-up procedure for massive historic buildings.

1.2.2 Local radiative heating

Local radiative heating is used in intermittently-heated buildings to provide comfort in a limited part of the building without heating the whole building. In addition to saving energy, local radiative heating also saves objects from the consequences of unnecessary heating and drying. The convective air movements that often are a problem in intermittent heated churches will be reduced [43]. Local radiative heating is often performed with low-temperature radiant sources such as electric panels, integrated heating foils, electric heating glass, heated water pipes or water radiators, sub-floor floor heating coils, as well as infrared emitters and electric radiators [44]. Local radiative heating has been evaluated using the input of churchgoers sitting in pews such as in the church of Santa Maria Maddalena in Rocca Pietore, Italy [45] and Lau church on Gotland island, Sweden [46]. In these studies, the test participants in both churches experienced slight discomfort.

1.3 Climate control for conservation

This section describes how low energy and low invasive climate control methods can be used for occasionally-used historic buildings to maintain a climate that inhibits mould growth – i.e., lower RH.

1.3.1 Conservation heating

Conservation heating is a technique for climate control where heaters are controlled by humidistats rather than by thermostats. The temperature varies to adjust RH to the set value. This technique is also referred to as humidistatic heating control [47]. The term conservation heating was introduced by the National Trust, UK, in the 1990s, but the technique was used earlier, for example, by the Canadian Conservation Institute [48].

If there are no major moisture supplements to a building, power requirement for conservation heating is relatively small. For example, in Scandinavia, heating a building to a temperature 5 to 7 degrees above the outdoor temperature will keep RH at approximately 60% [49]. The required heating power can be five times lower compared with permanent heating [50]. Of course, the energy consumption depends on the building infiltration rate and U-value, but simulations have found that conservation heating consumes more energy than dehumidification if the heat is supplied by direct electric heating but less if the heat is supplied by heat pumps [51].

Conservation heating provides a stable indoor climate if the building is reasonably air tight. In addition, conservation heating is simple and cheap to implement if a heating system already exists. Of course, if a building requires a new heating system, there is some risk of damage when installing the system. Another drawback of conservation heating is that the temperatures may be uncomfortably high during the summer. If there are visitors in the building, one has to either accept poor thermal comfort or turn off the heat and accept a temporarily higher mould risk.

An additional potential problem is that the indoor air mixing ratio (MR), the mass of water vapour to the mass of dry air, will increase due to evaporation from floors or walls, counteracting the intended effect to reduce RH [50]. This problem is especially evident when there are any sources of humidity in the building such as moisture in walls or if a large part of the room is filled with hygroscopic material such as wood [53].

According to life time calculations, chemical degradation will increase with higher temperature, which can damage, for example, paper [54].

To summarise, conservation heating has some advantages and some disadvantages. Although the method has been used and has been investigated, it is still unclear whether conservation heating is more energy efficient than other forms of climate control. A systematic investigation of the performance in situ in a massive historic building with high temperature inertia and buffered moisture is needed to see how it performs when controlled to minimise the risk for mould growth in relation to other climate control methods.

1.3.2 Dehumidification

In practise, two techniques can be used to dehumidify air in historic buildings – sorption dehumidifying and condensing dehumidifying [47, 48].

The basic idea behind sorption dehumidifying is to pass the air over a desiccant that adsorbs or absorbs water vapour in the air. This type of dehumidifier operates in two stages. In the first stage, humid air streams through the desiccant, which adsorbs water vapour from the air. In the second stage, the desiccant is regenerated (i.e., dried), often by a hot air stream that heats the desiccant so that the water evaporates, removing the moisture from the desiccant. This drying process is often implemented by placing the desiccant on a turning wheel that rotates through the two air flows, alternately taking up moisture from the inlet air and releasing moisture into the regenerating air stream.

Condensing dehumidification uses a cooling element that cools the air below the dew point and therefore water will condense on the cooled element. The condensed water is either collected in a tank or drained through a tube. Some dehumidifiers have a built-in pump that empties the water tank when the water reaches a certain level. The cooling element is cooled by either a thermoelectric element [49] or a heat pump. Some dehumidifiers take advantage of the heat from the heat pump condenser (or if it is a thermoelectric element, the warm side of the thermoelectric unit) to reheat the air after it has been cooled down and dehumidified. This principle makes the condensing dehumidifier very energy efficient. Condensing dehumidifiers do not work efficiently under about 8°C [45] because frost forms on the cooling element. More advanced condensing dehumidifiers use the heat from the heat pump to defrost the cooling element periodically, which enables the dehumidifier to operate down to 0°C but with lower efficiency [47].

The two techniques work completely different. The sorption dehumidifier works adiabatic – i.e., there is almost no difference in enthalpy between inlets and dried exhaust air. This means that the temperature actually increases during the drying process as latent heat is taken from the air. Energy is instead consumed when heat is used to evaporate and evacuate the moisture and the moist air during the regenerating process. In a condensing dehumidifier, the air stream temperature is instead lowered to a level under the dew point and water starts to condense on the cooling coil. However, the indoor environment will gain heat from the condensing dehumidifying apparatus, which is larger than the cooling effect and often is welcomed in occasionally-used historic buildings [44]. As the condensing dehumidifier uses a container to store condensed water, it needs to be periodically emptied either manually or by an automatic pump, making condensing dehumidifiers unsuitable in buildings where the temperature drops below 0°C. The sorption dehumidifier works at any temperature but requires an outlet duct through the climate envelope for the moist regenerating air.

Dehumidification is a well-established and reliable method to reduce RH. To minimise energy use and ensure the right capacity, a study is needed that assesses the long-term performance of dehumidification systems installed to minimise the risk for mould growth under realistic conditions in massive historic buildings.

1.3.3 Equal-sorption humidity control

Equal-sorption humidity control is a climate control method developed for use in exhibitions and other locations where sensitive artefacts are stored and/or displayed. Equal-sorption humidity control targets the moisture content in the object rather than the RH or temperature of the ambient air [55]. Typically, climate control of historic buildings relies on HVAC systems controlling both RH and temperature, but because the large thermal inertia of massive stone walls makes controlling temperature more expensive than controlling humidity. By focusing on the EMC of the material, the temperature can be allowed to fluctuate a little while the EMC is compensated by adjusting RH. As it is not practical to directly measure the moisture content of the historic objects, the equal-sorption humidity control method is based on a mathematical model that predicts the EMC in the material using the RH and temperature of the ambient air.

Zitek and Vyhlidal use the logarithmic Henderson three parameter model [56, 94] for the equal sorption control method [55]:

$$u = \left[\frac{-\ln\left(1-\frac{\varphi}{100}\right)}{A(\vartheta-B)}\right]^{C} = \Psi(\varphi,\vartheta), \qquad (3)$$

where $\varphi \epsilon [0, 100]$ is RH of the surrounding air, ϑ is the temperature of the ambient air, and u is the EMC expressed as the ratio of the mass of water to the mass of dry material. A, B (B<273,16 K), and $C \in [0, 1]$ are material-specific parameters.

If RH is the controlling parameter, it can be expressed as follows:

$$\varphi_D = 100\left(1 - e^{ln\left(1-\frac{\varphi_0}{100}\right)\left(\frac{(273{,}16+\vartheta-B)}{(273{,}16+\vartheta_0-B)}\right)}\right), \qquad (4)$$

where ϑ_0, φ_0 is the reference state and ϑ is the actual temperature, and φ_D is the set point value to an air handling device controlling the RH in the room.

Equal-sorption humidity control has been tested in two sites with good results. In the Chapel of Holy Cross at Karlštejn Castle, about 30 km southwest of Prague, a full air handling system is controlled by the equal-sorption humidity control. Although the chapel's ambient RH is affected by the many visitors, the system keeps the chapel's artefacts at an even EMC level [55]. In the Historical Collection in State Archives in Třeboň Castle, Czech Republic, previous studies show that a dehumidifier was the only needed air handling device. Measurements showed that the EMC level in the archives was very stable during the period tested [57].

A revision of the equal-sorption humidity control has been developed within a European project Climate for Culture: the Quasi equal-sorption humidity control [77]. In this new approach, the system is designed to avoid unrecoverable plastic deformation caused by anisotropic swelling or shrinking due to variations in moisture content in hygroscopic materials. Therefore, the allowed variations are larger than in the original version [58].

Equal-sorption humidity control is an innovative and energy-efficient method to control moisture content in historic objects and wooden buildings, but its main purpose is to maintain stable moisture content to prevent mechanical degradation, not to prevent mould growth. As such, this method will not be further evaluated in this thesis.

1.3.4 Adaptive ventilation

The traditional method to reduce humidity, bad smells, or pollutants is to ventilate, either by manually opening windows and doors to let fresh air into the building or uncontrolled by infiltration. However, in occasionally used unheated or intermittently-heated historic buildings, the humidity levels can fluctuate, sometimes being higher and sometimes lower than outdoors. Therefore, ventilating when outdoor humidity is higher than indoor humidity is counter-productive. The highest risk for this is during spring and the beginning of the summer when warm and humid outside air is cooled down by cold massive historic buildings.

An adaptive ventilation system has sensors for RH and temperature both indoors and outdoors allowing the system to calculate the absolute humidity and compare the humidity levels and decide when to ventilate. The system ventilates only when the humidity is lower outside compared to inside. An adaptive ventilation system is thus a type of natural dehumidifier that uses the difference in humidity between outside and inside air. When the humidity is lower outside, a fan draws air from the outside into the inside, beginning the drying process.

In the church in Zillis, Switzerland, adaptive ventilation was used to stabilize the climate for the painted wooden ceiling [59]. The system had pre-set limits for both RH and temperature; if humidity and temperature were lower than the limits, the system turned off. As a result, the system did not run during the winter. The results showed that the system had a positive effect on the RH when running, but the air leakage was probably significant as the humidity levels went back as soon as the fans shut off. During the two years the system was in use, it ran approximately half the time and removed approximately 3 400 litres of water.

In the Antikentempel in Potsdam-Sanssouci Park, an adaptive ventilation system was used to avert mould growth on the walls and ceiling from May to September 2005 [60]. The study showed a positive result as the absolute humidity was 1-2 g/m^3 lower inside compared with outside during the whole test period. Between May and September 2007, measurements made without the adaptive ventilation system in operation showed that the absolute humidity was 1-2 g/m^3 higher inside than outside.

Case studies of adaptive ventilation were also conducted in Torhalle in Lorsch, Germany where the goal was to prevent condensation on the wall paintings in the building [61]. The system, which controlled the fan, had sensors for temperature and RH both inside and outside. The system was designed to keep the dew point of the inside air below the surface temperature of the walls. The system was used only for a short time as it was shut down by a sceptical conservator [62].

Hagentoft, Sasic, Kalagasidis, Nilsson, and Thorin tested and made simulations for adaptive ventilation of cold attics to prevent mould growth [63]. Their system ran if the partial pressure of the water vapour in the outside air were lower than the attic air. The study showed that the mould risk substantially decreased after the adaptive ventilation system was installed.

Hagentoft and Sasic conducted a field measurement campaign in eight different cold attics in Sweden. Their results showed that the adaptive ventilation, compared with traditional ventilation, gave lower and more stable RH during the winter. The risk of mould growth was reduced significantly as the humidity levels became lower [64]. In both studies, Hagentoft et al. pointed out the importance of air tight attics, but they also concluded that normal air tightness measures are enough to get a positive effect of the adaptive ventilation system.

Antretter, Kosmann, Kilian, Holm, Ritter, and Wehle developed hygrothermal simulations with WUFI®-Plus for two historic buildings with different ventilation strategies, including adaptive ventilation [62]. They concluded that it is possible to lower the absolute humidity during some periods of the year with adaptive ventilation, but it is more effective if run in a building with some internal moisture loads such as dampness wicking through foundations.

Antretter et al. notes that the fluctuations in temperature and RH increase with the use of ventilation and point out the relationship between fluctuating indoor climate and salt damage, which often can be a problem in historic stone buildings with plaster on the internal walls as every phase change of the salt increases the risk for flaking plastered walls and wall paintings.

One study of heat supported adaptive ventilation was conducted on a building with many visitors. The major purpose of the system was to lower the CO_2 level in the visitor's zone [65]. The supportive heaters were used only when the RH level was higher than maximal allowed RH indoors combined with the mixing ratio outdoors was higher than indoors. Otherwise, the system operated like any other adaptive ventilation systems. At the same time, the indoor temperature set point during the winter was decreased from 19,5°C to 14,5°C. This lowered temperature resulted in less occasions with dangerous low RH indoor values during winter as well as for the whole year.

Adaptive ventilation can be a very cost effective way to reduce RH and could be an alternative for preventing mould growth in historic buildings. However, the results and control methods of previous studies diverge with respect to achieving stable RH. Thus adaptive ventilation needs to be further validated and closely analysed in situ in massive historic buildings to refine control algorithms and to define the need for auxiliary moisture control.

1.4 Modelling and control

Hygrothermal models for buildings can be used to better climate control in terms of comfort, conservation, and energy efficiency.

Generally building models can be categorized in three groups: black box, white box, and grey box models [66]. As the name implies, black box models are developed from empirical methods. That is, the parameters of a black box model do not have any physical significance but reflect the behaviour of the modelled system when tested with input data [67]. However, black box models require a vast amount of data to identify parameters and the models are not as effective when non-training data are used. In addition, as the parameters are not physical, they are not suitable for optimization of real buildings [66]. Neural networks are examples of black box models. Unlike black box models, white box models, such as a lumped capacitance models, are based on physical laws. However, it is difficult to develop a white box model that considers all possible parameters in a building, especially for a monumental building where it is impossible to know the exact hygrothermal properties of the building structures [68]. A grey box model, as the name implies, combines properties of both black box and white box models such as combining a white box building model with a black box subsystem model [66]. In many cases, linear parametric models are considered grey box models as a linear model is a black box model that uses parameters derived from physical data [69].

Using lumped capacitance models for both thermal and hygroscopic models, Kramer et al. have developed a method to estimate a building model that includes both thermal and hygroscopic properties of a building [68]. Yearly data processed in an optimisation algorithm in MATLAB gives the parameters for the model. As full building models are complex and time-consuming to develop and use, the trend is to use simplified mathematical models when controlling the indoor climate [68, 70, 71].

In modern houses and offices that are intermittently heated on a diurnal schedule, first-order or second-order building models have been applied [72, 73]. Model Predictive Control have been used to control intermittent heating in and also using a low order model [74, 75]. However, low-order models will not work in a massive historic building as the heat-up procedure in a massive historic building does not follow a linear pattern and a model for controlling this procedure must mirror the behaviour of the temperature increase. Therefore, massive historic buildings will need a new nonlinear model. To date, building models for temperature and humidity in massive historic buildings that are intermittently heated have not been developed except for the church heating models mentioned in section 1.2.1.

2 Problem statement

Climate control of historic buildings is a complex task where the climate must meet a number of requirements, some of them contradictory. If humidity is too high, risk for mould growth increases; if humidity is too low, risk for mechanical damage increases. Similarly, if temperature is too high, energy consumption increases and if temperature and RH fluctuations are too large, risk for mechanical damage increases. An optimal situation is when temperature and RH are stable at levels that entail no or low damage risk. The overall challenge is to achieve this without intrusive installations and large energy consumption.

Today, intermittent heating systems in historic buildings are often controlled by on-off control and are turned on manually. During a heat-up event, the system is turned on some arbitrary time before use and, as a rule, the maximum heating power is used to minimise the heat-up time and thereby energy use. Poor timing will lead to either insufficient heating or excessively high energy use. Furthermore, sensitive objects may require a limited RH as well as a limited change rate of RH. To provide an acceptable comfort and to minimise energy use and detrimental effects on valuable objects, the timing and heating power of intermittent heating are crucial, because RH decreases as temperature increases. In massive buildings with masonry walls, the large change rate of RH is to some extent counteracted by moisture buffering in the walls. As the indoor RH decreases, moisture is released from the walls. This is a complex interaction, specific for each building and can also change throughout the year [38]. Therefore, a control system for intermittent heating is needed where three factors must be balanced: comfort for visitors; conservation of the building and its interiors; and energy use.

By controlling the switch-on time as well as the heating power of a heat-up event, the temperature change rate can be controlled and thereby also the RH change rate. The downside is that the heat-up time will be prolonged and energy use may increase. Using hygrothermal dynamical models can improve a climate control system, saving energy and improving indoor climate. This leads to the first objective defined in the next section. Zitek and Vyhlidal used an analogous model-based technique to derive the equilibrium moisture content (EMC) control method [55] (see section 1.3.3); however, the EMC control method was designed to vary the RH set-point for a dehumidifier based on temperate variation (4) with the objective to keep the equilibrium moisture content constant in long-term operation using the static Henderson model (3). No dynamical models of the indoor climate response were involved in the design. For intermittent heating, however, no direct relative humidity control by dehumidification is considered. The well-known dependence of RH on temperature coupled with simple indoor climate models are to be used to keep the conditions safe in this unsolved optimised intermittent heating task.

When a building is not being used, energy efficient control of RH, mainly to prevent mould growth, is needed. Adaptive ventilation has been shown to be a cost effective option, but there are still questions about the method and whether it really is an effective measure to prevent mould growth. Thus, adaptive ventilation needs to be further validated and analysed and compared to other low energy and low invasive climate control measures. This leads to the second objective of the thesis.

There are mainly two measures – conservation heating and dehumidification – that are used to reduce RH in order to reduce mould growth. In addition, adaptive ventilation could also be used to help prevent mould growth. No previous case studies have compared the energy efficiency and mould prevention effectiveness of these three RH-reducing technologies in massive historic buildings [51]. This forms the third objective of the thesis.

3 Thesis objectives

The objectives of the thesis are defined based on the identified research gaps in the non-invasive control methods of indoor climate in historic buildings.

Objective 1: Propose and validate a methodology for shaping the heating power for intermittent heating in massive historic buildings with regard to heat-up time and change rate of RH.

The objective is to propose and validate a low-cost and energy efficient methodology for the heat-up procedure for intermittently-heating massive historic buildings (typically churches) with regard to creating a safe indoor climate for valuable historic objects. In the first stage, an approximate hygrothermal model of air temperature and relative humidity during a heat-up procedure in such a building will be developed as well as a method for finding the model parameters based on measured data. The subsequent and main task is to design a model-based control strategy for shaping the heating power so indoor climate safety and low energy consumption are established. In addition to achieving the desired indoor temperature in the predefined time, the objective is to avoid fast changes of relative humidity at the beginning of the heating procedure as the fast changes in relative humidity are identified in the literature as very risky for the upper layers of hygroscopic objects (e.g., objects made of wood, canvas, and paper).

Objective 2: Perform validation and analysis of adaptive ventilation method for relative humidity control in historic buildings

The objective is to perform a case study analysis of indoor climate control of historic buildings that use adaptive ventilation. The particular task is to investigate whether adaptive ventilation is an efficient alternative to other climate control measures for lowering relative humidity in order to prevent mould growth. Therefore, adaptive ventilation systems are designed, tested, and validated in real case studies in situ to uncover the practical and theoretical obstacles. The control methods are evaluated and refined based on the analysis of measured data.

Objective 3: Propose and validate improvements of indoor climate control methods in historic interiors with the focus of mould growth prevention.

The objective is to propose improvements of interior relative humidity control in historic buildings, taking into account recently quantified mould growth characteristics. A subsequent task is to evaluate selected climate control measures for lowering relative humidity in order to prevent mould growth in massive historic buildings in terms of energy efficiency, mould prevention effectiveness, and stable relative humidity. These goals are addressed in a case study of an historic building under comparable parameters of the controlled interior. The analysis is based on recent developments in indoor climate analysis.

3.1 Thesis outline

Objective 1, addressed in Chapter 4, analyses a hygrothermal model based on the heat conduction equation. The model is validated against measured data from three churches. A method for how to derive parameters to the models from a step response test is studied and further developed. Objective 2, addressed in Chapter 5, analyses a system for adaptive ventilation using two case studies. Objective 3, addressed in Chapter 6, analyses a three-year comparative study on climate control to prevent mould in Skokloster Castle. In the study, adaptive ventilation is compared with conservation heating and dehumidification.

4 Intermittent heating of massive historic buildings

Intermittent heating, introduced in detail in Section 1.2.1, is a common heating strategy in many historic buildings. The systems are often on-off controlled and the heat-up procedure is not controlled at all. The lack of control is evident as the buildings do not reach a comfortable temperature during winter or are heated unnecessarily long time (days) before use, ultimately wasting energy. The fast increase of temperature during a heating event induces a fast decrease in relative humidity (RH) that can be harmful for the building and its interior. This section will solve the problem stated in Objective 1 by developing a hygrothermal model for intermittent heating and designing a control method for limiting large fluctuations in RH at the beginning of the heating event. This section is an extension of a published papers [1, 2] (the author of this thesis is the lead author of both papers).

4.1 Model for intermittent heating of massive buildings

In this section, an approximate model for air temperature in response to a constant heat input in a massive historic building is developed. First, known equations based on heat balance in a building and the wall heat transfer equation are presented. Then, as the main result of this section, an approximate model under specified assumptions is developed.

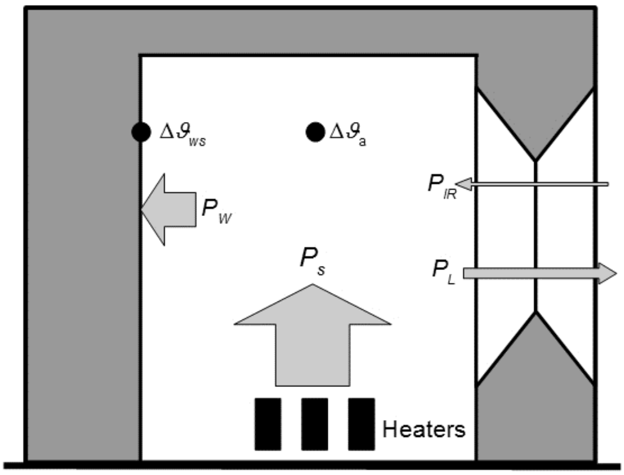

Figure 4.1. Major heat flux and temperatures during intermittent heating according to the simplified model, where ϑ_{ws} is the surface temperature (°C), $\vartheta_a$is the air temperature (°C), P_s is the supplied heat (W), P_{IR} is the irradiation (W), P_L is the losses (W), and P_W is the heat transferred to the walls (W).

In Figure 4.1, the main heat fluxes at a heat-up event are shown schematically. The supplied heat from the heaters, P_s (W), is mainly divided in two main fluxes. The large part, $P_W(W)$, heats the walls and interiors via the air. The smaller part, $P_L(W)$, represents losses due to infiltration and conductive losses. Irradiation, $P_{IR}(W)$, also contributes to the temperature in the building. The heat balance can then be described as follows:

$$V_a \rho_a c_{pa} \frac{d\vartheta_a}{dt} = Ah\big(\vartheta_w(0,t) - \vartheta_a(t)\big) + P_s - P_L + P_{IR}, \tag{5}$$

where V_a (m^3) is the indoor volume, $\rho_a (kg\, m^{-3})$ is the density of the indoor air, c_{pa} $(J\, K^{-1} kg^{-1})$ is the heat capacity of indoor air at constant pressure, A (m^2) is the effective indoor wall surface area, and h $(W\, m^{-2} K^{-1})$ is the heat transfer coefficient. In addition, $\vartheta_w(0,t)$ (°C) is the wall surface temperature and $\vartheta_a(t)$ (°C) is the indoor air temperature.

The model (5) is rather simple as it only relies on a single differential equation. Therefore, it is very useful for control design purposes. However, next to the control input by the heater, P_s, there are two additional inputs, P_L and P_{IR}, which create disturbances in relation to the model on the air temperature (ϑ_a) evolution. Further derivation of the model for intermittent heating in massive building is based on the following simplifying assumptions:

- **Assumption 4.1:** Heat loss due to infiltration, P_L, is a small and constant fraction of the supplied heat compared to the heat flowing into the wall.
- **Assumption 4.2:** Heat gain due to irradiation, P_{IR}, has a negligible impact on a single heat-up event.

Assumption 4.1 is valid for a typical medieval massive stone building. The overall area of windows and doors in such a building is small compared to the wall area, so the infiltration rate is small. In buildings with wooden floors built on a ventilated crawl space or a wooden ceiling, the infiltration rate can be higher [98]. However, the heating power in intermittently-heated buildings is usually very large compared to heat loss due to infiltration, so P_L can be assumed to be a small and constant fraction of the supplied heat compared to the heat flowing into the wall.

Similarly, Assumption 4.2 is due to the small window area and the relatively short heat-up time during which irradiation does not have a substantial impact on a single heat-up event. While irradiation has an influence on the long-term conditions [99] during a single heat-up event, which often lasts from half a day to a few days, the impact is small and assumed to be negligible. An estimation of the average diurnal temperature variations, which to some extent mirror the effect of irradiation, can be calculated by the root mean square (RMS) of the difference between indoor temperature and a five-day running average of indoor temperature. For example, for Fide Church, which will be discussed later, RMS is 0.69°C from September 1 to April 31, which indicates that the contribution from irradiation during this period is low. Furthermore, heating is mostly required during the winter months, where the contribution from irradiation is low.

The following steps in deriving the model for intermittent heating are preconditioned by Assumptions 4.1 and 4.2, which are due to the considered building type. However, the infiltration and irradiation phenomena are not entirely neglected. They are covered by the constant loss factor, F_1 ($F_1 \leq 1$), which accounts for all losses in the building (assuming $P_L > P_{Ir}$) and forms the effective power used for heating, $P_e = F_1 P_s$. The heat balance at a heat-up event can then be simplified as follows:

$$\frac{V_a \rho_a c_{pa}}{Ah} \frac{d\vartheta_a}{dt} = (\vartheta_w(0,t) - \vartheta_a) + \frac{1}{Ah} F_1 P_s. \tag{6}$$

Since building volume, effective wall area, and the heat transfer coefficient between air and wall will not be determined using real physical parameters, the equation is further simplified as follows:

$$T_1 \frac{d\Delta\vartheta_a}{dt} + \Delta\vartheta_a = \Delta\vartheta_w(0,t) + b_1 P_s, \tag{7}$$

where $\Delta\vartheta_a$ and $\Delta\vartheta_w$ are increments of temperatures from equilibrium,

$$T_1 = \frac{V_a \rho_a c_{pa}}{Ah} \tag{8}$$

is the time constant, and

$$b_1 = \frac{F_1}{Ah} \tag{9}$$

is the static gain. The two parameters T_1 and b_1 of model (7) are determined experimentally based on input-output data using the grey box modelling approach. To simplify the notation, the wall surface temperature is denoted by $\Delta\vartheta_{ws} = \Delta\vartheta_w(0,t)$.

Note that the quasi-linear model (7) is valid under the assumption that the heat transfer coefficient h, influencing both the time constant T_1 and gain b_1, is approximately constant. This assumption also applies to classic convective heating. However, due to the well-known dependency of h on air velocity, model (7) needs to be used carefully if heating by ventilation is applied. If the air velocity by the ventilator changes, parameters T_1 and b_1 are likely to change too.

4.1.1 Model for massive wall surface temperature

The temperature increase at the wall surface, $\Delta\vartheta_{ws}$, can be calculated using the heat partial differential equation (PDE):

$$\frac{\partial^2 \vartheta_w}{\partial x^2} = \frac{c_w \rho_w}{\lambda_w} \cdot \frac{\partial \vartheta_w}{\partial t}, \tag{10}$$

where ϑ_w $(°C)$ is the wall temperature, λ_w $(Wm^{-1}K^{-1})$ is the heat conductivity of the wall, c_w $(J\ kg^{-1}K^{-1})$ is the specific heat of the wall, $\rho_w (kg\ m^{-3})$ is the density of the wall, t (s) time, and x (m) is the distance into the wall from the wall surface. Equation (10) can be solved both analytically and numerically in one dimension, for example, by using the numerical Finite Difference Method (FDM) [78]. FDM was recently applied to a structurally analogous problem of moisture sorption in a wooden desk [12]. The method is adapted to the problem at hand (10) in section 4.1.7 and used for the cross-comparison of further derived results.

An analytical solution of equation (10) is solved for the case of a constant heat flux into a semi-infinite slab [79] with initial conditions typical for intermittent heating of massive buildings:

- At the start of the heat-up event (i.e., $t = 0$), the temperature distribution in the wall is constant and equal to the indoor and outdoor air temperature, $\vartheta_w(x) = \vartheta_{a0}$.
- The heat flux, P_w, into the wall is considered constant during the heat-up process,

$$\frac{\partial \vartheta_w}{\partial x} = \frac{P_w}{A\lambda_w}, \; x = 0. \tag{11}$$

- The heat-up process is short enough that only a part of the wall is affected by the heat wave. Thus, the problem can be reformulated to the case of a semi-infinite wall:

$$\frac{\partial \vartheta_w}{\partial t} = 0, \; x \to \infty.$$

Under the above assumptions, the wall inner surface ($x = 0$) temperature can be expressed as

$$\vartheta_{ws} - \vartheta_{ws0} = \frac{P_w}{A} \cdot \frac{2}{\sqrt{\pi}} \cdot \frac{1}{\sqrt{\lambda_w c_w \rho_w}} \cdot \sqrt{t}, \tag{12}$$

where ϑ_{ws0} ($°C$) is the wall surface temperature at the beginning of the heat-up event [79]. To simplify equation (12), the following parameter is used:

$$a_1 = \frac{F_2}{A\sqrt{\pi}} \cdot \frac{2}{\sqrt{\lambda_w c_w \rho_w}}, \tag{13}$$

considering $P_w = F_2 P_s$ where F_2 is a constant factor ($F_2 \leq 1$). Because equation (12) expresses the increase in temperature from the initial temperature as a function of elapsed time of a heat-up event, the incremental form can be more appropriately represented as

$$\Delta\vartheta_{ws} = a_1 P_s \sqrt{t}. \tag{14}$$

4.1.2 Approximate model for air temperature

If equation (7) is coupled with equation (14), the following equation can be formulated:

$$T_1 \frac{d\Delta\vartheta_a(t)}{dt} + \Delta\vartheta_a(t) = a_1 P_s \sqrt{t} + b_1 P_s. \tag{15}$$

Equation (15) has the following solution for a step input, P_s

$$\Delta\vartheta_a = P_s \left(a_1 \left(\sqrt{t} - \sqrt{T_1} \cdot \frac{\sqrt{\pi}}{2} \operatorname{erfi}\left(\sqrt{t/T_1} \right) e^{-t/T_1} \right) + b_1 \left(1 - e^{-t/T_1} \right) \right), \tag{16}$$

where $\operatorname{erfi}(z)$ is the imaginary error function and $\frac{\sqrt{\pi}}{2} \cdot \operatorname{erfi}\left(\sqrt{t/T_1} \right) \cdot e^{-t/T_1}$ is the Dawson's integral [80].

4.1.3 Model parameter identification from measured data

Because it is difficult to determine the construction and the materials of historic masonry walls, it is difficult to determine their thermal parameters. The heat transfer coefficient between the wall and the air depends on the air flow close to the wall surface, which also is difficult to determine. However, these parameters can be estimated from measurements of the temperature during a step response test (i.e., a heat-up event) [38]. The task is to find parameters T_1, a_1 and b_1 which then determine the dynamic equation (15) or its solution (16). Here, it is supposed that the response data are available from earlier heat-up events with step-wise change in heating power, P_s. If this is not the case, smaller values of heating power, P_s (e.g., a half of $P_{s,max}$), are recommended in the step response test to lower the risk of damage due to associated RH decay.

According to equation (16), after the first stage, where the effect of the time constant dominates, the increase in air temperature is very close to a linear function of the square root of time ($\sqrt{t}$). Parameters a_1 and b_1 can then be determined by linear regression of air temperature measurements at the step response test, as demonstrated in the following case study. The regression must be conducted on the latter part of the data, where the influence of time constant accumulation has none or very little impact. From the equation of the regressed line, parameters a_1 and b_1 can be derived by the following equations:

$$a_1 = \frac{K_1}{P_s}, \quad \text{and} \tag{17}$$

$$b_1 = \frac{(\vartheta_{ar0} - \vartheta_{a0})}{P_s}, \tag{18}$$

where K_1 is the slope of the regressed temperature line when plotted against the square root of time $\left(\sqrt{t}\right)$, ϑ_{ar0} is the intercept of the regressed temperature line, and ϑ_{a0} is the air temperature at the start of the heat-up process.

The time constant, T_1, for the indoor air and interiors can then be found by integration of equation (15) [81]:

$$\int_0^{t_m} \left(T_1 \frac{d\Delta\vartheta_a(t)}{dt} + \Delta\vartheta_a(t)\right) dt = \int_0^{t_m} \left(a_1 P_s \sqrt{t} + b_1 P_s\right)\, dt, \tag{19}$$

and solving for T_1,

$$T_1 = \frac{\frac{2}{3} a_1 P_s t_m{}^{3/2} + b_1 P_s t_m - \int_0^{t_m} \Delta\vartheta_a(t) dt}{\Delta\vartheta_a(t_m)}, \tag{20}$$

where $\Delta\vartheta_a(t_m)$ are measurements of the air temperature increment from the equilibrium state and t_m is duration of step response. As equation (20) depends on the single value $\Delta\vartheta_a(t_m)$, T_1 is likely to be very sensitive to noise. To reduce the undesirable influence of noise on the measured value, equation (15) is integrated twice, resulting in

$$T_1 = \frac{\frac{4a_1 P_s t_m^{5/2}}{15} + \frac{b_1 P_s t_m^2}{2} - \iint_0^{t_m} \Delta\vartheta_a dt dt}{\int_0^{t_m} \Delta\vartheta_a dt}. \qquad (21)$$

4.1.4 Case study analysis and discussion

The proposed model identification procedure was tested on data collected from three 13th century churches. Figure 4.2, next to the photographs of the churches, shows the floor plans with dimensions and heater types and positions. All the churches are equipped with pew heaters (orange) and radiators (red). In Fide Church, the walls and floor are made of sandstone. The wall and vault are rendered with lime mortar both inside and outside. The roof is constructed with two cross vaults without a central pillar. The total indoor volume is approximately 1000 m^3. The three parts of the building form one connected large space. The church is heated with electric pew heaters located in the hall and three electrical radiators located in the chancel and tower. The total heating power of the heating system is 32 kW.

Hangvar Church's walls and vault are constructed of limestone, which is rendered with lime mortar both inside and outside. The roof has four cross vaults and a central pillar in the middle of the hall. The church has wooden floors. The church has three connected areas – hall, chancel and tower – that form a large open space. The indoor volume is approximately 1000 m^3. Hangvar Church is heated with electric pew heaters located in the hall and three supplemental electrical radiators located in the tower. The total heating power in the church is 27 kW. Tingstäde Church's walls and vault are constructed of limestone, only the inside is rendered with lime mortar. The roof consists of four cross vaults and a pillar in the middle of the hall. It has wooden floors. The indoor volume is approximately 1200 m^3. Tingstäde Church is heated with a hydronic pew heating system in the hall and two supplemental hydronic radiators – one in the tower and one in the chancel. The total heating power is 50 kW.

In all the churches, temperature and RH were measured hourly by data loggers located approximately 2,5 m above the floor in the middle of the church (see the blue circle in Figure 4.2). In Hangvar Church and Fide Church, Testo 175 H1 data loggers were used, while a Tiny Tag plus 2 data logger was used in Tingstäde Church. Due to practical constraints, measurements of the wall surface temperature were not conducted. The step response tests were carried out during winter: in Fide Church, from March 8, 9:00 to March 9, 14:00; in Hangvar Church from February 2, 20:00 to February 3, 10:00; and in Tingstäde Church from January 11, 13:00 to January 11, 24:00.

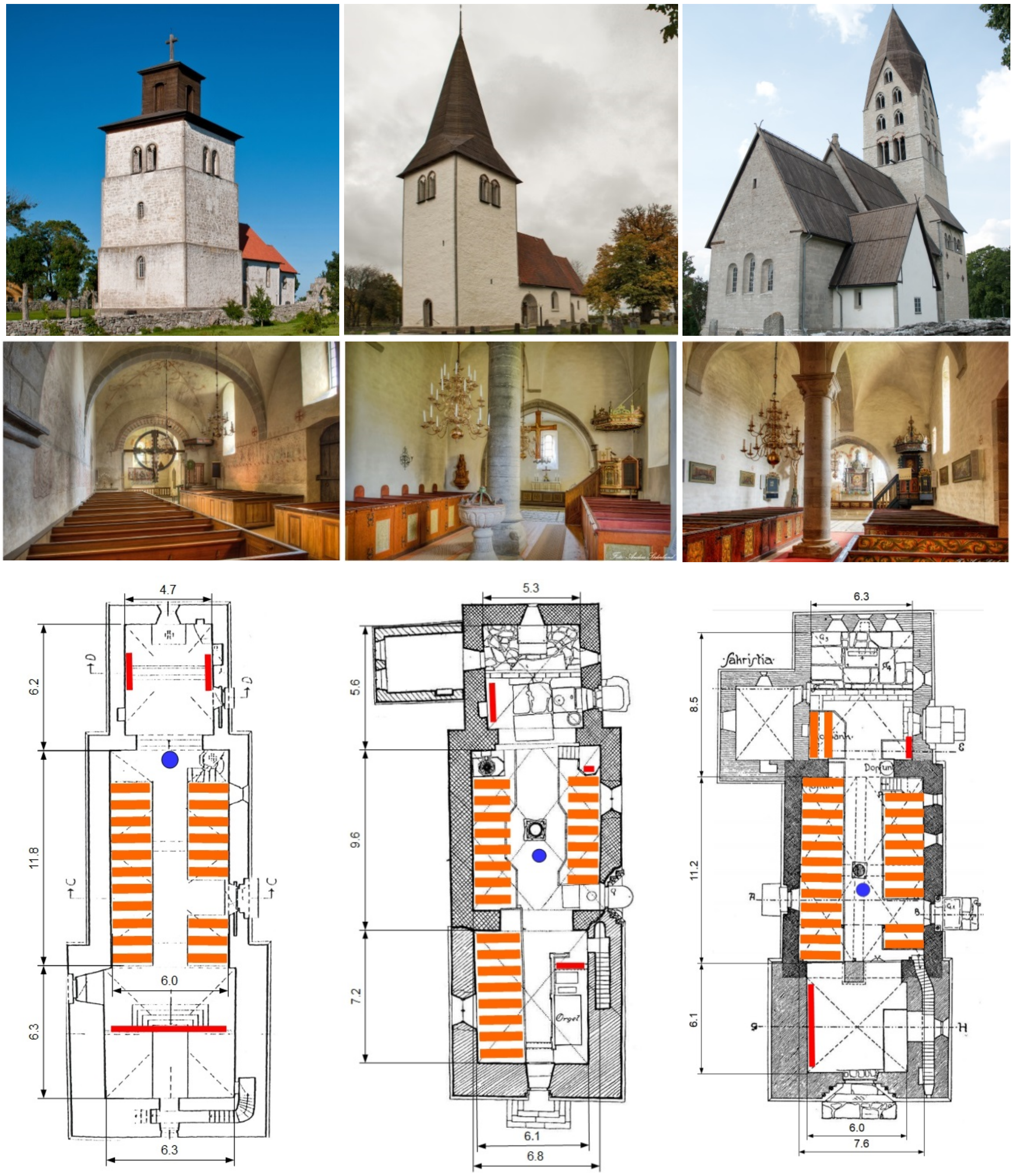

Figure 4.2. Fide Church (left), Hangvar Church (middle), and Tingstäde Church (right). The blue spot in the floor plan shows the location of the temperature and RH instruments, the orange area shows the location of the pew heaters, and the red shows the location of the radiators. (Photo Anders Söderlund).

4.1.5 Model parameter identification

The step responses measured at the churches can be seen in Figures 4.3-4.5. All three responses agree with the theoretical assumption outlined above. The transient part at the beginning of the responses is followed by a linear part along a square-root time axis. If this linear part in the given time-scale were missing, the methodology proposed here cannot be applied for the given building. As a result, a classical linear model with exponential characteristics would have been applied, leading to a lower complexity of control not considered here.

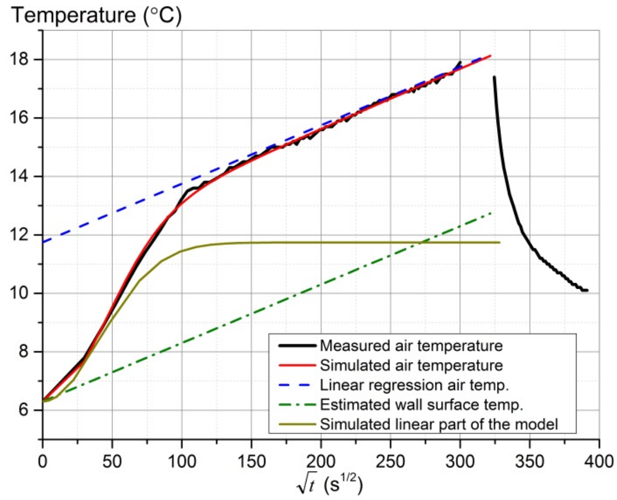

Figure 4.3. Heat-up event in Fide Church – measured versus simulated responses by the model (16) with identified parameters in Table 4.1.

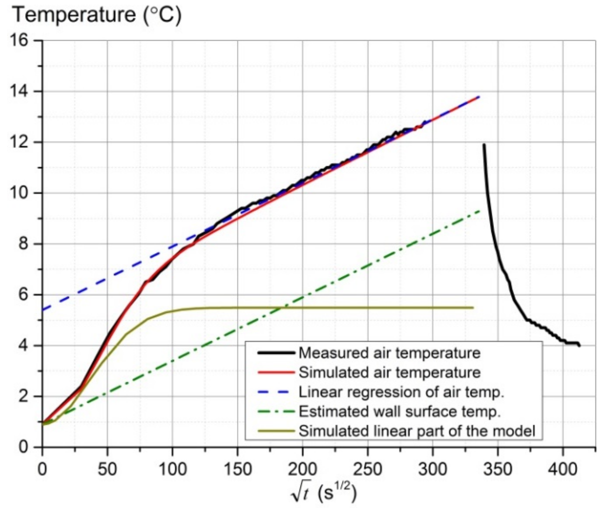

Figure 4.4. Heat-up event for Hangvar Church – measured versus simulated responses by the model (16) with identified parameters in Table 4.1.

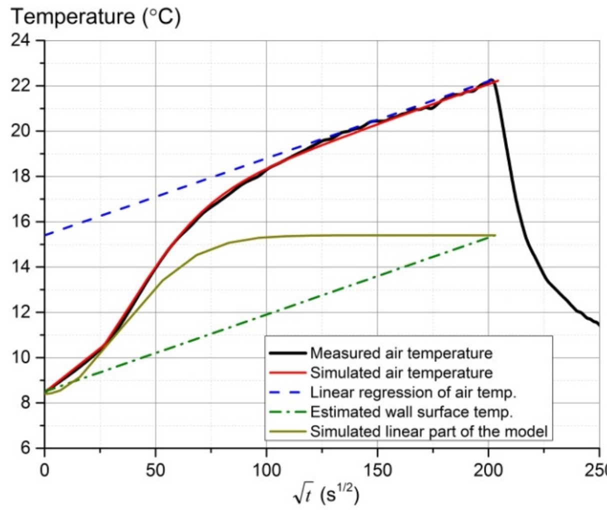

Figure 4.5. Heat-up event in Tingstäde Church – measured versus simulated responses by the model (16) with identified parameters in Table 4.1.

As can be seen in the figures, the duration of the transient part is approximately three hours for all three churches. The upper blue dashed line corresponds to the linear regressed air temperature. The linear regression is performed only on the latter part of the step response, where the dynamics with time constant, T_1, have no or very little impact. From the linear regression line, the slope, K_1, and the intercept, ϑ_{ar0} , are determined. Parameters a_1 and b_1 are calculated using equations (17) and (18), respectively. All identified parameter values are given in Table 1. Compared to the other two churches, the slope, K_1, was considerably higher for Tingstäde Church due to the higher heating power. However, Hangvar Church had the highest value for parameter a_1, indicating lower relative heat loss due to heat accumulation in the wall compared to the other two churches. The highest losses (mainly due to infiltration) can be expected for Tingstäde Church, which has the lowest gain parameter, b_1.The time constant is determined by equation (21) using MATLAB, where integrals $\iint_0^{t_m} \Delta\vartheta_a \, dtdt$ and $\int_0^{t_m} \Delta\vartheta_a dt$ are performed numerically on the measured data. The integration limit, t_m, is set to the time where the linear part of the data in the square-root time scale starts.

The resulting time constants, T_1, are given in Table 4.1. As expected, the time constants do not differ substantially due to similar indoor air volumes. The differences are presumably due to differences in heat transfer coefficients and material constants. The simulation results from equation (16) are shown in Figures 4.3-4.5 in comparison with the measured data. As seen, a very good match between the measured and simulated data has been achieved for all three churches.

To highlight the contribution of slow heat exchange between the massive walls due to $a_1 P_s \sqrt{t}$ in the input of equation (15), a response of the linear part of equation (15) considering $b_1 P_s$ as the only input (i.e., assuming $a_1 = 0$) is shown for each church in Figures 4.3-4.5. Such an exponential response is expected in buildings where the walls are well insulated (wooden) or rather thin (typical modern buildings). As seen from the differences between the partial model responses and overall responses of equation (15), the influence of slow heat exchange between the massive walls and interior air volume is significant after the initial transient part. It is evident that slow heat exchange cannot be neglected or approximated using a standard first-order linear model.

Table 4.1. Thermal parameters from a step response test. See Figures 4.3, 4.4, and 4.5.

	ϑ_{a0} (°C)	ϑ_{ar0} $(°C)$	K_1 $(°C/s^{1/2})$	P_s (kW)	a_1 $(°C/kW/s^{1/2})$	b_1 $(°C/kW)$	T_1 (s)
Fide Church	6,3	11,8	0,020	32	$5{,}7 \cdot 10^{-4}$	$1{,}7 \cdot 10^{-1}$	3400
Hangvar Church	0,9	5,4	0,025	27	$9{,}3 \cdot 10^{-4}$	$1{,}7 \cdot 10^{-1}$	2800
Tingstäde Church	8,4	15,4	0,034	50	$6{,}6 \cdot 10^{-4}$	$1{,}4 \cdot 10^{-1}$	2250

Although there are only three parameters in the simplified model parametrised at the single step response test, very good conformity between models and measurements has been achieved. Parameter a_1 is a material specific constant, as seen in equation (13), but it can change during the year depending on the wall moisture content. Static gain, b_1, includes the heat transfer coefficient and is therefore temperature dependent, as seen in equation (9). However, step response tests, which were conducted under different seasons in different churches, showed that the variations in these parameters are relatively small and slightly influenced by seasonal changes [38]. If the seasonal differences in responses are substantial, design models can be identified and used for the design for each of the seasons.

4.1.6 Alternative model with discretized PDE of heat transfer in the wall

For comparison, the FDM model of the wall (10) described in section 4.1.7 has also been parametrized for the data measured at the three churches. Coupling the discretized model of the wall in the state space form (40) with the single accumulation model (7), a good fit of the simulated and measured data was obtained for the three churches (Figures 4.7-4.9). The model parameters have been tuned to obtain this good fit. As the starting point, parameters from Table 4.1 were considered together with the wall parameters: thickness ($L = 1$ m), number of slices (i.e., order) ($N = 100$), slice thickness ($\Delta L = 0{,}01$ m), and material parameter of limestone (($\lambda_w = 1{,}9$ ($\mathrm{Wm^{-1}K^{-1}}$), $\rho = 2750$($\mathrm{kg\,m^{-3}}$), $c_w = 840$ ($\mathrm{J\,kg^{-1}K^{-1}}$), and $h = 10{,}0$ ($\mathrm{Wm^{-2}K^{-1}}$)). Some parameters were then slightly tuned (within 15% range) for a better fit with the measured data, in particular b_1 and h. The purpose of parametrizing the coupled and discretised high-order models (7-10) is to justify the simplifying assumptions that will be applied to model (15) in the indoor climate control design presented in Section 4.3. The control procedure synthetized for model (15) will be validated on this higher-order model. In addition to the simulated air temperature, which fits very well with the measured data, simulated wall temperature is visualized in the node points in the left parts of Figures 4.7-4.9. In the right parts of Figures 4.7-4.9, comparisons of the two considered models are visualised. A very good match can be seen for all the three simulation sets.

4.1.7 Discrete approximation

One dimension discrete approximation of the heat conduction equation perpendicular to a masonry wall surface is derived following the discretization scheme applied in [12]: a masonry wall in a massive building denoted by L (m) divided by equidistant parallel planes into N slices of equal thickness, $\Delta x = L\,/\,N$. These planes determine $N + 1$ nodes of the discrete representation of the thickness variable x. At the beginning (i.e., $t = 0$), the building is unheated, so the temperatures inside the building, on the surface of wall, and outside the building are considered equal: $\vartheta_w(0, x) = \vartheta_0$, $\vartheta_a = \vartheta_0$, and $\vartheta_{out} = \vartheta_0$. During a heat-up event, the wall model described by PDE (s) is theoretically considered semi-infinite; that is, the heat wave from inside will not reach the outside of the wall. For the numerical implementation of the model, the width of the wall is fixed to L, which needs to be large enough so that the heat wave would not influence the outside side of the wall substantially.

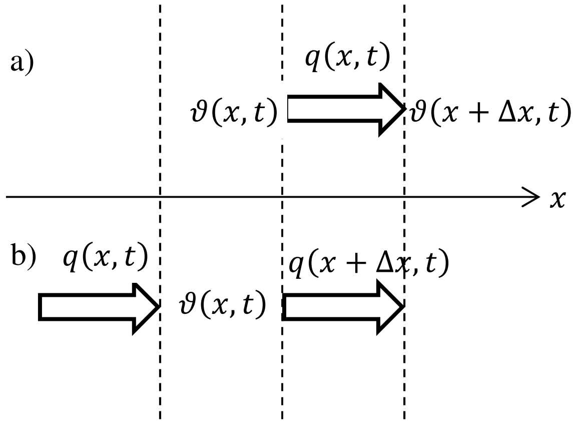

Figure 4.6. a) Heat flux through a plane and b) conservation of energy.

Considering the heat flux scheme in Figure 4.6 (a), the heat flux through a small plane of a masonry wall is given by

$$q(x,t) = -\lambda_w \cdot \frac{\vartheta_w(x+\Delta x,t)-\vartheta_w(x,t)}{\Delta x}, \quad (22)$$

which turns to

$$q(x,t) = -\lambda_w \cdot \frac{\partial \vartheta_w(x,t)}{\partial x}, \quad (23)$$

for $\Delta x \to 0$, where ϑ_w $(°C)$ is the temperature, λ_w $(W/m\,°C)$ is heat conductivity of the wall, t (s) is time, and x (m) is the distance into the wall from the wall surface. The change of heat flux with respect to x through the wall is given by

$$\frac{\partial q(x,t)}{\partial x} = \frac{\partial}{\partial x}\left(-\lambda_w \cdot \frac{\partial \vartheta_w(x,t)}{\partial x}\right) = -\lambda_w \cdot \frac{\partial^2 \vartheta_w(x,t)}{\partial x^2}. \quad (24)$$

The conservation of energy reveals that the change of energy level in a small slice Δx during a short Δt depends on the difference of the heat in the slice, as sketched in Figure 4.6b,

$$\frac{\Delta \vartheta_w(x,t)}{\Delta t} = -\frac{1}{c_w \rho_w} \cdot \left(\frac{q(x+\Delta x,t)-q(x,t)}{\Delta x}\right), \quad (25)$$

which turns into

$$\frac{\partial \vartheta_w(x,t)}{\partial t} = -\frac{1}{c_w \rho_w} \cdot \frac{\partial q(x,t)}{\partial x} \quad (26)$$

for $\Delta x \to 0$. Now equation (24) can be substituted into equation (26) and the result becomes

$$\frac{\partial \vartheta_w(x,t)}{\partial t} = \frac{\lambda_w}{c_w \rho_w} \cdot \frac{\partial^2 \vartheta_w(x,t)}{\partial x^2}, \quad (27)$$

where $c_w (J\,kg^{-1}\,°C^{-1})$ is the specific heat of the wall and $\rho_w (kg\,m^{-3})$ is the density of the wall. Equation (27) is a Partial Differential Equation also known as the Heat Equation.

To numerically simulate the temperature in the wall and the wall surface, a discretisation of the heat equation must be carried out. At the boundaries, the heat flow is described by

$$\lambda_w \frac{\partial \vartheta_w(x,t)}{\partial x}\bigg|_{x=0} = h_{in}\big(\vartheta_a(t) - \vartheta_w(0,t)\big) = -q(0,t), \text{ and} \tag{28}$$

$$\lambda_w \frac{\partial \vartheta_w(x,t)}{\partial x}\bigg|_{x=L} = h_{out}\big(\vartheta_w(L,t) - \vartheta_{out}(t)\big) = -q(L,t), \tag{29}$$

where h_{in} and h_{out} is the inside and outside heat transfer coefficient $(W\, m^{-2} K^{-1})$ and ϑ_a and ϑ_{out} is the indoor and outdoor temperature. For the discrete approximation of the second order derivatives with respect to x, the three-node method can be applied [78] [12]:

$$\frac{\partial^2 \vartheta(x,t)}{\partial x^2}\bigg|_{x=i} \cong \frac{1}{\Delta x^2}[\vartheta(i-1,t) - 2\vartheta(i,t) - \vartheta(i+1,t)]. \tag{30}$$

Where feasible, the symmetrical formulae are preferred. Only the boundary nodes $x = 0$ and $x = L$ require an asymmetrical version. At the boundaries, the asymmetrical Lagrangian three-point formula for the heat flow is applied:

$$\frac{\partial q(x,t)}{\partial x}\bigg|_{x=0} \cong \frac{1}{2\Delta x}\big(-3q(0,t) + 4q(1,t) - q(2,t)\big). \tag{31}$$

The heat flux at the first $(x = 1)$ and the second $(x = 2)$ slice is described by

$$q(1,t) = -\frac{\lambda_w}{2\Delta x}\cdot\big(\vartheta(2,t) - \vartheta(0,t)\big), \quad \text{and} \tag{32}$$

$$q(2,t) = -\frac{\lambda_w}{2\Delta x}\cdot\big(\vartheta(3,t) - \vartheta(1,t)\big). \tag{33}$$

By substituting equation (28) and (29) for boundary and equation (32) and (33) for $x = 1$ and $= 2$, respectively, into equation (31), the result becomes

$$\frac{\partial q(x,t)}{\partial x}\bigg|_{x=0} \cong \frac{3h_{in}}{2\Delta x}\big(\vartheta_a(t) - \vartheta_w(0,t)\big) + \frac{\lambda_w}{4\Delta x^2}\big(4\vartheta(0,t) - \vartheta(1,t) - 4\vartheta(2,t) + \vartheta(3,t)\big). \tag{34}$$

Finally, by using equation (26),

$$\frac{\partial \vartheta(x,t)}{\partial t}\bigg|_{x=0} = a\big(\vartheta_a(t) - \vartheta_w(0,t)\big) + \frac{K}{4}[-\vartheta(3,t) + 4\vartheta(2,t) + \vartheta(1,t) - 4\vartheta(0,t)], \tag{35}$$

and

$$\frac{\partial \vartheta(x,t)}{\partial t}\bigg|_{x=L} = b\big(\vartheta_{out}(t) - \vartheta_w(L,t)\big) + \\ + \frac{K}{4}[-\vartheta(L-3,t) + 4\vartheta(L-2,t) + \vartheta(L-1,t) - 4\vartheta(L,t)], \tag{36}$$

at the boundaries, where

$$a = \frac{3h_{in}}{2c_w \rho_w \Delta x}, \tag{37}$$

$$b = \frac{3h_{out}}{2c_w \rho_w \Delta x}, \tag{38}$$

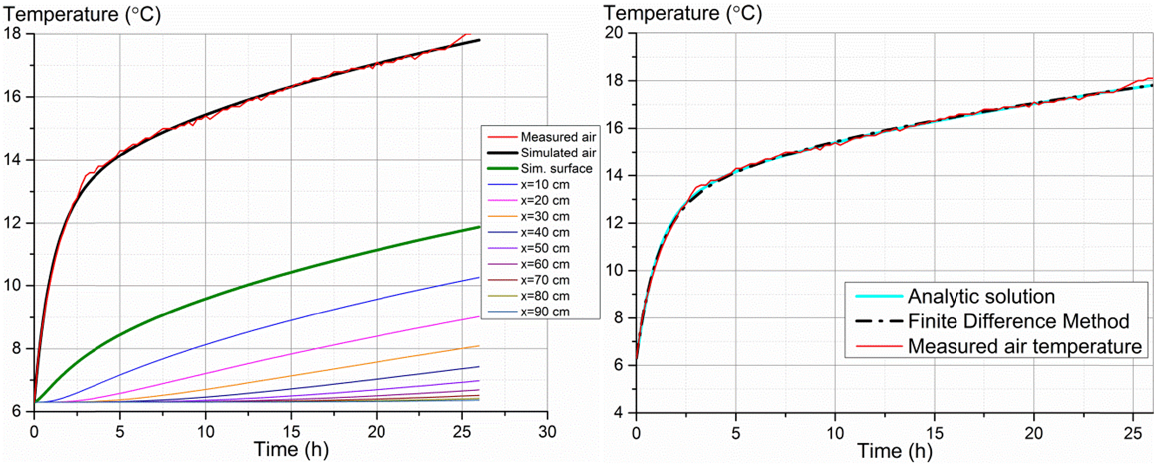

Figure 4.7. Fide Church: Left – measured versus simulated data by model (7) coupled with heat equation (10) approximated by FDM. Right – comparison of air temperature simulated by model (16) and (7) coupled with (10) approximated by FDM.

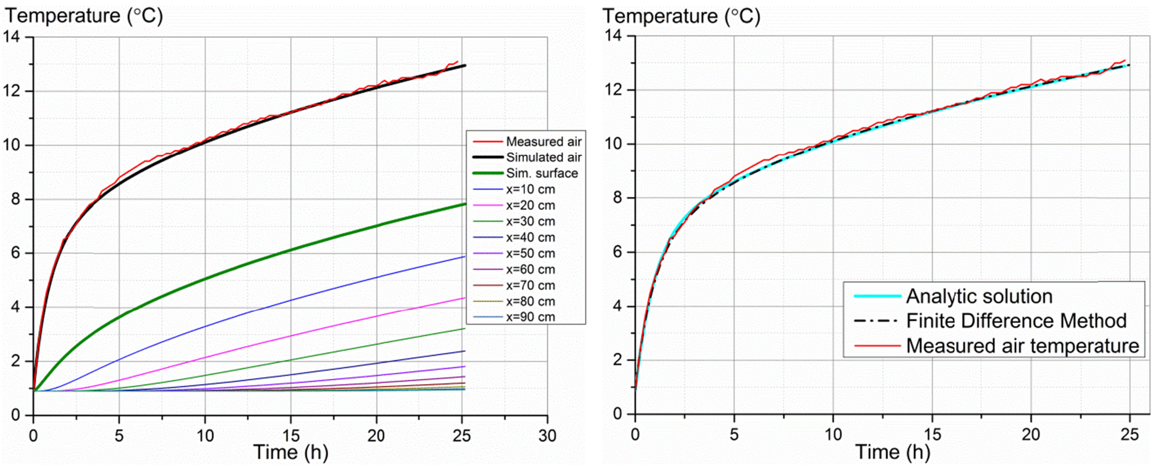

Figure 4.8. Hangvar Church: Left – measured versus simulated data by model (7) coupled with heat equation (10) approximated by FDM. Right – comparison of air temperature simulated by model (16) and (7) coupled with (10) approximated by FDM.

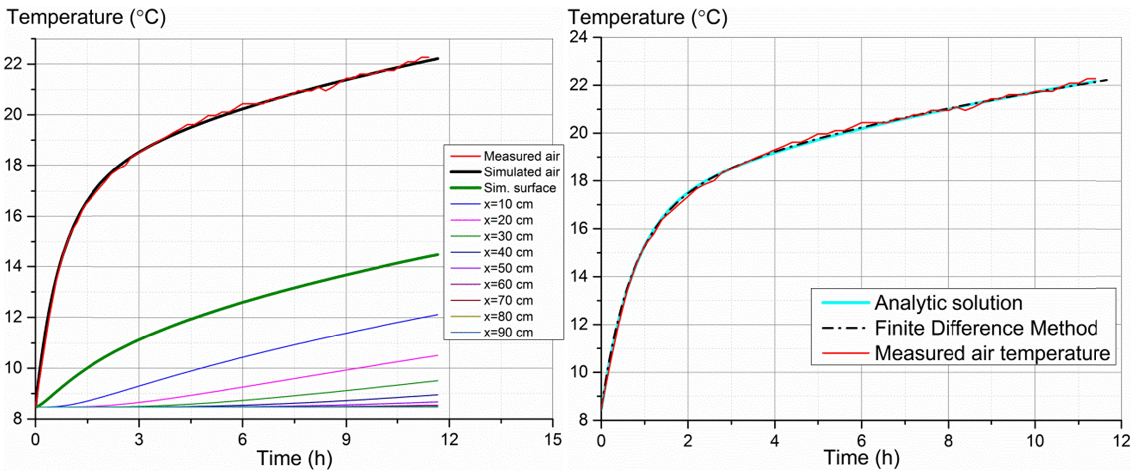

Figure 4.9. Tingstäde Church: Left – measured versus simulated data by model (7) coupled with heat equation (10) approximated by FDM. Right – comparison of air temperature simulated by model (16) and (7) coupled with (10) approximated by FDM.

$$K = \frac{\lambda_w}{c_w \rho_w \Delta x^2}. \tag{39}$$

Then, the following state space model of order $N + 1$ can be obtained:

$$\frac{dx(t)}{dt} = \boldsymbol{A}\boldsymbol{x}(t) + \boldsymbol{B}\boldsymbol{u}(t) \tag{40}$$

$$y(x) = \boldsymbol{C}\boldsymbol{x}(t) \tag{41}$$

with the state vector $\boldsymbol{x}(t) = [\vartheta_w(0,t), \vartheta_w(1,t), \ldots, \vartheta_w(N,t)]^T$, input vector $\boldsymbol{u}(t) = [\vartheta_A(t), \vartheta_B(t)]^T$ and the output $y(t) = \vartheta_w(0,t)$ and with the following matrices:

$$\boldsymbol{A} = \begin{bmatrix} -a-K, & K/4, & K, & -K/4, & \ldots & 0, & 0, & 0, \\ K, & -2K & K, & 0, & \ldots & 0, & 0, & 0, \\ 0, & K & -2K & K & \ldots & 0, & 0, & 0, \\ --- & --- & --- & --- & --- & --- & --- & --- \\ 0, & 0, & 0, & \ldots & K, & -2K, & K, & 0, \\ 0, & 0, & 0, & \ldots & 0, & K, & -2K, & K, \\ 0, & 0, & 0, & \ldots & -K/4, & K, & K/4, & -b-K \end{bmatrix},$$

$$\boldsymbol{B} = \begin{bmatrix} a, & 0 & 0, & 0 & \ldots & 0, & 0, & 0, \\ 0, & 0 & 0, & 0, & \ldots & 0, & 0, & b \end{bmatrix}^T,$$

$$\boldsymbol{C} = [1, \quad 0, \quad 0, \quad 0, \quad \ldots \quad 0, \quad 0, \quad 0].$$

This model has been implemented in MATLAB-Simulink.

4.1.8 Simplified model to determine heat-up time with no constrains on RH change rate

The air temperature at the end of the heat-up process as a function of elapsed time is relevant for practical calculations. The time constant has a significant impact only at the first part of the heat-up process, but at the final temperature its impact is only a few tenths of a centigrade. If the heat-up time is larger than five time constants ($5T_1$) and constants a_1 and b_1 are known from the step response test, the final temperature can be approximated with the following simplified equation:

$$\vartheta_{af} - \vartheta_{a0} = P_s\left(a_1\sqrt{t_f} + b_1\right), \tag{42}$$

where ϑ_{af} is the target temperature at the end of the heat-up time, t_f. Equation (42) can in turn be rearranged to calculate the heat-up time:

$$t_f = \left(\frac{\vartheta_{af} - \vartheta_{a0} - P_s b_1}{P_s \cdot a_1}\right)^2, \tag{43}$$

which is very useful for knowing when to turn on the heat. Equation (42) can also be rearranged to determine required power,

$$P_r = \frac{\vartheta_{af} - \vartheta_{a0}}{a_1\sqrt{t_f} + b_1}, \tag{44}$$

to reach the required final temperature as a function of time t_f. This simplified model was proposed and analysed in [1], presenting preliminary results to this paper.

It should, however, be stressed that this single step intermittent heating procedure may be risky for the interior due to the fast change rate of RH, especially at the starting part of the heat-up procedure. In Section 4.3 of this thesis, this is demonstrated in the left parts of Figures 4.13-4.15, which provide simulation results of temperature and RH using the single step intermittent heating for the three churches. For the purpose of estimating the change rate of RH, an approximate hygric model with parametrisation procedure is developed below, similar to the temperature model proposed above.

4.2 Simplified hygric model for intermittent heating of massive buildings

Similar to the thermal balance model, in this section an approximate hygric model for air humidity in a massive building in response to the heat input step is developed. Both the coupled thermal and hygric models will then be useful for planning a safe heat-up procedure. During a heat-up event, with the increase in temperature, the indoor air mixing ratio (MR) increases as moisture evaporates from the indoor walls and interiors. The mass balance during such a heat-up event is expressed by

$$K_a A\left(x_w(t) - x_a(t)\right) = \rho_a V_a \frac{dx_a}{dt} + n\rho_a V_a\left(x_a(t) - x_{out}(t)\right), \tag{45}$$

where K_a ($kg\ m^{-2}s^{-1}$) is a evaporating constant, A (m^2) is the effective evaporating wall area, x_w ($g\ kg^{-1}$) is the saturated MR at the wall surface, x_a ($g\ kg^{-1}$) is the indoor air MR,

$\rho_a (kg\ m^{-3})$ is the air density, $n\ (s^{-1})$ is the air exchange rate, $V_a\ (m^3)$ is the volume of the indoor air (the building interior), and $x_{out}\ (g\ kg^{-1})$ is the outdoor air MR. Large variations in MR in the outdoor air will influence the humidity inside if the infiltration rate is large. However, during a single heat-up event, the variation is usually not large enough to affect the indoor air significantly. Thus, x_{out} can be regarded as a constant [38].

Equation (45) can consequently be simplified to

$$T_2 \frac{d\Delta x_a(t)}{dt} + \Delta x_a(t) = C_2 \Delta x_w(t), \tag{46}$$

where

$$T_2 = \frac{\rho_a V_a}{K_a A + n \rho_a V_a}, \tag{47}$$

and

$$C_2 = \frac{1}{1 + n\frac{\rho_a V_a}{K_a A}}. \tag{48}$$

Moreover, it is assumed that due to capillary action, the RH at the wall surface is 100%. Therefore, MR at the wall surface can be assumed to be dependent only on the wall surface temperature [38]. As the wall surface temperature at the intermittent heat-up process is a function of square root of time, similar to equation (15), the right-hand side of equation (46) can be approximated as

$$C_2 \Delta x_w(t) = P_s\left(a_2\sqrt{t} + b_2\right), \tag{49}$$

where a_2 and b_2 are constants. The expression for air MR then becomes

$$T_2 \frac{d\Delta x_a(t)}{dt} + \Delta x_a(t) = P_s\left(a_2\sqrt{t} + b_2\right), \tag{50}$$

which has the same type of solution for a heating-power step as for temperature:

$$\Delta x_a = P_s\left(a_2\left(\sqrt{t} - \sqrt{T_2}\cdot\frac{\sqrt{\pi}}{2}\operatorname{erfi}\left(\sqrt{t/T_2}\right)e^{-t/T_2}\right) + b_2\left(1 - e^{-t/T_2}\right)\right). \tag{51}$$

To determine the parameters a_2, b_2, and T_2, the same approach as used for air temperature can be applied, using measured data from a step response test. A linear regression is performed from the time when the impact of the time constant has subsided to the end of the heat-up time. From the slope K_2 of the regressed line, the intercept x_{ar0} and air MR at the start x_{a0}, parameters a_2 and b_2 are derived as follows:

$$a_2 = \frac{K_2}{P_s} \text{ and} \tag{52}$$

$$b_2 = \frac{(x_{ar0} - x_{a0})}{P_s}. \tag{53}$$

The time constant T_2 can be determined by signal integration of equation (50) twice:

$$\iint_0^{t_m} \left(T_2 \frac{d\Delta x_a(t)}{dt} + \Delta x_a(t)\right) dtdt = \iint_0^{t_m} \left(a_2 P_s \sqrt{t} + b_2 P_s\right) dtdt, \tag{54}$$

and solving for T_2 gives

$$T_2 = \frac{\frac{4 a_2 P_s t_m^{5/2}}{15} + \frac{b_2 P_s t_m^2}{2} - \iint_0^{t_m} \Delta x_a dtdt}{\int_0^{t_m} \Delta x_a dt}. \tag{55}$$

4.2.1 Experimental verification

The identification procedure has been tested on the data measured in the three churches given in Figure 4.2. MR is calculated from measured data of RH and temperature using standard psychrometric formulas [83]. The calculated MR, its slope (K_2), and its intercept (x_{ai}) are shown in Figures 4.10-4.12. The resulting parameters are given in Table 4.2. As seen from the simulation results in Figures 4.10-4.12, model (51) fits the data very well for all the churches. As the moisture conditions of the wall are likely to change over the seasons, the hygrothermal parameters of the model must be adjusted to the current conditions of the wall.

To show the contribution of desorption from the massive walls, a response of the linear part of model (26) – i.e., $b_2 P_s$ as the only input ($a_2 = 0$) – is seen in Figures 4.10-4.12. As seen from the difference between this response and the overall response of the model, except Hangvar Church, the contribution of moisture desorption from the walls is significant after the initial transient part of the response. Furthermore, the largest time constant value is obtained for Hangvar Church. Together with a low value of a_2, this indicates that the moisture desorption in Hangvar Church is less than the other two churches. On the other hand, the largest moisture desorption from the walls took place in Tingstäde Church, which has the highest values for both a_2 and b_2.

Table 4.2 Humidity parameters from step response tests.

	x_{a0} (g/kg)	x_{ai} (g/kg)	P_s (kW)	K_2 $(g/kg\ /s^{1/2})$	a_2 $(g/kg/kW/s^{1/2})$	b_2 $(g/kg/kW)$	T_2 (s)
Fide Church	3,8	4,96	32	0,0072	$230 \cdot 10^{-6}$	$36 \cdot 10^{-3}$	3600
Hangvar Church	3	3,99	27	0,00071	$27 \cdot 10^{-6}$	$36 \cdot 10^{-3}$	5900
Tingstäde Church	5,86	8,2	50	0,0135	$270 \cdot 10^{-6}$	$47 \cdot 10^{-3}$	3500

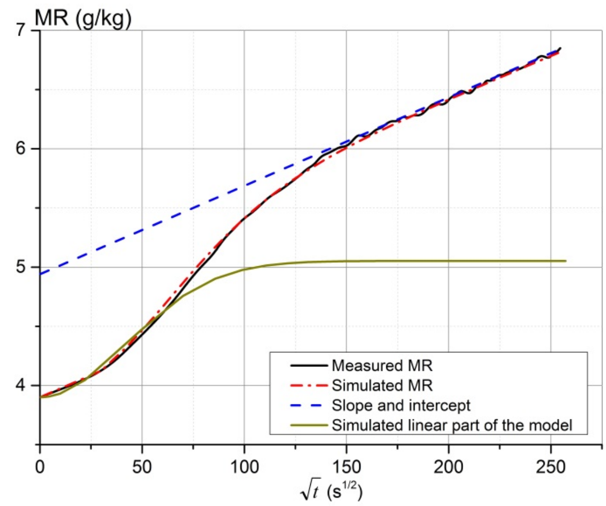

Figure 4.10. Indoor air MR response at the heat-up event in Fide Church – measured versus simulated responses by the model (51) with identified parameters in Table 4.2.

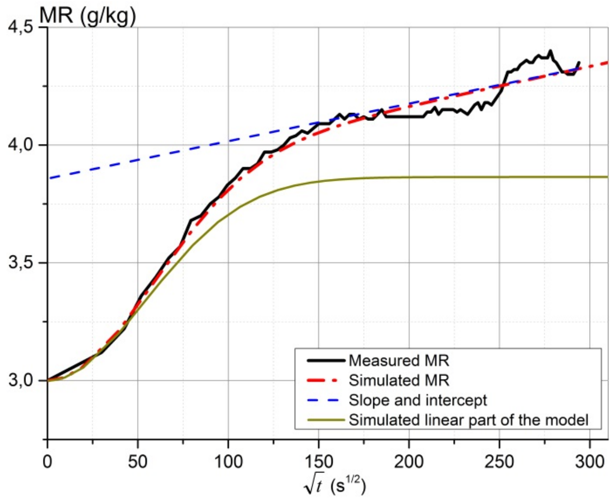

Figure 4.11. Indoor air MR response at the heat-up event in Hangvar Church – measured versus simulated responses by the model (51) with identified parameters in Table 4.2.

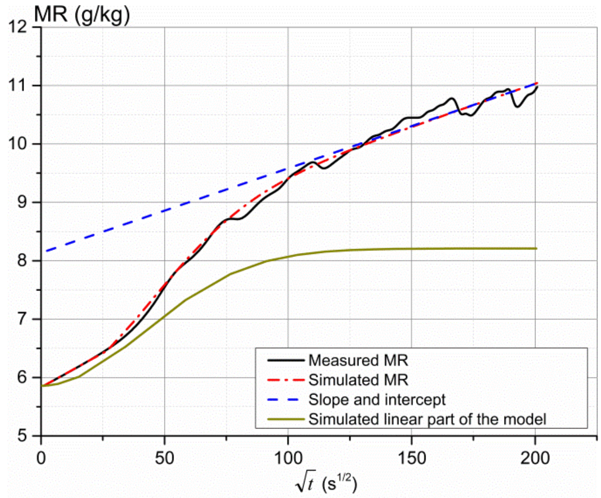

Figure 4.12. Indoor air MR response at the heat-up event in Tingstäde Church – measured versus simulated responses by the model (51) with identified parameters in Table 4.2.

4.3 Procedure to control the RH change rate by step-wise modulation of the heating power

The primary objective of deriving the approximate hygrothermal models above is to involve them in the optimisation of the heat-up procedure in intermittently-heated massive buildings. The control strategy for intermittent heating of a heavy masonry building should have the following requirements:

- **RH change**: To minimize the risk associated with fast variation of RH, the heating power should be adjusted so that the magnitude of RH change rate associated with temperature increase does not exceed a specified value.
- **Energy consumption**: The longer the heating lasts, the larger the heat losses due to both heat accumulation in the wall and infiltration. Thus, to keep the energy consumption low, the heater should be turned on for the shortest possible time before using the building and with as much power as possible considering safety constraints on the RH change rate requirement.
- **Comfort temperature:** The predefined comfort temperature needs to be achieved at a specific time.

To follow the recommendations for RH variations in interiors of historic buildings [23], the magnitude of RH change rate at the beginning of the heating period is limited. Therefore, the hourly RH change rate magnitude $\Delta\varphi_{a,s} = 2\%$ per hour suggested in [82] is considered further in the text for demonstration (the observed time period is $\Delta t = 1$ h). However, the user can define different values for both RH change rate and time period.

Next, a step-wise adjustment of heating power in time intervals $i\Delta t, i = 0, 1, 2, \ldots$ is determined by satisfying the given maximum change rate of RH per Δt. As a preliminary step, equations (16) and (51) are expressed in the following form:

$$\Delta\vartheta_a(t) = K_\vartheta(t)\Delta P_s \text{ and} \tag{56}$$

$$\Delta x_a(t) = K_x(t)\Delta P_s, \tag{57}$$

where

$$K_\vartheta(t) = a_1\left(\sqrt{t} - \sqrt{T_1} \cdot \frac{\sqrt{\pi}}{2}\operatorname{erfi}\left(\sqrt{t/T_1}\right)e^{-t/T_1}\right) + b_1\left(1 - e^{-t/T_1}\right), \tag{58}$$

$$K_x(t) = a_2\left(\sqrt{t} - \sqrt{T_2} \cdot \frac{\sqrt{\pi}}{2}\operatorname{erfi}\left(\sqrt{t/T_2}\right)e^{-t/T_2}\right) + b_2\left(1 - e^{-t/T_2}\right). \tag{59}$$

For fixed t, $K_\vartheta(t)$ and $K_x(t)$ are constant gains. Considering this, the design task at $t = 0$ is to determine ΔP_s for which

$$\Delta\varphi_a(\Delta t) \le \Delta\varphi_{a,s}. \tag{60}$$

Using the simplified Magnus formula [83,18], changes in $\Delta\vartheta_a$ and Δx_a can be transformed to change in $\Delta\varphi_a$:

$$x_a = 3.795 \cdot 10^{-5} \cdot \varphi_a \cdot 10^{\frac{a\vartheta_a}{b+\vartheta_a}}, \tag{61}$$

where $a = 7.65$ and $b = 243.12°C$ [83]. From (61), the RH value can be determined as

$$\varphi_a = f_\varphi(x_a, \vartheta_a) = \frac{1}{3.795} \cdot 10^5 \cdot x_a \cdot 10^{-\frac{a\vartheta_a}{b+\vartheta_a}}. \tag{62}$$

Assuming the variations of $\Delta\vartheta_a$ and Δx_a from the equilibrium initial values $\vartheta_{a,0}$ and $x_{a,0}$ (determining $\varphi_{a,0}$) within Δt are small, equation (62) can be reformulated into the linear incremental form

$$\Delta\varphi_a = C_x(\vartheta_{a,0}, x_{a,0})\Delta x_a + C_\vartheta(\vartheta_{a,0}, x_{a,0})\Delta\vartheta_a, \tag{63}$$

where

$$C_x(\vartheta_{a,0}, x_{a,0}) = \left.\frac{\partial f_\varphi(x_a,\vartheta_a)}{\partial x_a}\right|_0 = \frac{1}{3.795} \cdot 10^5 \cdot 10^{-\frac{a\vartheta_{a,0}}{b+\vartheta_{a,0}}}, \tag{64}$$

$$C_\vartheta(\vartheta_{a,0}, x_{a,0}) = \left.\frac{\partial f_\varphi(x_a,\vartheta_a)}{\partial \vartheta_a}\right|_0 = -\frac{1}{3.795} \cdot 10^5 \cdot x_{a,0} \cdot 10^{-\frac{a\vartheta_{a,0}}{b+\vartheta_{a,0}}} \cdot \frac{ab}{(b+\vartheta_{a,0})^2} \cdot \ln(10). \tag{65}$$

Substituting (56) and (57) for (63) and considering $t = \Delta t$, the following formula is obtained:

$$\Delta\varphi_a = C_x(\vartheta_{a,0}, x_{a,0})K_x(\Delta t)\Delta P_{s,0} + C_\vartheta(\vartheta_{a,0}, x_{a,0})K_\vartheta(\Delta t)\Delta P_{s,0}. \tag{66}$$

The heating power step at $t = 0$ to achieve maximal allowable RH change rate $\Delta\varphi_{a,s}$ over the period Δt can be then determined as

$$\Delta P_{s,0} = \frac{1}{C_x(\vartheta_{a,0},x_{a,0})K_x(\Delta t) + C_\vartheta(\vartheta_{a,0},x_{a,0})K_\vartheta(\Delta t)}\Delta\varphi_{a,s}. \tag{67}$$

The subscript in $\Delta P_{s,0}$ indicates the heating-power step at $t = 0$. In the unlikely case $\Delta P_{s,0} \geq P_{s,m}$, where $P_{s,m}$ indicates the maximal available heating power, the guidelines proposed in section 4.1.8 are to be followed. If the inequality is not satisfied, proceed as described below.

As a consequence to the determined heating power step $\Delta P_{s,0}$, values of $x_a(t)$ and $\vartheta_a(t)$ at $t = \Delta t$ can be expressed as

$$\vartheta_{a,1} = \vartheta_{a,0} + K_\vartheta(\Delta t)\Delta P_{s,0} \text{ and} \tag{68}$$

$$x_{a,1} = x_{a,0} + K_x(\Delta t)\Delta P_{s,0}. \tag{69}$$

Consequently, the RH change is given by

$$\varphi_{a,1} = f_\varphi(x_{a,1}, \vartheta_{a,1}). \tag{70}$$

Next, the subsequent heating-power step $\Delta P_{s,i}$ is added at $t = i\Delta t$, and $i = 1,2, \dots$ are determined. First, two key assumptions are stated:

- **Assumption 4.3:** To determine the heating-power step $\Delta P_{s,i}$, the nonhomogeneity of temperature distribution in the wall caused by the previous heating-power steps $\Delta P_{s,k}, k = 0,1, \dots i-1$ is neglected.
- **Assumption 4.4:** Under the linearity assumption, the overall response to a stepped heating-power distribution consists of a superposition of single heating-power steps $\Delta P_{s,i}$ at $t = i\Delta t$, $i = 0,1,2, \dots$.

To justify Assumption 4.3, let us recall that equations (16) and (51) were derived and identified considering the equilibrium distribution of temperature in the wall. This is not valid after applying the first (and possibly subsequent) heating-power step(s). However, due to high thermal inertia of the wall, the non-homogeneity of temperature distribution of the initial steps at the beginning of the heating period is likely to be small, so it is neglected in the next steps. Assumption 4.4 arises from a linearity assumption [84] where equations (16) and (51) are used to assess the responses of subsequent heating-power steps. The overall response is then derived as a superposition of the partial responses to the heating-power steps $\Delta P_{s,i}$, taken at $t = i\Delta t, i = 0,1,2,\dots$. To justify these assumptions, simulation-based validation is performed on a higher-order model derived in Section 4.1.6, which models the heat distribution in the wall more precisely, including temperature non-homogeneity.

To determine the power increment at $t = \Delta t$, the superposition of the first and the second step needs to be considered. For this purpose, values of $\bar{x}_a(t)$ and $\bar{\vartheta}_a(t)$ at $t = 2\Delta t$ (as a consequence of $\Delta P_{s,0}$) are expressed as

$$\bar{\vartheta}_{a,2} = \vartheta_{a,0} + K_\vartheta(2\Delta t)\Delta P_{s,0} \text{ and} \tag{71}$$

$$\bar{x}_{a,2} = x_{a,0} + K_x(2\Delta t)\Delta P_{s,0}, \tag{72}$$

which leads to $\bar{\varphi}_{a,2} = f_\varphi(\bar{x}_{a,2}, \bar{\vartheta}_{a,2})$ using equation (70). Then, the maximal possible RH decrement due to $\Delta P_{s,1}$ is given by

$$\Delta\varphi_{a,r_1} = \Delta\varphi_{a,s} + (\varphi_{a,1} - \bar{\varphi}_{a,2}). \tag{73}$$

That is, the maximum RH drop $\Delta\varphi_{a,s}$ is reduced by the drop caused already by $\Delta P_{s,0}$. The power increment can then be determined as

$$\Delta P_{s,1} = \frac{1}{C_x(\vartheta_{a,1}, x_{a,1})K_x(\Delta t) + C_\vartheta(\vartheta_{a,1}, x_{a,1})K_\vartheta(\Delta t)} \Delta\varphi_{a,r_1}. \tag{74}$$

In this case, $C_x(\vartheta_{a,1}, x_{a,1})$ and $C_\vartheta(\vartheta_{a,1}, x_{a,1})$ are evaluated for $\vartheta_{a,1}$ and $x_{a,1}$. Therefore, these coefficients slightly differ from those applied to determining the first step. If $\Delta P_{s,0} + \Delta P_{s,1} < P_{s,m}$, the above procedure is repeated; if not, $\Delta P_{s,1} = P_{s,m} - \Delta P_{s,0}$ and the procedure stops. The procedure can be generalized for the $i - th$ step, considering Assumptions 4.3 and 4.4, as described below.

Algorithm 4.1: Determining the power increment $\Delta P_{s,i}$ at $i-th$ step

1. Values $x_a(t)$ and $\vartheta_a(t)$ at $t = i\Delta t$ are determined as

   $\vartheta_{a,i} = \vartheta_{a,0} + \sum_{k=0}^{i-1} K_\vartheta\big((i-k)\Delta t\big)\Delta P_{s,k}$ and (75)

   $x_{a,i} = x_{a,0} + \sum_{k=0}^{i-1} K_x\big((i-k)\Delta t\big)\Delta P_{s,k}$ (76)

   leading to the RH value $\varphi_{a,i}(t) = f_\varphi\big(x_{a,i}, \vartheta_{a,i}\big)$ by equation (62).

2. Auxiliary values $\bar{x}_a(t)$ and $\bar{\vartheta}_a(t)$ are determined at $t = (i+1)\Delta t$:

   $\bar{\vartheta}_{a,i+1} = \vartheta_{a,0} + \sum_{k=0}^{i-1} K_\vartheta((i-k+1)\Delta t)\Delta P_{s,k}$ and (77)

   $\bar{x}_{a,i+1} = x_{a,0} + \sum_{k=0}^{i-1} K_x((i-k+1)\Delta t)\Delta P_{s,k}$, (78)

   leading to the RH value $\bar{\varphi}_{a,i+1}(t) = f_\varphi\big(\bar{x}_{a,i+1}, \bar{\vartheta}_{a,i+1}\big)$ by equation (62).

3. The reduced RH decrement is given as

   $\Delta\varphi_{a,r_i} = \Delta\varphi_{a,s} + (\varphi_{a,i} - \bar{\varphi}_{a,i+1})$. (79)

4. The heating-power step at $t = i\Delta t$ is finally estimated as

   $\Delta P_{s,i} = \frac{1}{C_x(\vartheta_{a,i}, x_{a,i})K_x(\Delta t) + C_\vartheta(\vartheta_{a,i}, x_{a,i})K_\vartheta(\Delta t)}\Delta\varphi_{a,r_i}$. (80)

5. If the following inequality is satisfied,

   $\sum_{k=0}^{i} \Delta P_{s,k} \geq P_{s,m}$, (81)

   then $\Delta P_{s,i}$ is reduced to $\Delta P_{s,i} = P_{s,m} - \sum_{k=0}^{i-1} \Delta P_{s,k}$ and the procedure stops; if not, then $i = i+1$ and the procedure is repeated from step 1.

After shaping the heating-power distribution at the beginning of the heating period, the last task is to estimate the overall heating time t_f to reach the temperature $\vartheta_{a,f}$. Following the superposition rule, the time can be determined as a solution of the following nonlinear equation:

$$\vartheta_{a,f} = \vartheta_{a,0} + \sum_{k=0}^{i} K_\vartheta\big(t_f - k\Delta t\big)\Delta P_{s,k}, \tag{82}$$

considering $t_f > i\Delta t$. The equation can be solved using an established numerical method, such as Newton's method [85], or simply by sweeping time t_f starting from $t_{f,0} = i_{max}\Delta t$. Similar to equation (43) in Section 4.1.8, considering the assumption that the heat-up time of each step is larger than five time constants (i.e., $5T_1$), equation (82) can be considerably simplified as

$$\vartheta_{af} = \vartheta_{a,0} + \sum_{k=0}^{i}\big(a_1\sqrt{t_f - k\Delta t} + b_1\big)\Delta P_{s,k}. \tag{83}$$

Equation (83) is still nonlinear and a numerical solution is required to determine t_f.

4.3.1 Simulation-based validation of the proposed indoor-climate control

Figures 4.13-4.15 show the simulation results validating the control procedure for adjustment of the heating power by Algorithm 4.1 in the three churches. The target temperature was selected as $\vartheta_{af} = 20°\mathrm{C}$ for all the three churches. Initial values of temperature and RH are given as $\vartheta_{a,0} = 6°\mathrm{C}, \varphi_{a,0} = 69{,}5\%$ for Fide, $\vartheta_{a,0} = 1{,}3°\mathrm{C}, \varphi_{a,0} = 74{,}7\%$ for Hangvar, and $\vartheta_{a,0} = 8°\mathrm{C}, \varphi_{a,0} = 85\%$ for Tingstäde. The responses of temperature and RH to a single heating-power step discussed in Section 4.1 are shown in the left parts of the figures. The heating time to achieve $\vartheta_{af} = 20°\mathrm{C}$ was determined by equation (43) as $t_f = 47$ h for Fide, $t_f = 94$ h for Hangvar, and $t_f = 6{,}2$ h for Tingstäde. As seen in the figures, a considerably high change rate of RH can be observed at the beginning of all heating events, which may be risky for the building interior, particularly for wooden objects. As seen in the right part of the figures, the predefined RH drop $\Delta\varphi_{a,s} = 2\%$ per hour is achieved for all three churches when the above-defined control procedure is applied. For Fide, the heating-power increase is divided into five full and one shortened sub-step determined by Algorithm 4.1 (i.e., with $i_{max} = 5$). For both Hangvar and Tingstäde, the number of steps $i_{max} = 7$. According to Algorithm 4.1, the magnitude of the heating-power substeps tends to decrease as i increases. By solving equation (83) using the sweeping method, the heating time over predefined dense grid is determined as $t_f = 48{,}5$ h for Fide, $t_f = 97$ h for Hangvar, and $t_f = 9{,}4$ h for Tingstäde. When compared to the heating time for single step alternative, relatively small heating-time increments can be observed for all three churches.

To justify Assumptions 4.3 and 4.4, which are necessary to determine the complete control design procedure, a more accurate model from coupling model (7) and PDE (10) discretised by FDM and parametrised in Section 4.1.6 is used for validation. The stepped power signal generated by applying the above-derived control design procedure is considered as the input of model (7) coupled with FDM wall model (40). On the other hand, the results by equation (15) are the sum of partial responses to $\Delta P_{s,i}$ at time instants $i\Delta t$, $i = 0,1,\ldots i_{max}$. As seen in Figures 4.13-4.15, both models practically provide the same results: a perfect match. This agreement justifies Assumption 4.1: ignore the temperature non-homogeneity in the wall when determining the heating-power steps $\Delta P_{s,i}$. In addition, for obtaining the RH estimation, superposition of step responses simulated by equation (51) to get $\Delta x_{a,i}$ was applied, which was used to calculate RH by equation (62).

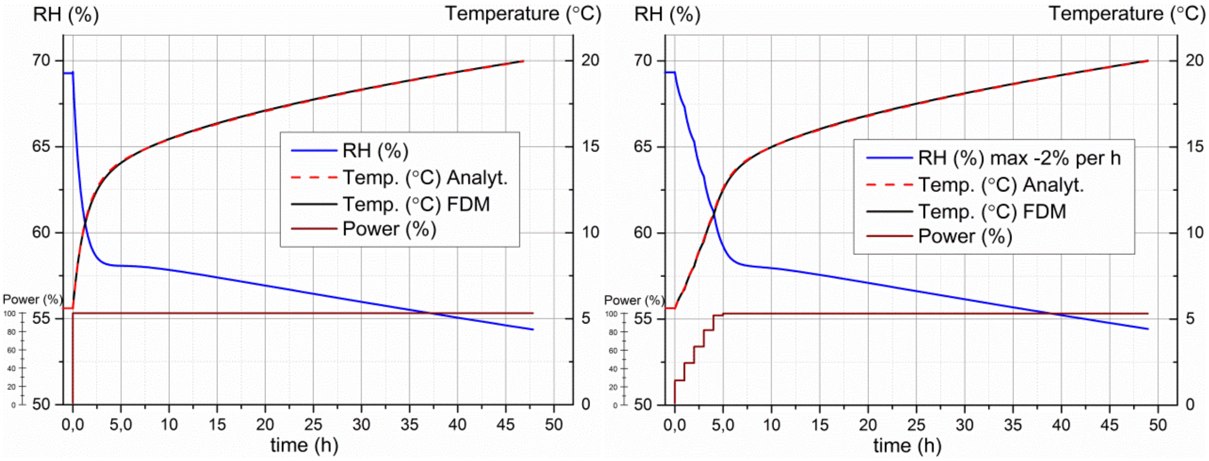

Figure 4.13. Fide Church: Simulation of heating event. Left – a single heating power step; Right – a stepped heating power distribution determined by the proposed control method (75)-(81) with $i = 0, .., 5$. (Temperature simulation performed with both FDM and analytical method).

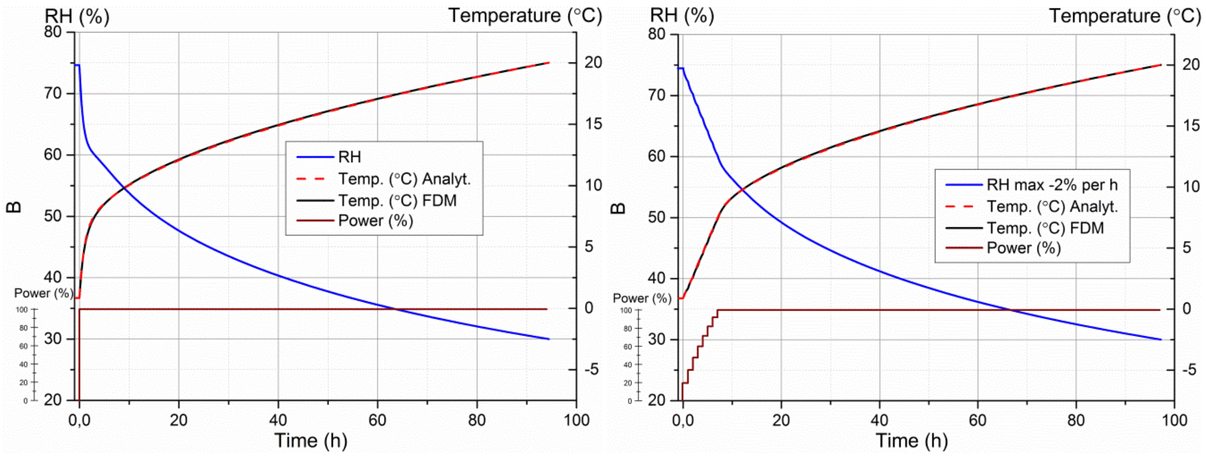

Figure 4.14. Hangvar Church: Simulation of heating event. Left – a single heating power step; Right – a stepped heating power distribution determined by the proposed control method (75)-(81) with $i = 0, .., 7$. (Temperature simulation performed with both FDM and analytical method).

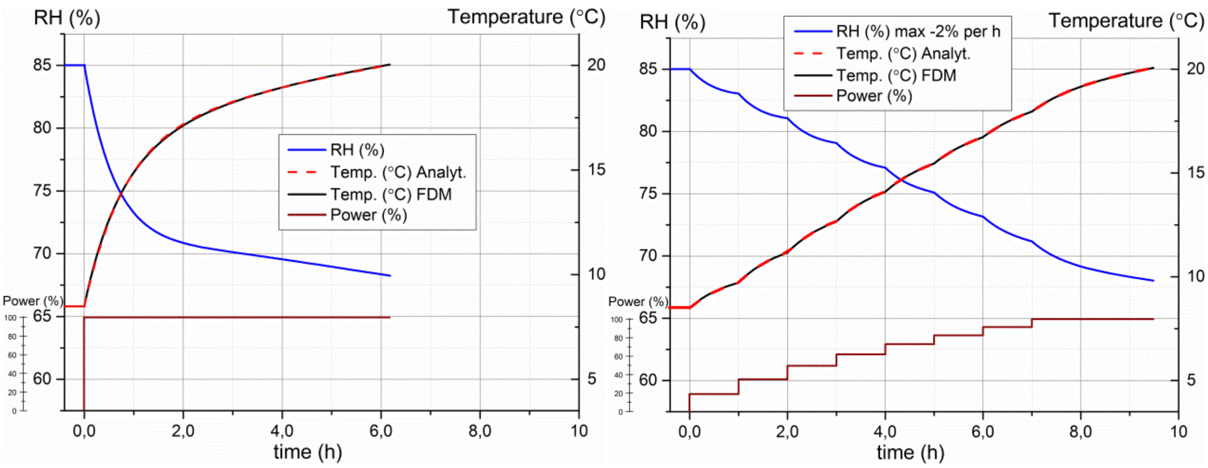

Figure 4.15. Tingstäde Church: Simulation of heating event: Left – a single heating power step; Right – a stepped heating power distribution determined by the proposed control method (75)-(81) with $i = 0, .., 7$. (Temperature simulation performed with both FDM and analytical method).

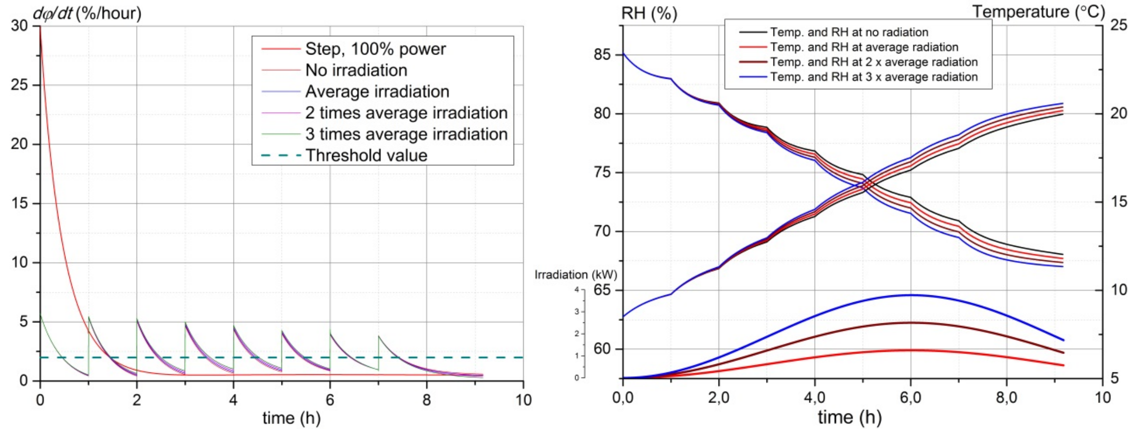

Figure 4.16. Tingstäde Church. Simulation of continuously evaluated change rate $\frac{d\varphi}{dt}$ (%RH/hour) for the single heating power step and proposed multistep intermittent heating procedures taking into account the disturbance by solar irradiation for the latter case (left). The effect of solar irradiation (shown in the bottom part of the figure) on the temperature and RH (right).

The predefined change rate $\Delta\varphi_{a,s}$ per Δt is achieved in a discrete-time manner over the time samples. In between the time samples, it is likely that the maximum of continuously evaluated change rate $\frac{d\varphi}{dt}$ (%RH/h) is higher. The quantities $\Delta\varphi_{a,s}$ per Δt and $\frac{d\varphi}{dt}$ are linked using

$$\Delta\varphi_{a,s} = \int_{i\Delta t}^{(i+1)\Delta t} \frac{d\varphi(t)}{dt} dt. \qquad (84)$$

The differences between $\Delta\varphi$ per hour and $\frac{d\varphi}{dt}$ are visualised in Figure 4.16 (left) for the Tingstäde Church model. The change rate $\frac{d\varphi}{dt}$ exceeds the predefined threshold value $\Delta\varphi_{a,s} = 2\,\%$ per hour. The change rate is higher when the power is step-wise increased, with the maximum $\frac{d\varphi}{dt} = 6$ %/h at the first step. On the other hand, just before the heat steps, $\frac{d\varphi}{dt}$ is close to 0.5 %/h. According to the assignment, the predefined $\Delta\varphi_{a,s}$ by equation (84) is obtained for $i = 0,1 \ldots 6$.

To keep the continuously evaluated change rate $\frac{d\varphi}{dt}$ strictly below the threshold value $\Delta\varphi_{a,s}$ per Δt, the heating power would need to be adjusted continuously (i.e., with $\Delta t \to 0$), considerably increasing the complexity of the overall approach. The other option for achieving a strict constraint on the RH change rate is to lower the predefined $\Delta\varphi_{a,s}$ by a factor of at least 0,5. Of course, this adjustment would prolong the overall heating time and thus increase the heat demand. However, it needs to be stressed that in comparison with the change rate under the single full-heating power step, a substantial improvement has been achieved. At the beginning of the heat-up period, the change rate for the single step method is as high as 30% per hour, whereas the initial change rate due to stepwise heating is five times smaller (Figure 4.16).

Finally, the disturbance effect of solar irradiation is also studied for the Tingstäde Church model. The heat gain by the solar irradiation was determined by considering solar irradiation data from the nearby Visby airport (Visby, Sweden) and the effective glazing area of the church during a daily cycle. For the simulation, the heat gain by irradiation shown in the lower part of Figure 15 was considered as a disturbance input of the model in three scenarios. The first scenario considers an average solar irradiation intensity with the maximum $P_{IR,max} = 1250\ W$, which has almost negligible effect on the temperature, RH, and the RH gradient. Then responses are shown for the irradiation magnitudes multiplied by factors of two and three (i.e., with maxima $P_{IR,max} = 2500\ W$ and $P_{IR,max} = 3750\ W$.) Although the effect on the temperature and RH naturally increased, the effect on $\frac{d\varphi}{dt}$ is almost negligible (Figure 4.16, left). This justifies the Assumption 2.2 for Tingstäde Church. The impact of disturbances can also be lowered by considering a safety margin on $\Delta\varphi_{a,s}$.

4.4 Discussion on applicability and implementation aspects

It needs to be stressed that the approximative models were developed for massive historic buildings with heavy masonry walls and small window areas and assume a relatively small and constant infiltration rate as well as relatively small effects of solar radiation during the heat-up event. Typical representatives of such buildings are historic stone churches such as the ones considered here. The derived models are not directly applicable for more than one dominant dynamical mode. For example, if the moisture desorption from the floor is considerably faster or slower than the moisture desorption from the walls, the methodology is not directly applicable. In this case, second- or higher-order mathematical models with two or more distinct time constants are required. In this work, the case study churches were modelled as single zone buildings. The method is applicable to multi-zone buildings with massive walls only if there is no interaction between the zones during the intermittent heating event.

Implementing the proposed heat-power shaping can be carried out manually by increasing the power at regular time (e.g., every hour) based on tabularised values. Alternatively, the entire algorithm can be automated and implemented using a smart switch. Thus, the reduction of the risk due to large RH rate change can be achieved at no cost or at least a relatively low cost. However, the proposed method has limitations. In particular, the method does not compensate for external disturbances, such as substantial changes of infiltration rate, effect of solar radiation, and impact of visitors. Interestingly, these disturbances are not likely to influence the indoor climate of the churches during a short intermittent heating procedure. If the disturbances play a significand role, the method can be combined with a feedback control method following the model predictive control framework [74, 75]. However, the implementation cost of this advanced control method would be considerably higher.

4.5 Conclusions on optimised intermittent heating

A method of shaping the heating power and determine heat-up time of an intermittent heating event in historic buildings with heavy masonry walls is proposed. The primary objective is to keep the RH change rate within a safe range, as a fast change rate of RH can damage cultural heritage objects. The method is based on simplified thermal and hygric analytical models, both in a form of accumulation-type first-order nonlinear differential equations. For both models an easy-to-apply parameter identification procedures based on in-situ measurements are proposed. The proposed models and identification procedures were successfully validated on measured data collected from three churches in Sweden: Fide, Hangvar, and Tingstäde. To validate the simplification assumptions of the models, a dynamical model of higher order was proposed and parametrized, where the heat dynamics in the wall were modelled by the second-order partial differential heat equation solved by the finite difference method (FDM).

The parameterised models are then used in the synthesis of control design procedure. The indoor air RH change rate is predictable, as it is determined by the air temperature and the air RH. The key idea is to divide the available heating power to (hourly) sub-steps to limit the defined (hourly) RH change rate. An iterative procedure is based on sensitivity analysis using simplifying assumptions under which the whole response is composed of superposition of the responses to the heating power sub-steps distributed over time. Next to determining the magnitude of the heating power sub-steps, a method was proposed to determine the heat-up time to achieve the target temperature.

The control method is applied and successfully validated on the models of the three churches. The RH (hourly) change rate can be well controlled by the proposed sub-step procedure. As shown from the comparison with the single-heating power step response, the increase of heating time for the start-up step-wise power increase is relatively small. In addition, the heating power can be controlled manually at given times (e.g., every hour) based on tabularised values. Alternatively, the whole algorithm can be automated and implemented using a smart switch or a low-cost controller (e.g., Raspberry-Pi).

Future research should address the modelling issues mentioned in the discussion above as well the potential for a practical application of the proposed control method. This should include i) the validation of the control procedure in one or more of the test churches, ii) a test of the validity of assumptions for the models in a range of building types, and iii) a comparative testing of the simulations and in-situ, of the proposed control method in relation to conventional methods. In addition, as the presented model is only valid for the heat-up period of an event but not the cooling period, the next step would be to find a complete dynamic model that uses the parameters from the step response test. Another research direction is in design and analysis of feedback control approach, for example, by applying model predictive control. However, in this case, a considerably more powerful (and more expensive) control unit would need to be used to implement the control method.

5 Validation and analysis of adaptive ventilation method

The primary objective of this chapter is to determine whether adaptive ventilation (AV) is an efficient alternative to other climate control measures for lowering relative humidity (RH) to prevent mould growth. For this analysis, an adaptive ventilation system is designed and tested on real case studies in situ to find the practical and theoretical obstacles of the approach. The control methods must be evaluated and refined. Note that this section is an extension of previous studies ([3], [4], [5], and [6]) where the author of this thesis is either main author or a key co-author. The chapter is organised as follows. Sections 5.1-5.2 describe the development of a system for adaptive ventilation, section 5.3 addresses a first case study in an old farm house, and section 5.4 addresses a case study in Hangvar Church. Section 5.5 contains discussion and conclusions.

5.1 Introduction

Many historic buildings that are unheated or unheated between use have problems with high humidity levels, increasing the risk for mould growth. To preserve the building as well as the interior and its contents, climate control between the heating events must keep RH low. Adaptive ventilation is a potentially low-energy and low impact option but needs to be validated and developed. There are several questions that need to be answered: Does adaptive ventilation actually limit the risk for mould growth, how is the stability of RH affected and are the control methods optimized for this purpose?

In some congregations, the tradition has been to ‘let the spring into the church’ – i.e., to open the doors wide to bring the warmth into the winter-cold building. Sometimes this works, but sometimes this method causes condensation of warm and humid air on the still cold masonry walls. Ventilation by opening doors and windows is the traditional way of controlling the intake of outside air; however, as the example above shows, it is difficult to determine when the climatic conditions will improve or deteriorate the indoor climate. Therefore humidity controlled mechanical ventilation is required either to move outside air into the building or to move inside air out of the building [4].

Adaptive ventilation attempts to lower the humidity in the inside air using the outside air by taking advantage of the natural diurnal and seasonal variations in the outside humidity. That is, the outdoor air is brought into a building only when its air absolute humidity (AH) is lower than indoor air AH [4]. The best drying effect is achieved if the building is air tight as the building should also be closed when it is more humid outdoors than indoors. In a leaky building, the drying effect will be counteracted if humid air enters the house by natural air infiltration [3].

As air AH is not measurable, the adaptive ventilation control system must calculate air AH both indoors and outdoors from the measurable quantities temperature and RH. As can be seen in Figure 5.1, a fan is then controlled by a relay (on/off control) based on the value of the control error:

$$e = F_a - F_{out} - d, \tag{85}$$

where F_a and F_{out} are any of the quantities absolute humidity (AH) (used in early studies), mixing ratio (MR) (x), or water vapour partial pressure (p_w) (used in latter studies where the air temperature have significance) calculated using temperature and RH. d is a bias for safety margin (psychrometric formulas in Appendix 1).

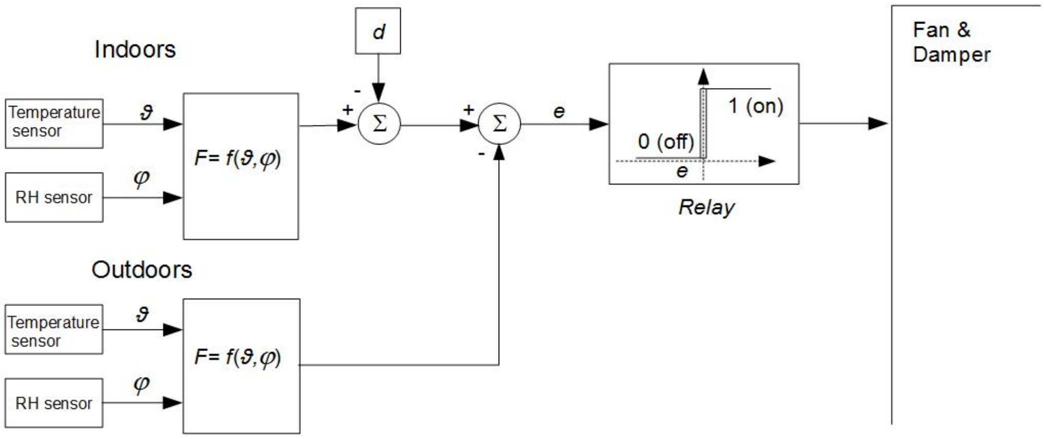

Figure 5.1. Principle of adaptive ventilation

5.2 Instrumentation

An adaptive ventilation control system can be designed on different levels. A low cost system can be designed with a small single-board computer such as Rasberry Pi[2] or Arduino[3] equipped with an IO-module connected to a relay for control of the fan. Sensors for a such system are preferably a system-on-a-chip solution (i.e., pre-calibrated integrated RH and temperature sensors on one chip). These sensor types have instrumentation amplifiers and A/D conversion embedded in the chip and the data are transmitted via I2C[4] bus interface to the single board computer. This type of sensor has become more and more used in these types of applications as they do not require instrumentation amplifiers or expensive calibration after manufacturing and assembly. For the outdoor sensor, a filter cap should be used to inhibit salt and other airborne pollutions from contaminating the sensor. In addition to the hardware, protective housing is required for the single-board computer, sensors, power modules, and cabling between computer and sensors. The hardware can be purchased for approximately 100-150 Euros, but it requires many work-hours for someone with electronics and software development skills to set up the instrument. Of course, producing such a system on a large scale would lower prices.

[2] www.raspberrypi.org

[3] www.arduino.cc

[4] www.i2c-bus.org

A perhaps more professional alternative is to integrate the adaptive ventilation system in a commercial off-the-shelf building automation system. The sensors must then be adapted for industrial interface. That is, the automation system is connected to sensors that have embedded amplifiers with industry standard 0-10 V or 4-20 mA analogue interfaces. There are combined sensor units with temperature and RH as well as pure temperature and RH units. Of course, a building automation system will be more reliable and sensors and installation material are designed and classified for outdoor use. Furthermore, a building automation system can include possibilities to store data and is also more user friendly with respect to programming although these features will make the system more expensive: as much as 10 times higher compared with the first solution. However, these added design features should lower the number of hours of engineering work required. Nonetheless, it is a low cost measure compared to the other common climate control measures.

To better understand how adaptive ventilation works in a real world setting and how it should be designed within a control system, the latter high-end configuration was developed. The AV controller was developed in LabVIEW on a PC with an NI Compact DAQ I/O chassis with modules for 0-10 V analogue automation signals, PT100 sensors, digital input with edge detection, and relay output. The Compact DAQ was connected via USB to the PC. The Compact DAQ was mounted in a cabinet together with two power supplies, one for measurements and one for control, to minimize the effect of disturbances. The outdoor sensor was a Vaisala Humicap for temperature and RH connected to a HMT100 transmitter. Between the transmitter and the LabVIEW CDAQ unit, two 0-10V analogue signal wires were connected. Indoor temperature and relative unit was measured with a Testo 6621 A01C01 with display. In addition, this unit was connected to the LabVIEW CDAQ unit with two 0-10V analogue signal wires. Four PT100 temperature sensors adapted for surface mounting were also connected to the LabWIEW CDAQ unit, only for the surface temperature measurements. The LabVIEW software saved data on the laptop hard drive with 10 minute sampling. To control the fan, a relay was connected to the NI Compact NAQ relay output modules. See Figure 5.3.

Figure 5.2. The cabinet with control equipment.

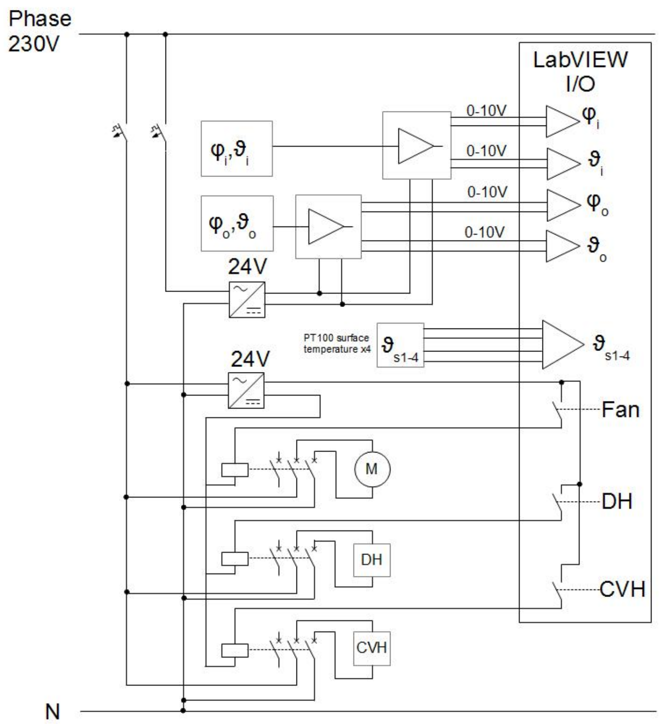

Figure 5.3. Schematic of the electrical peripheral components required for the control system.

The controller software was developed in the graphical environment from LabVIEV. See figure 5.4. The software compared indoor AH with outdoor AH, which was calculated from the respective temperature and RH sensors. A hysteresis of 0.1 g/m^3 was also implemented within the relay-based controller. In addition to the adaptive ventilation, optional controller functions were implemented that started a heater if the indoor temperature was below 5°C and started a dehumidifier if the indoor RH was over 75%. After development and programming, the control system was tested in situ in a small building to validate that the control system worked. To validate the adaptive ventilation controller, humidity tests were carried out by pouring water on the floor in the building at the same time as the system was running and comparative measurements were being carried out. The result showed that the adaptive ventilation control was running according to the requirements. In addition, the system's ability to handle power failures and its remote control (i.e., the ability to operate the PC off site) were tested. The remote control capabilities were developed using the software LogMeIn. Internet connection was established by a radio router connected to the PC. The tests revealed that the control system worked as required and was ready to be tested in real case studies.

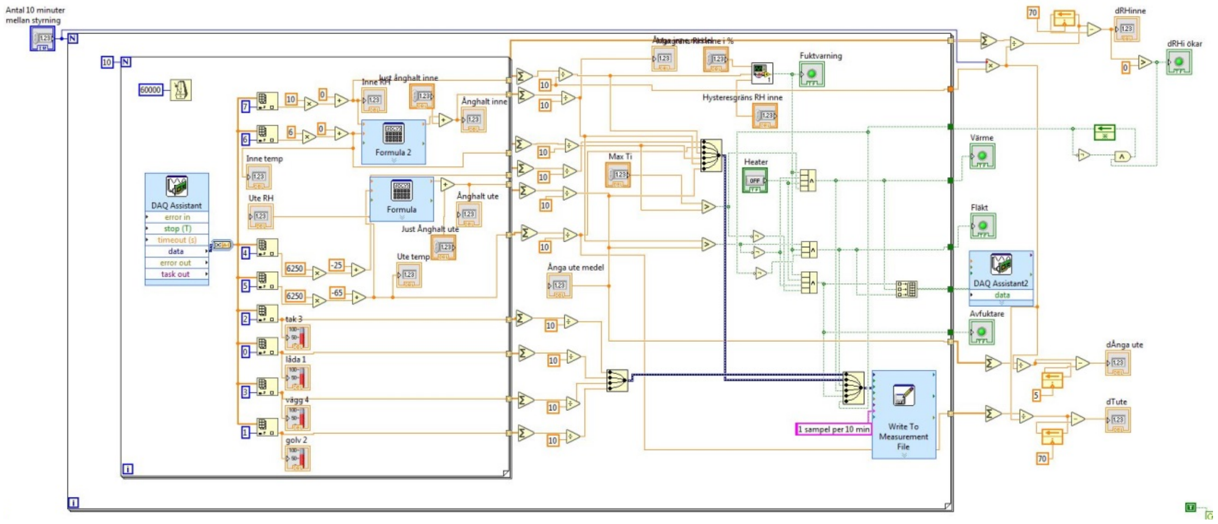

Figure 5.4. The LabVIEV software schematic for the control system.

5.3 Case study I – Klints old farmhouse

A case study in the first floor of an old split level farmhouse (Klints farmhouse) was carried out to evaluate the assembled adaptive ventilation control unit. As the split level house is partly located under ground level, the building is very humid. To validate only adaptive ventilation, this case study had no auxiliary climate control measures installed. The building used in the case study is located on the northern part of Gotland, Sweden. Built in the early part of the 18th century, the house has limestone construction with at least 60 cm thick walls. The walls are covered with lime plaster both inside and outside, with the exception of the western façade, which has no plaster on the outside. The windows are single glazed. The building was naturally ventilated, mainly through fireplaces. The building went through an extensive restoration in the 1990s after having been neglected for decades. After the restoration, the building was left unused and without any climate control. On the bottom floor of the southern part of the building (Figure 5.5, right), severe moisture problems were noticed only years after the restoration. Furniture and wooden floors show signs of wood worms and algae are growing on the walls. In the case study, an exhaust fan was placed in one of the fireplaces in the building (Figure 5.5, left). Inlet air was mainly through leakage as the flue pipes of other fireplaces were sealed (Figure 5.7). Except for the one-way damper on the fan, no controlled dampers were used. The indoor sensors where located in the same room as the extraction fan and the outdoor sensors were located in a solar radiation shield just outside the building's wall (Figure 5.6).

Figure 5.5. Left – the exhaust fan mounted in a wooden board used for sealing. Right – the investigation was carried out in the bottom floor of the left (southern) lower part of the split-levelled building.

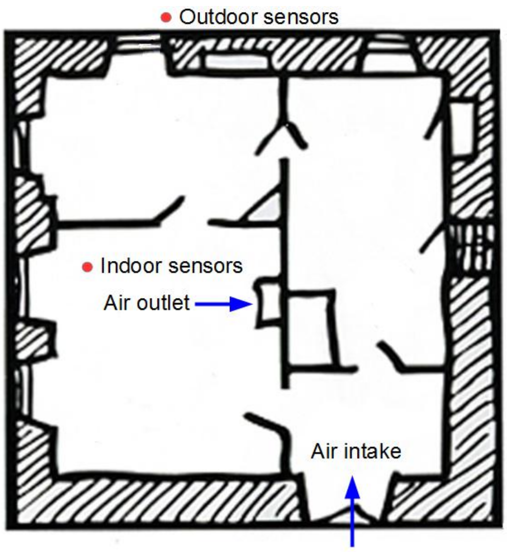

Figure 5.6. Plan over the farmhouse with indication of sensor and actuators positioning

5.3.1 Results and data analysis

The temperature and RH were monitored every 30 minutes for a year. Figure 5.7 shows the measured values of temperature and RH both inside and outside the building. A statistical summary is given in Table 5.1. The energy consumption of the fan during the test year was less than 200 kWh. Air exchange was measured using a passive tracer gas technique according to NORDTEST Method VVS118 [100]. Four measurements at different seasons gave a range of 2.3 to 3.1 air exchanges per hour.

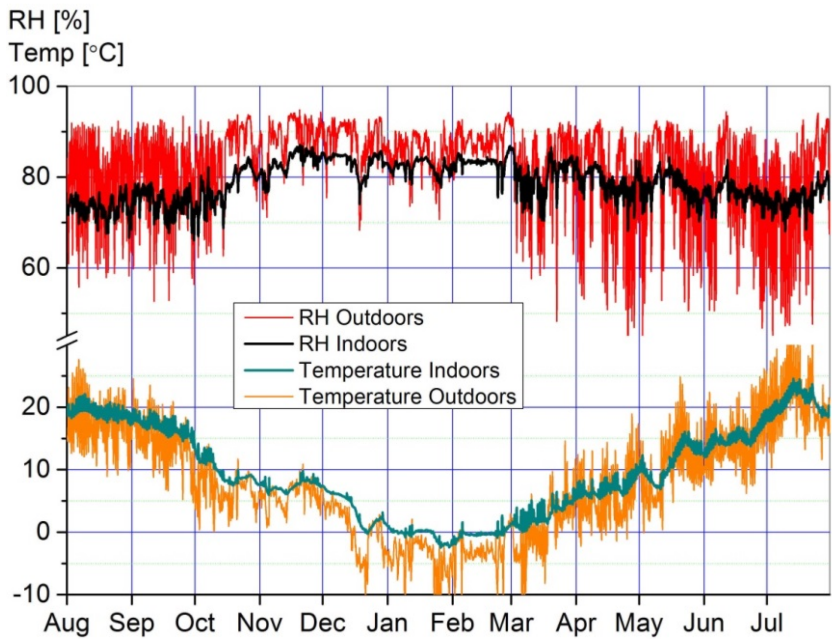

Figure 5.7. Temperature and RH in the outdoor air and in the ventilated space.

Table 5.1. A statistical summary of the indoor and outdoor climate for one year based on 30 min sampling.

	Average	Std dev	Max	Min
RH indoors (%)	79	4,2	87	66
RH outdoors (%)	82	9,1	95	40
T indoors (°C)	9,5	7,2	25	-2,5
T outdoors (°C)	7,5	8,6	33	-16
AH indoors (g/m^3)	7,7	3,2	17	3,1
AH outdoors (g/m^3)	7,2	3,6	20	1,0

The driving force of adaptive ventilation is the difference in indoor and outdoor AH. To show the long-term variations, a moving 30-day average was calculated for the difference in AH (Figure 5.8). The measurements range from -0,5 to 1,1(gm^{-3}) with an average of 0,4(gm^{-3}). This clearly indicates that there is an inside moisture source in the building. Most likely this is due to water evaporating from the building foundation and from the walls that are in contact with the foundations or are wetted by rain. Although the long-term differences are quite small, a closer look at the diurnal variations shown in Figure 5.8 gives a different picture. By taking advantage of the diurnal variation in AH, a drying effect can be achieved even during periods when the outside climate on average is more humid. Continuous ventilation would, on average, reduce the AH during most of the year. However, results in Figure 5.8 clearly show the greater drying potential of AV.

Figure 5.9 (left) shows a duration graph of the difference between the indoor and outdoor AH. Around 30% of the time, ventilation would actually increase the amount of moisture in the room. During these periods, the adaptive ventilation switches off the ventilation system. The average of the positive component is 0,99, and the average of the negative component is -0,85.

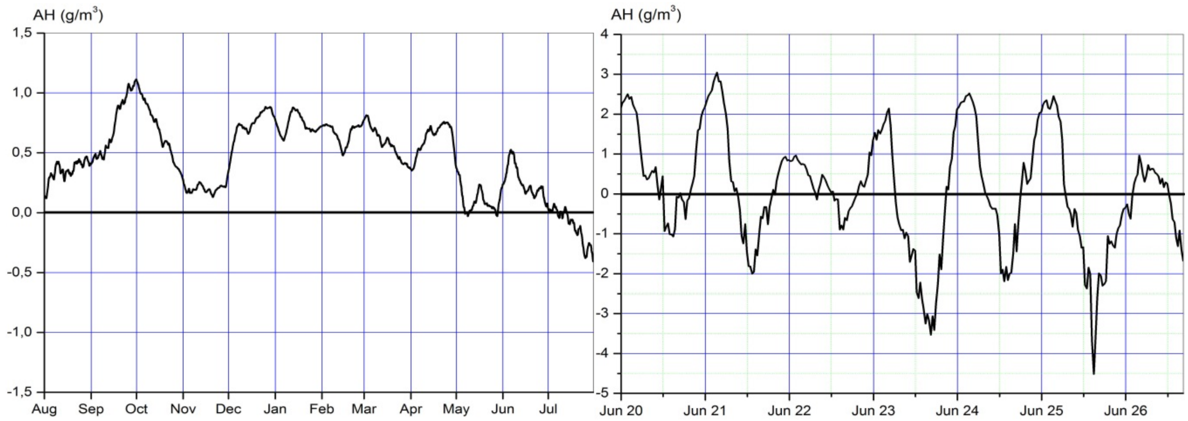

Figure 5.8. Measured difference between indoor and outdoor AH. Left – Moving 30 days average of AH indoors-AH outdoors. Right – AH indoors-AH outdoors one week in June.

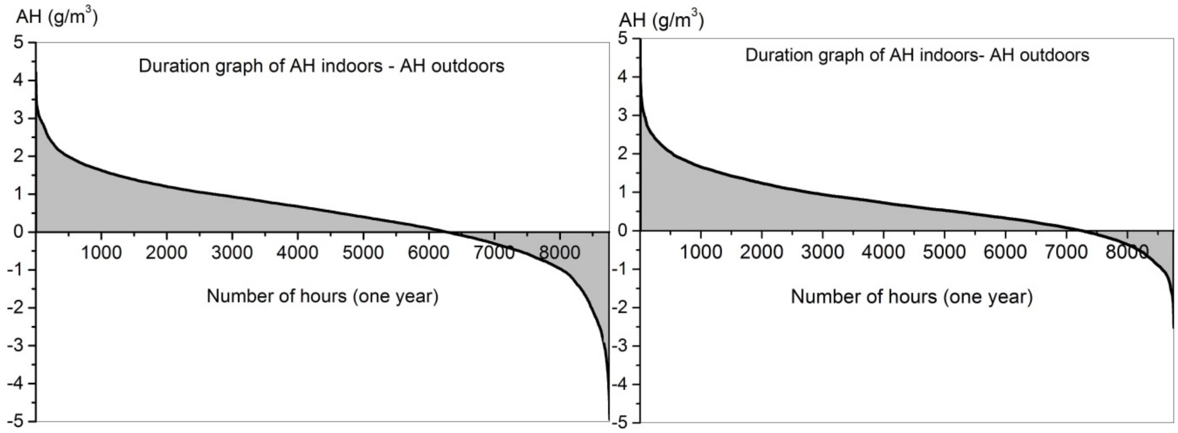

Figure 5.9. Duration graph for the difference in AH based on measurements. Left – with adaptive ventilation. Right – with conservation heating. Sampling time, every 30 minutes.

Figure 5.9 (right) shows a duration graph for the same building in 2008-2009 when conservation heating and natural ventilation were used. In this case, the average difference in AH is more than two times higher than with AV.

Based on the ventilation air flow and the actual difference in RH, an approximation of the amount of removed water from the building can be calculated:

$$RW = \int_0^{T_p} \Big(\big(x_a(t) - x_{out}(t)\big) Q_a(t) \rho_a \Big) \, dt, \qquad (86)$$

where $Q_a(t)$ is the air flow of the fan when it is running and $\rho_a$is the average density of the indoor air. During the year of the case study, some 1600 kg of water were removed from the building. The duration graph (Figure 5.9, left) shows that performance can be improved by enhancing ventilation for the positive part and improving air tightness to reduce the effect of the negative part of the curve. Even for an unheated building, ventilation has a dominant effect on the heat balance. In a typical diurnal cycle, the temperature will be lower outside when the AH is higher inside and the fan is running (Figure 5.10). This means that the ventilation has a cooling effect that would tend to increase RH even though moisture is removed at the same time.

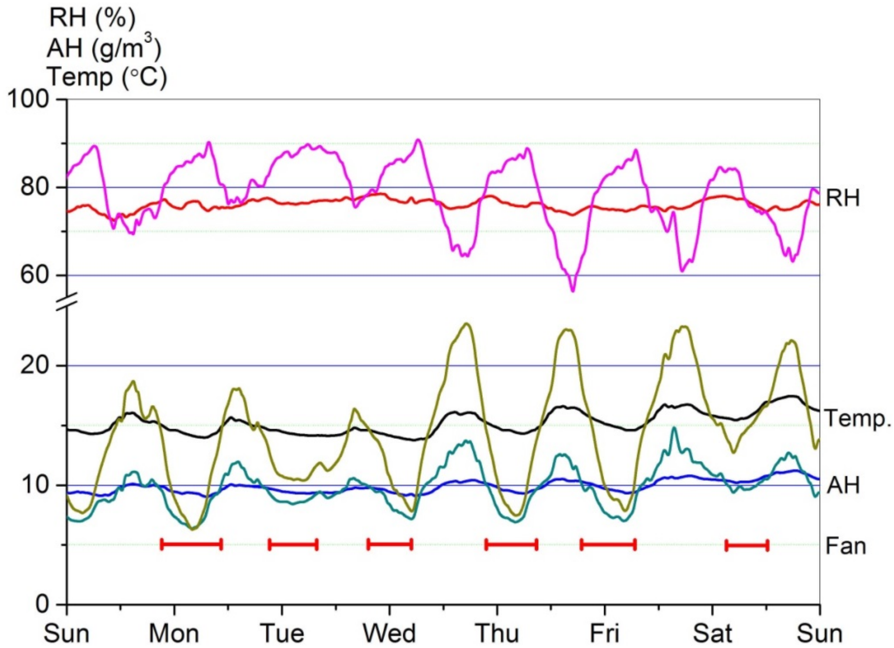

Figure 5.10. RH, AH, and temperature indoors and outdoors for one week in June. Indoor variations are small in relation to outdoors. The lowest line indicates when the fan was in operation.

With increased ventilation, indoor RH would approach the outdoor value. This is a complex phenomenon, involving the thermal inertia of the building in relation to diurnal variations of temperature as well as the long-term effects on the moisture balance and RH inside. Further investigations will aim to investigate if and how control can be improved with respect to this effect. The RH in the building shows no obvious long-term trend after ventilation was introduced (Figure 5.10). Looking closer at the daily cycles, there is no distinct pattern that shows a short-term effect on RH indoors. Gathering from experience with adaptive ventilation in attics [64] and other historic buildings, one would expect a relatively small, but significant, change in RH. Thus long-term effects on the moisture balance of the building may have to be evaluated over several years.

Consequently, the influence of RH on mould risk is assessed based on a method used in [3]. As a measure of the mould risk, a mould risk potential has been defined, which is RH divided by the critical RH – i.e., the LIM I for mould to start growing at the actual temperature [34]. Theoretically, mould growth is possible only when $RH/RH_{LIM\ I} > 1$, but as time is also important for mould to start growing, the mould risk potential must be larger than one for some consecutive time (days) before mould starts to grow. However, number of hours when $RH/RH_{LIM\ I} > 1$ makes it possible to evaluate risk for mould growth and mould control measures. The mould risk potential for the case study is shown in Figure 5.11 (left). The mould growth potential stays below one for most of the year except for short periods. Here heating or dehumidification would be needed to further reduce mould risk. To keep $RH/RH_{LIM\ I}$ below 1, auxiliary climate control would be needed for around 1400 hours (Figure 5.11, right).

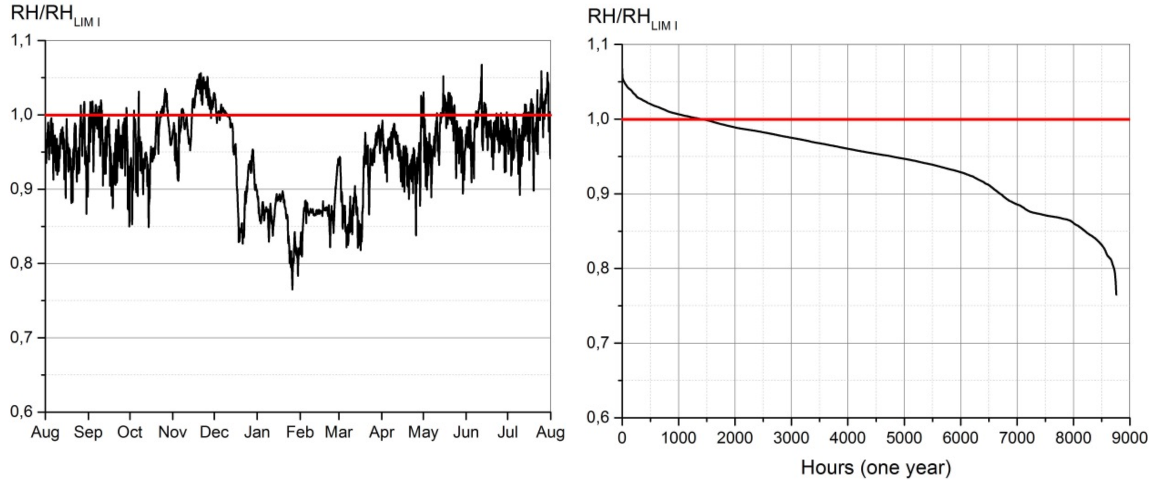

Figure 5.11. Left – mould risk during the test period. Right – mould risk represented as a duration graph.

As single periods shorter than 24 hours with mould potential larger than one are still considered safe, a deeper analysis shows that only on nine occasions did the risky events ($RH/RH_{LIM\ I} > 1$) last longer than 24 hours. If an auxiliary climate control would have been run only during those nine occasions, the number of hours would be reduced to 907. The longest consecutive period of dangerous mould risk potential was 328 hours, which is too long to be acceptable.

In Section 1.1.3, the European standard EN15757 [23] was presented. The standard specifies allowable fluctuations in RH based on historic climate and gives a method to examine, quantify, and compare RH fluctuations during a given period with another period. A fluctuation from the seasonal cycle is considered outside the safe range when the magnitude is more than 1,5 of standard deviation. Deviations of less than ±10% RH are considered safe. By definition, adaptive ventilation should enhance short-term variations in the indoor climate. In this case, both short-term and long-term variations are moderate or even small in relation to comparable buildings. Even though the building is actively ventilated during most of the year, the indoor climate is still much more stable than the outdoor climate both in the short- and long-term (Figure 5.7 and Table 5.1). The calculated range is ±3,3% RH, which is much less than the minimum level of ±10% RH suggested in the standard [23]. Thus, according to the EN15757 standard, the variations in RH are acceptable. If necessary, one could easily add a secondary control condition to reduce short-term variations in relation to the seasonal cycle. A control method based on the standard EN 15757 is presented in [9].

5.4 Case study II – Hangvar Church

From the previous case study in Klints farmhouse, it was apparent that when the outdoor air is drier then the indoor air, the outdoor air is also cooler than the indoor air. Cool air is counterproductive when it comes to lowering the RH, so the effect on RH inside a building is limited. In the short-term, this means that the ventilation has a cooling effect, which would tend to increase RH, even though moisture is simultaneously being removed from the building. This situation occurs when the MR, $x_{out} < x_a$ and at the same time as RH, $\varphi_{out} > \varphi_a$ are fulfilled. The obvious mitigation measure is to heat the inlet air a few degrees to decrease RH, thereby decreasing the mould risk. But heating inlet air is energy consuming so the new concept applied in the Hangvar case study was to let the inlet air be slightly heated with energy produced by solar panels placed just outside the churchyard's wall.

The concept operates as follows:

1. In the day time, solar energy is collected and stored.
2. At night, when the outside air generally is drier but also cooler, the inlet air is preheated using the stored energy.

The system can either be electric (photovoltaic) or thermal depending on costs and practical aspects. In this study, considering the installations and other practical aspects, an electric system was used. Solar energy was seen as a sustainable solution both in terms of resource use and economy and the parish's requirements. Of course, preheating can also be achieved by conventional means.

Hangvar Church is a 13th century stone church situated on the northwest Gotland, Sweden. The construction is typical for Gotland churches with outer walls and vaults made of limestone and lime mortar and a roof construction of wood and tiles. The volume of the nave and chancel in total is 1000 m^3. The church is used about ten times per year, mostly for funerals and weddings. The church is intermittently heated for services and unheated when not used. The church has been very humid. During spring, condensation forms on the walls and floors. In the winter, the indoor temperature can drop below 0ºC and in July gate as warm as 20ºC, but typically the temperature rarely exceeds 18ºC. The members of the parish have complained about bad smells and algae and mould is evident in corners and on the northern wall. Many tourists visit the church during summer and the church door is often left open in the day time.

To improve the indoor climate conditions, the adaptive ventilation system was installed in the church. A vent pipe was installed from an opening in the tower staircase to the fan and then through a new temporary tower door with built-in exhausts (Figures 5.12. and 5.13). Air was exhausted through leaks in the building envelope and the doors.

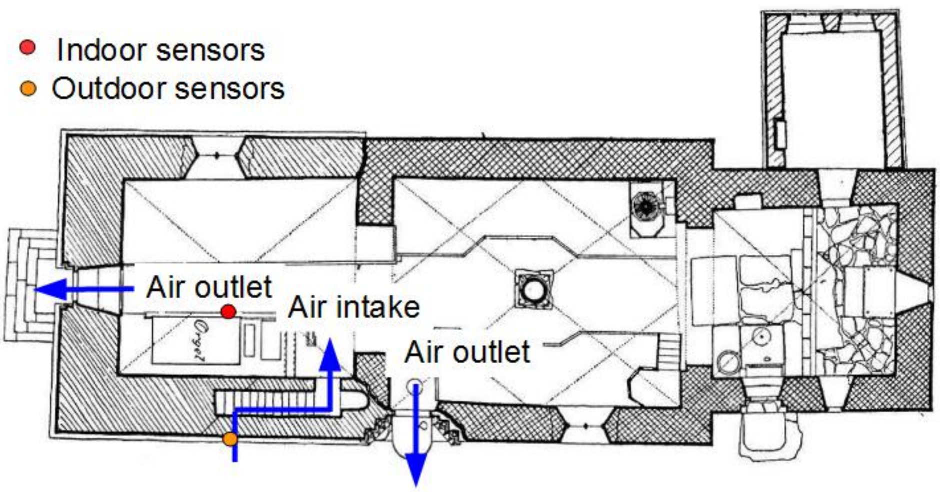

Figure 5.12. Floor plan for Hangvar church with indication of sensor and actuator positions.

5.4.1 System

In this study a commercial system originally developed for ventilation of attics were used. The fan had a capacity of 500 m^3 per hour. The indoor sensors for RH and temperature were located in the rear part of the church. The outdoor sensor was located close to the air intake in an opening in the church wall. The control unit was programmed to compare indoor and outdoor water vapour partial pressure with a ratio instead of a difference. The fan was thus running if the ratio between indoor and outdoor water vapour partial pressure were larger than 1,05. A hysteresis of 0,05 was also implemented:

$$F_{p_w}\left(\frac{p_{wa}}{p_{wout}}\right) = \begin{cases} 1, \text{if } \frac{p_{wa}}{p_{wout}} > 1{,}05 \\ 0, \text{if } \frac{p_{wa}}{p_{wout}} < 1{,}05 \end{cases}. \tag{87}$$

The control system had no other limits for the inside RH, but there was a lower limit of -10˚C for the outside air temperature – i.e., if the outdoor temperature were lower than -10˚C, the fan stopped. The inlet air duct had two electric heaters with a total power of 1800 W. At the given air flow, when the two heaters were on, it gave a temperature increase $\Delta\vartheta$ of the inlet air of 11 ˚C.

Figure 5.13. Left – the air intake and outdoor sensor. Middle – the fan and the flexible air duct. Right – the new temporary tower door.

The case study was designed for 25 m^2 of photovoltaic elements, but due to costs, heritage regulations and the fact that this set up was experimental, only 5 m^2 were installed. Therefore, the amount of produced energy was multiplied by 5 in the control system. The photovoltaic elements were placed outside the church yard to avoid a discussion on the visual impact of roof placement (Figure 5.15). In this case, the electric grid was used to store the energy rather than local storage. A commercial off the shelf DC to AC converter was connected between the photovoltaic panels and the grid via an energy meter that was connected to the control system (Figure 5.14).

The heaters were controlled by a control system developed in the LabVIEW environment on a PC with an NI Compact DAQ I/O chassis with modules for PT100 temperature sensors, digital input with edge detection, and relay output. The Compact DAQ chassis was connected via USB to the PC. The energy meter that measures the produced solar energy sends 1000 pulses per kWh, and the edge sensing LabVIEW module detected and counted pulses from the energy meter .The system software could thus keep records of both energy produced by the voltaic panels and the energy consumed by the heaters. Consumed energy was not measured but calculated in real-time by the system. Therefore, the total amount of stored energy produced by the photovoltaic elements could be compared with the total amount of energy consumed by the heaters.

A signal, *AV Running*, indicating when the fan was running, was connected to a digital input on the control system (Figure 5.14). The heater was turned on only if this signal indicated and the energy difference between produced energy and consumed energy was larger than zero. In this way, the heaters only consumed stored energy produced from the voltaic panels. A problem that occurred was the frequent power grid failures, resulting in LabVIEW losing data when the PC shut off. The solution was to program the LabVIEW software to store all data on the PC's hard drive device every 10 minutes and to make calculations using the most recently-recorded data.

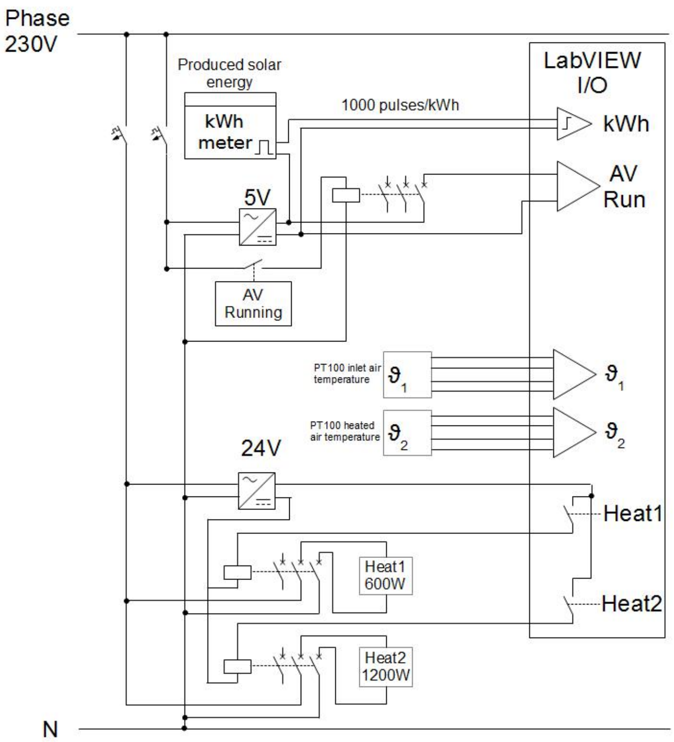

Figure 5.14. Electrical schematic of the peripheral circuits for the heating system.

Figure 5.15. Hangvar church and the photovoltaic elements placed outside the church fence.

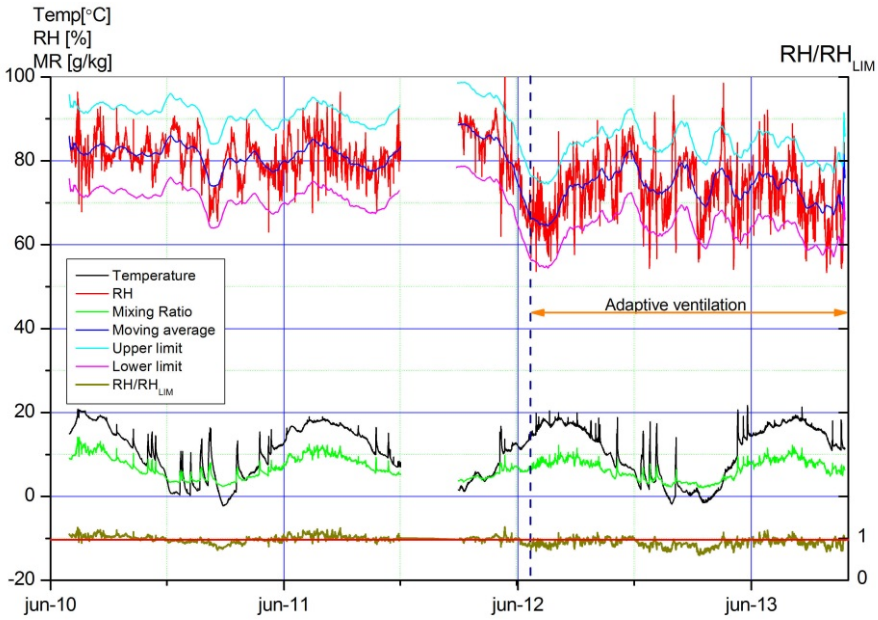

Figure 5.16. Indoor climate in Hangvar church. The graph shows that during the period with adaptive ventilation the RH on average has decreased, but the variations have increased.

Table 5.2. Statistics for the two periods

Period	Average Temperature	Average RH	Average MR	Standard deviation of short term fluctuations SD30
Without climate control	9,6	81	6,5	3,5
Adaptive ventilation	9,3	75	5,9	5,2

5.4.2 Results and analysis

From July 2010 to June 2012, there was no climate control in the church except for the intermittent heating periods for services. Solar augmented adaptive ventilation was installed in July 2012. There was no climate monitoring between December 2011 and March 2012. Figure 5.16 shows indoor climate over three years: The average RH decreased after the introduction of adaptive ventilation, but the short-term variations increased.

Table 5.2 shows a statistical comparison between the period without any climate control, September 2010 to August 2011, and the period with adaptive ventilation, September 2012 to August 2013. The comparison shows that average RH decreased from 81 to 76%. The average temperature was approximately the same in the two periods, with only 0.2 degrees of difference. The short-term variations in RH are important from a conservation point of view. Deviations of less than ±10% RH are considered safe. Figure 5.16 shows that when using adaptive ventilation, there are more short-term excursions outside the target range, which can be considered as a negative feature for increasing risk of mechanical damage of wooden objects. The standard deviation, in relation to the moving average, increased from 3,5 to 5,2%.

Two methods were used to measure the church's air tightness (August 2013). The blower door test [89] showed a result of Q_{50} = 0,89 L/s/m^2 and the pressure pulse method [90] showed for a resulting equivalent leakage area at 4 Pa of 0,051 m^2. Both methods showed a result of Q_4 = 138 L/s, which is on the same order of magnitude as adaptive ventilation. However, this result is regarded as a relatively air tight church.

In the next step of the analysis, mould risk was assessed in relation to the isopleth curve LIM I for biologically recyclable building materials [34]. Figure 5.17 (left) shows the period without climate control and Figure 5.17 (right) shows the period with adaptive ventilation. It is clear that the risk for mould has decreased during the year when adaptive ventilation was used. The year without climate control, 44% of the overall time, the indoor climate was above the LIM. When the adaptive ventilation system was running 16.7% of the time the indoor climate was above the LIM. Thus, the adaptive ventilation improved the indoor climate in this aspect.

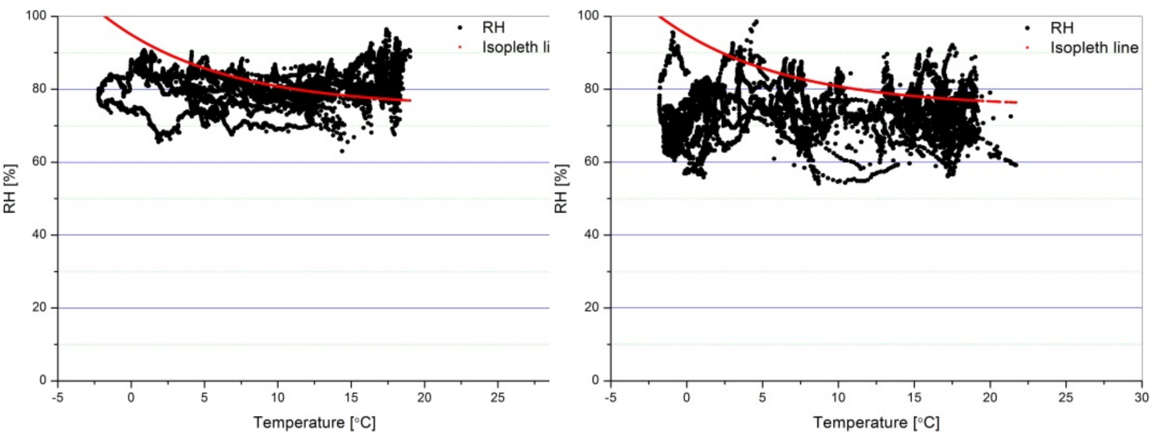

Figure 5.17. Damage functions for mould growth. Left – time period without climate control. Right – time period with adaptive ventilation.

Figure 5.18 shows RH/RH_{LIM} where RH_{LIM} represents the RH values corresponding to lowest isopleth for mould that can be seen in Figure 5.17. If the value is above 1, the climate is beneficial for mould growth. The duration in the area above LIM is critical for mould growth. According to [34], RH/RH_{LIM} has to be above 1 for longer periods (days) for mould to grow. In the year without climate control, the average duration length above LIM was 72 hours and the longest period was 826 hours. In the year with adaptive ventilation, the average was 32 hours and longest period was 134 hours. In the latter case, the extended periods were in the summer. Consequently, the overall duration graph in Figure 5.19 shows that even small changes in the RH levels have a significant impact on climate control requirements. The figure shows the duration graph for RH/RH_{LIM} for the year with adaptive ventilation (black) and the year without (red). If the requirement is $RH/RH_{LIM} < 1$, the time of operation for auxiliary climate control was 1450 hours in combination with adaptive ventilation, and the time of operation for auxiliary climate control was 3750 hours the year without AV. Therefore, the number of hours with mould risk was reduced by 2300 hours.

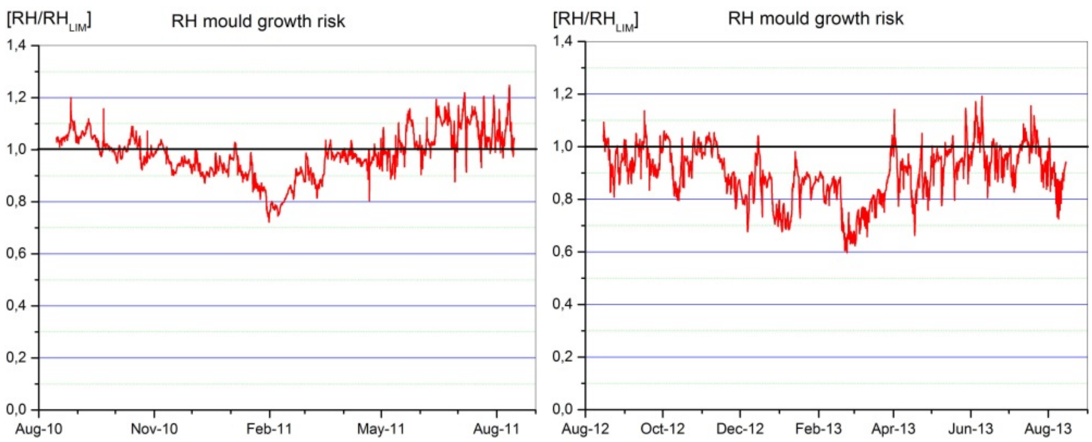

Figure 5.18. RH/RH_{LIM}. Left – time period without climate control. Right – time period with adaptive ventilation.

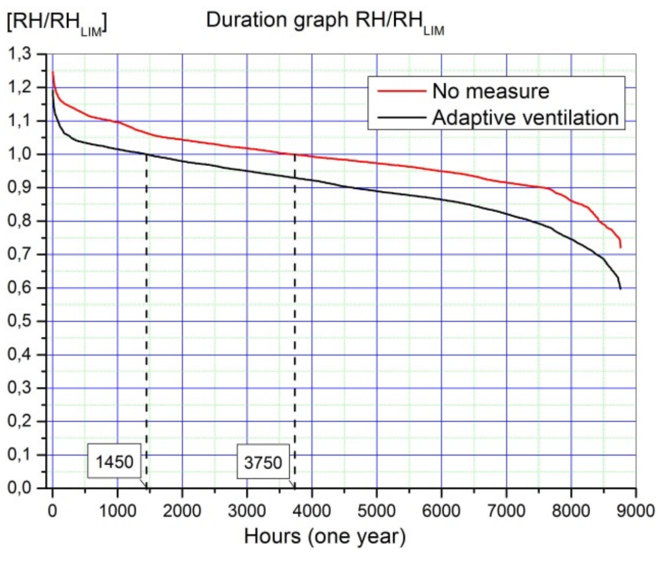

Figure 5.19. Duration graph of RH/RH_{LIM}.

Based on the difference between RH indoors and outdoors every hour and the air flow, the total moisture transport during the test period is calculated with equation (86). From September 2012 to August 2013, 1100 *kg* of water was transported out of the church. The ventilator consumed 250 kWh of electrical energy during the same period. This gives a drying efficiency of 4.4 kg water per kWh.

The inlet air heaters were used only when stored solar energy was available and the ventilator was running. In October, November, December, and half of January the 25m^2 'nominal' photovoltaic panels did not produce enough energy for preheating the whole time when the ventilation was in operation. In the rest of the year, the produced energy was larger than the amount of consumed energy (Figure 5.20).

From September 2012 to August 2013, the 5m^2 photovoltaic panels produced 645 kWh, thus the 'nominal' panels of 25m^2 produced 5 × 645kWh = 3 225 kWh. The amount of energy used for the inlet air heaters was 2 066 kWh. When the fan was running at full speed, the heaters gave a temperature difference of 11°C. When solar energy was available, this has generally been sufficient to counteract or mitigate the cooling effect without causing any harmful temperature variations. In January 2013, there was no solar energy available. During one week, the adaptive ventilation ran without preheating and the indoor temperature decreased by 6°C. At the same time, the MR decreased, but RH was still around 65%.

Concerning the user perspective, the church's indoor air quality improved after installation of AV. 'Bad smell' was no longer a problem. Because the fan was too loud to operate during services, it was manually turned off for the duration of the services. Overall, the parishioners were positive towards this solution and want to make it permanent.

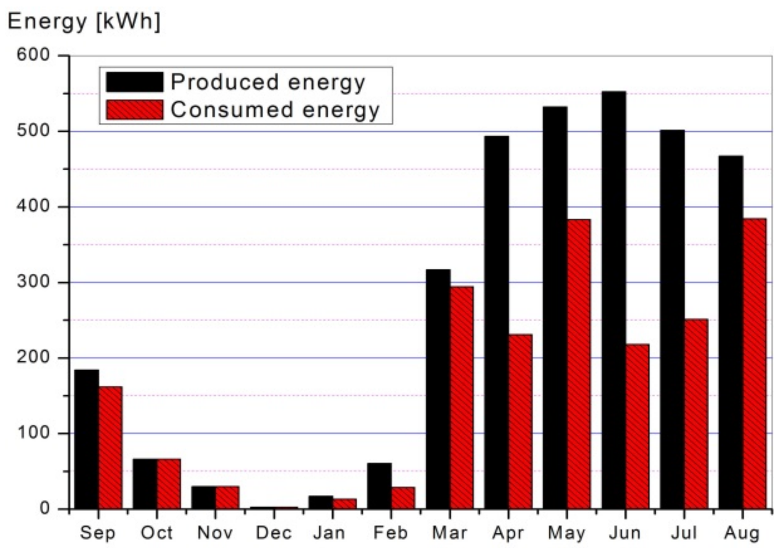

Figure 5.20. Monthly produced and consumed solar energy.

5.5 Conclusions on Adaptive Ventilation

In the two case studies, adaptive ventilation has had a significant drying effect, removing about 1600 kg of water in Klints farmhouse and 1100 kg in Hangvar church in one year. The mould risk was kept at an acceptable level with exception of some periods. Concerning the RH fluctuations, AV considerably increased a number of events when the fluctuation peaks were above the ±10% RH with respect to the moving average proposed in the standard EN 15757. This can be considered as a negative aspect, but this can be removed by adjusting the control algorithms.

The members of Hangvar parish judged that the indoor air quality improved, mainly in the elimination of bad smell. In these two case studies, adaptive ventilation is not sufficient to eliminate mould risk throughout the whole year; however, it does significantly reduce the operational time and energy demand for auxiliary measures such as dehumidification or additional heating. The results presented in this paper are from one year of operation. Over a longer period, the massive structure is expected to slowly become dryer thus reducing indoor RH levels.

Adaptive ventilation is a low-cost and low-energy option as compared to conventional humidity control. The annual energy consumption for the operation of the fan in Hangvar church was only 250 kWh. This gives an efficiency of 0,22 kWh/kg of exhausted water, which is about a tenth of energy per kg compared to conventional dehumidifiers. The preheating of the inlet air in Hangvar church counteracted the cooling effect, which was reported in the Klints study and other previous studies. However, during one year, the contribution from the solar panels was 2000 kWh, which is not economically viable unless the solar panels are subsidised. During the winter, the amount of energy produced by the solar panels was not enough to heat the inlet air; however, during the summer, the system used a fraction of the energy the solar panels produced.

Both case studies confirmed that adaptive ventilation is particularly useful when there are internal moisture sources in the building, resulting in absolute humidity levels higher than outside. This situation is quite common in historic buildings due to evaporation of moisture from the floor or through the walls.

Generally, adaptive ventilation is best suited for unheated or occasionally heated buildings. For buildings with constant comfort or conservation heating, more elaborate control strategies are needed. A general problem with adaptive ventilation in historic buildings is achieving sufficient air tightness. The air tightness measurements in Hangvar church indicate that the air leakage may be of the same order of magnitude as the fan air flow. In Klints farmhouse, air leakage was larger. The effect of the ventilation can be improved by increased fan capacity and improving air tightness to reduce leakage when the fan is not in operation.

Given the complex interaction between the thermal inertia and the RH and T of the incoming air, control by water vapour partial pressure rather than RH has proven to be a robust method. Further research will investigate the effect of the hygrothermal inertia of the building, long-term effects on the moisture balance, the potential for improving performance, and the further integration of heating or dehumidification.

In summary, the two case study experiments reveal several pros and cons of the adaptive ventilation. These are presented below.

Positive aspects:

- substantial reduction of mould risk;
- low-cost and low energy demand;
- non-invasive technical installations;
- improved indoor air quality as perceived by people;
- reduction of indoor temperature during hot periods.

Negative aspects:

- increase of RH short-time fluctuations;
- function is highly dependent on outdoor conditions;
- decrease of indoor temperature in winter months; and
- needs auxiliary measures (i.e. heating or dehumidification) to fully prevent mould risk.

5.5.1 Overall recommendation on AV implementation and its enhancement

Adaptive ventilation is a useful measure to lower RH in unheated historic buildings and occasionally heated buildings, especially when there are internal moisture sources in the building such as rising damp or humid walls due to precipitation. AV prevents mould growth by decreasing the number of hours with mould risk; however, for part of the year, the measure will probably be insufficient. As it is mentioned in Section 5.5, the dehumidification capacity depends on appropriate outdoor climate. To improve the technique (and the indoor climate), the following actions should be considered.

During cold periods, the outdoor air is mostly dry (in absolute terms); however, there are often some occasions between October and December where the risk for mould growth increases (i.e., $x_{out} < x_a$ but $\varphi_{out} > \varphi_a$). This means the MR in the indoor air will decrease but the RH will still increase On those occasions, the best measure is to combine adaptive ventilation with conservation heating – i.e., to heat the in inlet air a few degrees to mitigate the decreased temperature, which increases RH. According to [49], a temperature increase of about 2-6 °C mitigates the increased RH. As it was shown in Section 5.4.3, the energy consumption is low for that measure.

Between May and September, the outdoor air contains more humidity and the outdoor climate can be disadvantageous for adaptive ventilation. During this period, a portable condensing dehumidifier with embedded water tank controlled by mould growth control is recommended. If this method is used, an auxiliary dehumidifier will run only when the adaptive ventilation is unable to keep down the risk for mould growth.

A larger ventilating system will increase the dehumidification capacity, but it will also increase the fluctuations in RH. A larger system must thus be combined with a more advanced control system that controls the fan not only using the difference in indoor and outdoor air moisture content but also differences in RH level and RH change rate. A speed control of the fan can be used, and in this case conservation heating is useful for limiting the RH fluctuations. Finally, it is very important for buildings using AV to be airtight as the positive effect of adaptive ventilation will effectively be counteracted by a leaky envelope.

6 Comparison of control methods with the emphasis on mould growth

One significant climate-related problem in massive historic buildings is high levels of relative humidity (RH) that cause mould growth. To mitigate these high humidity levels, conservation heating and dehumidification have been used with good results on the indoor climate. Additionally, adaptive ventilation, which is analysed in the previous chapter, has emerged as an energy-efficient measure that could be a candidate for mould growth prevention. Studies on adaptive ventilation and dehumidification have been carried out before as outlined in the state of the art section. A new aspect of the presented analysis is cross-comparison of the methods with respect to mould prevention. The applied measures will be controlled in a way to mitigate mould growth while keeping the energy demands as low as possible. The objective of this section is thus to evaluate these three climate control measures for lowering RH to prevent mould growth in massive historic buildings in terms of energy efficiency, mould prevention effectiveness, and stability. This requires a case study in a real massive historic building where the three climate control measures can be compared and evaluated. This section is an extension of published papers [7] where the PhD candidate is the main author. This section also includes results presented in 'Built Cultural Heritage in times of Climate Change' [8] and Deliverable report D7.1.2; 'New algorithms for optimal control of relative humidity' [11] of the FP7 European project Climate for Culture, which the author contributed to. The section is organized as follows. Sections 6.1 – 6.4 presents mould growth control. Sections 6.2 and 6.3 presents simulations of mould growth control and compares traditional humidity control in terms of energy efficiency. Section 6.4 describes a case study in Fide church where mould growth control was implemented and tested. Section 6.5 presents a comparative study of three different climate control measures in Skokloster castle.

6.1 Mould growth climate control using isopleths

Traditionally, when a climate control measure is installed to mitigate mould growth, the RH set-point is often set to a constant level 5-10% below 75%. This approach, however, is unnecessarily restrictive and will cause higher energy consumption than needed. By using a predictive criterion for mould growth, a set-point strategy can be developed for climate control. To assess the climate induced risk for mould growth in a building, Sedlebauer et al. have developed a predictive model [34] that describes mould fungus activity dependence on hygrothermal conditions allowing for the prediction of mould growth based on surface temperature and RH. The growth conditions for mould are nutrients, warmness, and RH, which must exist simultaneously for a certain period. The growth conditions are described in the so-called isopleth diagrams, as outlined in the state of the art section. These diagrams describe the germination times or growth rates (Figure 6.1). Recall that the resulting lowest boundary line of possible fungus activity is called LIM (Lowest Isopleth for Mould). LIM I, which according to Sedlebauer, is the lowest isopleth for mould growth on biological recyclable building materials (Figure 6.1) [34].

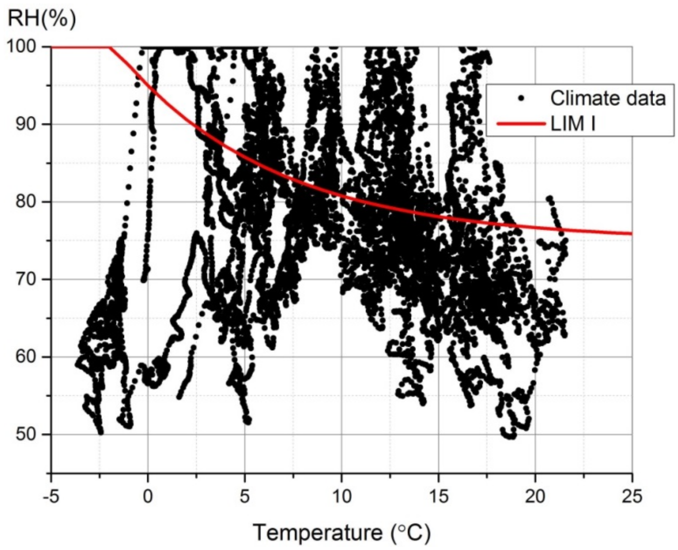

Figure 6.1. The red curve shows the Lowest Isopleth for Mould, LIM 1. Data from simulation of Hangvar church.

The LIM I curve in Figure 6.1 can be approximated by the following exponential function

$$\varphi(\vartheta) = f_{\varphi}(\vartheta) = 75 + 20\mathrm{e}^{-0{,}1241\vartheta}. \tag{88}$$

All the temperature and RH $[\vartheta, \varphi]$ combinations in Figure 6.1 positioned below the LIM boundary red line are considered safe with regard to mould growth. However, the isopleth is based on empirical research and the damage risk cannot be determined exactly in absolute numbers. Furthermore, when working with microclimate in historic buildings, microclimate can vary within a room. For example, if the climate is measured in the middle of a room, the temperature can be a few degrees higher or lower on the walls, ceiling, and floors, affecting the RH in these spots. If the LIM I isopleth is used as the set point for climate control, it requires a safety margin to be sure to avoid damage within the whole interior.

One possible mitigation measure against mould growth is dehumidification. The control objective is to keep the microclimate conditions in the safe region (Figure 6.1). This can be achieved by adjusting the set-point value of the dehumidifier, φ_{set}, based on the current (measured) temperature, ϑ_m, as

$$\varphi_{set}(\vartheta_m) = f_{\varphi}(\vartheta_m) = 75 + 20\mathrm{e}^{-0{,}1241\vartheta_m} - d, \tag{89}$$

where d is a bias, $d > 0$, which should guarantee that the humidity stays safely below the line given in Figure 6.1. The overall control scheme implementing the given control objective is shown in Figure 6.2. As can be seen, the dehumidifier is controlled by a relay (on/off control) based on the current value of control error:

$$e = \varphi_{set}(\vartheta_m) - \varphi_m, \tag{90}$$

where $\varphi_{set}(\vartheta_m)$ is given by (89) and φ_m is the actual value of the measured RH. In assessing the parameter d, one needs to consider the hysteresis of the relay h (usually 1-5% RH), such that $d \geq h$. The temperature measurement readings could be filtered by a low pass-filter (e.g., Butterworth seconds-order filter with cut-off frequency $\omega \in [0{,}2; 1]\ \mathrm{h}^{-1}$) with the objective to decrease the effect of projecting the short-time fluctuations of temperature to the generated RH set-point value. However, in many historic buildings, the short-time temperature fluctuations are limited due to the heavy building construction.

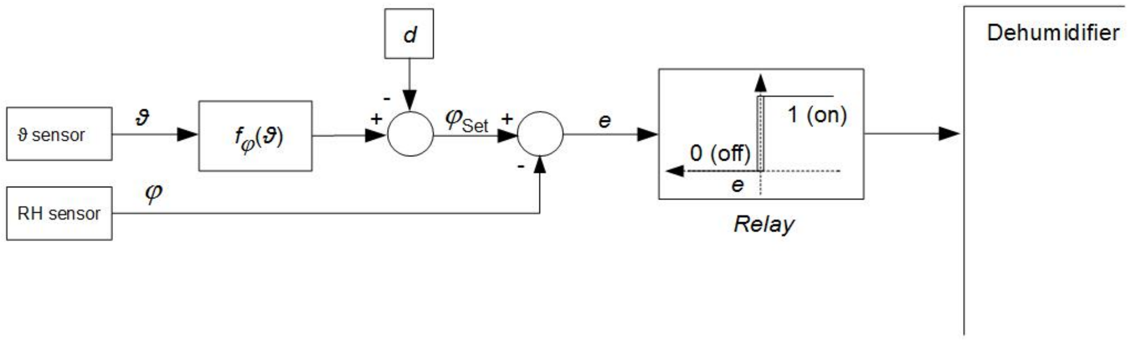

Figure 6.2. Control scheme to keep the microclimate in a safe region against mould growth using dehumidification.

6.1.1 Simulation analysis on Hangvar church model

The designed microclimate control method is demonstrated by simulation tests with the hygrothermal model for the Hangvar church on Gotland, Sweden, which was implemented in Hambase tool [92] and parametrized based on the measured data. The model and its parameters are described in Appendix 2.

In Figure 6.3, simulated (ϑ, φ) indoor data points of one year are shown in the subject to the given mould growth damage function. A large number of data points are found above the LIM I transformed to the figure scale by (88). Thus, according to the model and the given climate conditions, the risk of mould growth in the church is very high. Implementing the control algorithm (89), (90) and Figure 6.2, with hysteresis $h = 2\%$ and bias $d = 2\%$ controlling a model of a sorption dehumidifier (described in the Appendix 2) used together with the model of the church, the microclimate simulation data shown in Figure 6.4 are obtained. In Figure 6.4 (right), the simulated running hours by dehumidification are shown. The number of hours for one year is 915h. As can be seen in Figure 6.4, almost all the data points are now located below the boundary of the risky region. The couple of points located above are due to very rapid indoor climate changes, which the dehumidifier could not handle. Thus, the implementation of the humidity control specified above would prevent mould growth.

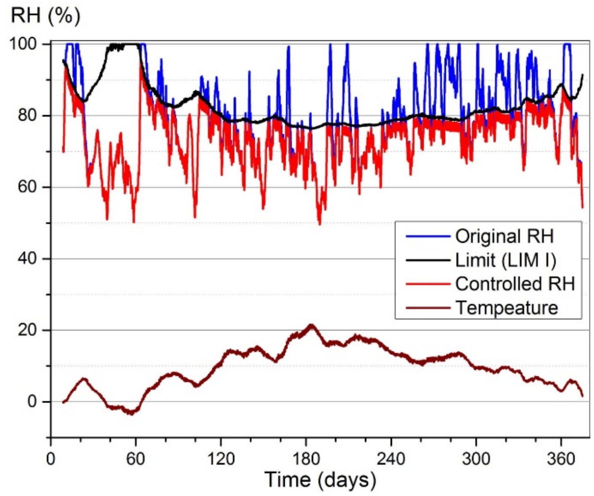

Figure 6.3. Results of RH control according to scheme in Fig. 2 with $h = \pm 2\%, b = 2\%$.

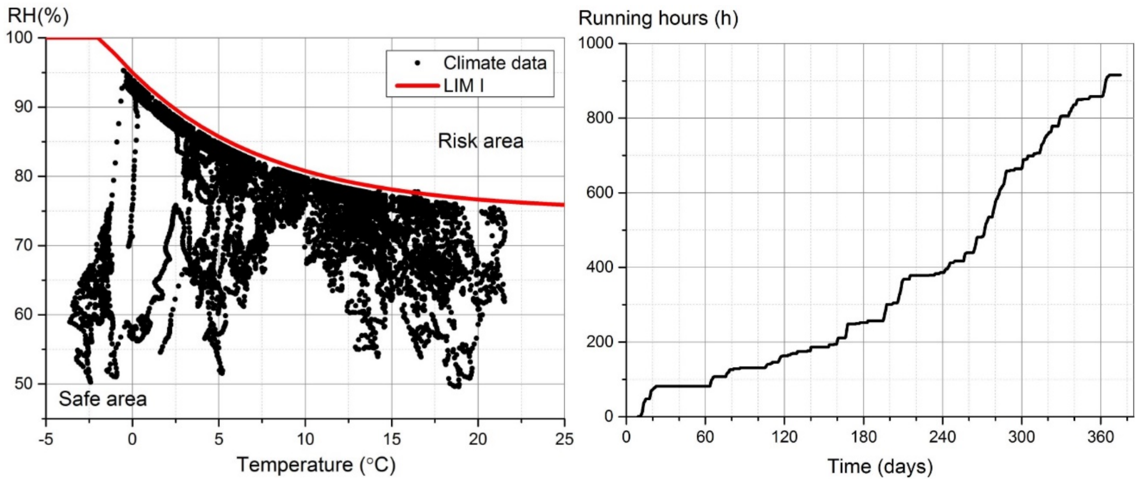

Figure 6.4. Left, simulated $[\vartheta, \varphi]$ data points of one year period of mould growth damage function under the humidity control according to Figure 6.3. Right, running hours for dehumidification.

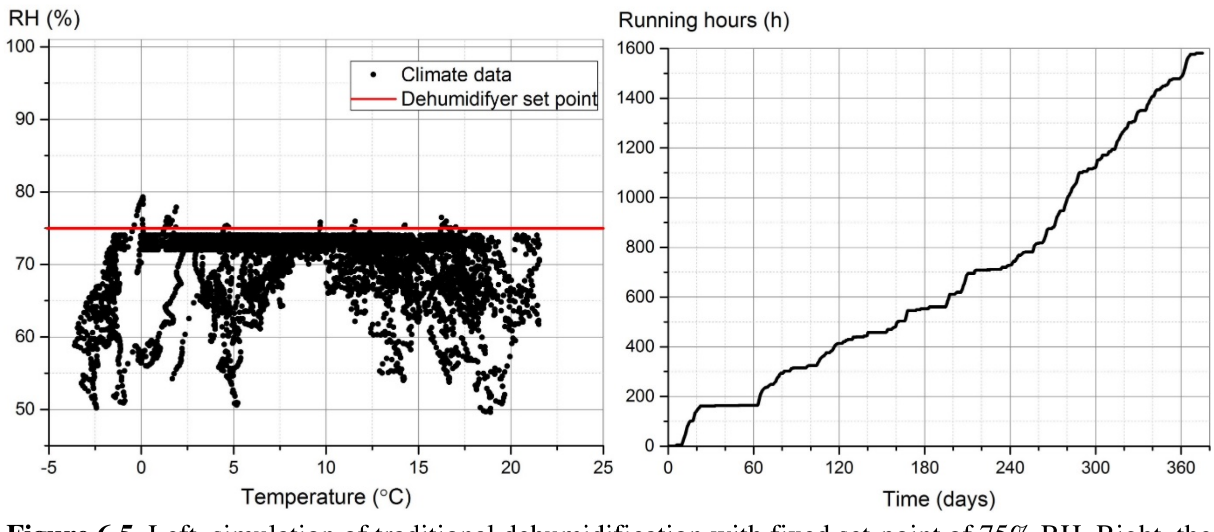

Figure 6.5. Left, simulation of traditional dehumidification with fixed set-point of 75% RH. Right, the number of running hours with traditional dehumidification. Set point 75% RH.

To compare the result of mould growth control with traditional dehumidifier use, a new simulation was carried out with a fixed RH set point of 75% with the same model of a sorption dehumidifier. Figure 6.5 (left) shows the result of dehumidification and Figure 6.5 (right) shows the number of running hours. The runtime for this setup was 1581h, which is 72% more compared with the mould growth control. To conclude, the adjustment of the RH control proposed in the previous section can bring substantial energy savings, compared to the traditional dehumidification to a fixed RH value.

6.2 Case study in Fide church

A case study on mould growth control was carried out in Fide church during one year from March 11 to March 11 the following year. A dehumidifier (DR-010B) with nominal capacity of 0.5 (kg/h) was installed in the organ loft and the dehumidifier was controlled with the Culturebee system [93], a wireless measurement and control system based on ZigBee-technology, which was evaluated and tested by the author. Mould growth climate control was implemented according to equation (89) and the set point for the dehumidifier was implemented according to equation (88). The bias was at first set to $d = 0\%$ and the hysteresis $h = 1\%$. The capacity of the dehumidifier was too small and therefore a larger dehumidifier (DR-020) with nominal capacity of 0,8 kg/h was installed in mid-September. To achieve a larger safety margin, the bias was adjusted to $d = 7\%$ and the hysteresis was set to $h = 2\%$. Figure 6.6 shows the *temperature-RH* diagram for the case study. The black curve represents the period from March to September, when the dehumidifying capacity was too small. The green curve represents the period from September to March, when the larger dehumidifier was installed. In connection with services, the church was heated and the dehumidifier was turned off to avoid noise. As a consequence, RH increased on one occasion to risky levels. The total running time of the dehumidifiers was 4340 hours during the year. It would have been less if a dehumidifier with a higher capacity had been installed from the beginning.

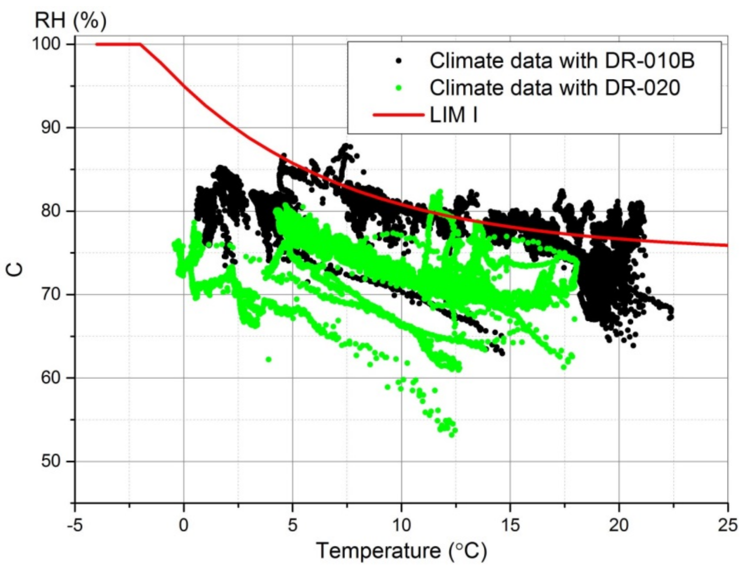

Figure 6.6. Black – climate data from March to mid-September. Green – climate data from mid-September to March.

6.3 Comparative study in Skokloster Castle

The Skokloster castle study compares three RH-reducing technologies used to minimize the long-term risk for mould growth with minimum energy use [51]. Hence, the objective of this study is to evaluate and compare in situ the relative performance of these technologies in terms of mould prevention, energy consumption, and indoor climate stability of conservation heating (CH), dehumidification (DH), and adaptive ventilation (AV).

The study was carried out at Skokloster castle, a unique Baroque palace museum (Figure 6.7). Most the objects in the collection, which is dominated by objects from the 17th century, are on display in their original historic setting. A series of detailed inventories beginning in 1716 reveal the status of individual objects. The castle has been a state-operated museum since 1967, is mainly open during summer, although there are occasional guided tours in winter.

Due to a massive and relatively leaky building envelope, the indoor climate is characterized by high thermal inertia and high and unstable RH [10]. The upper floors of the castle have been unheated for centuries. A few rooms on the ground floor are permanently heated to provide thermal comfort for staff and visitors. An increase of mould growth, especially in rooms facing north, has called for preventive indoor climate control. In the 1990s, it was decided that to reduce the risk for mould growth it would be beneficial to increase the air exchange rate. The chimneys, packed with centuries of old bird's nests, were cleared out to increase the infiltration of outdoor air. The doors in rooms with mould problems were kept open to provide more ventilation.

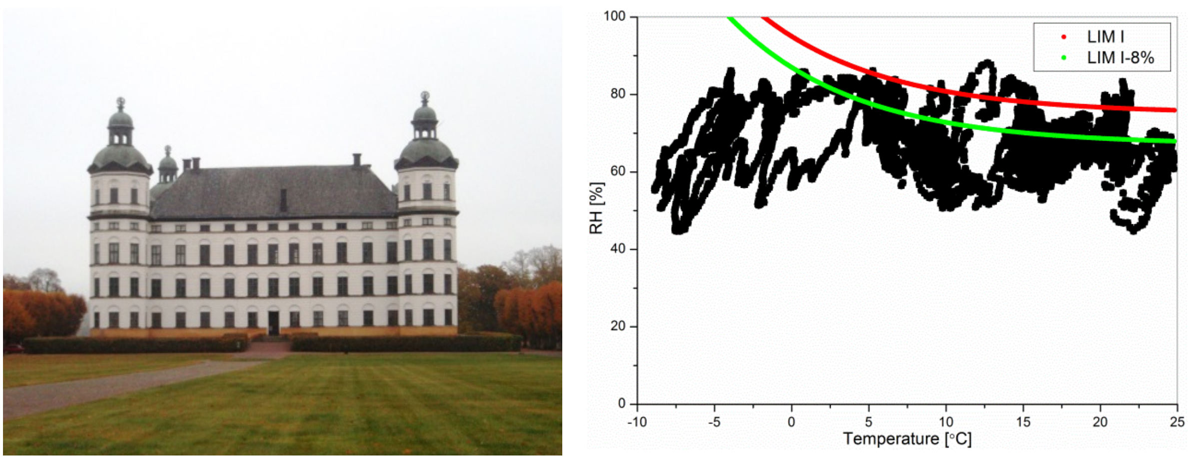

Figure 6.7. Left, Skokloster castle. Right, temperature and RH in *Grå rummet* (Grey Room) during the reference year. The red line shows the isopleth LIM I, values above which indicate a risk for mould growth. The green line shows LIM I of 8%, which gives a conservative safety margin.

In 2008-2010, an extensive measuring campaign was performed to determine the impact of the building envelope on the indoor climate and to assess indoor climate-related risks [95].

There were two main results. On an average, the indoor and outdoor absolute humidity were about the same, which implies that there were no sources of moisture except from infiltration. Considerable differences in RH stability were evident in the rooms. Therefore, draught-proofing the rooms could decrease the amplitude of RH fluctuations without increasing the average RH level. In addition, this measure would decrease the risk for mechanical damage to the objects without increasing the risk for bio-deterioration. It was also suggested that relying only on passive climate control would not be sufficient to eliminate the risk for future mould growth (Figure 6.7).

6.3.1 Methods

Three rooms known to have problems with bio-deterioration due to the indoor climate were chosen as case study rooms. The active measures were rotated annually (Table 6.1). Three similar rooms with no active climate control were used for reference. Case study rooms CS1 CS2 and reference rooms RF1 and RF2 are north-northeast facing, and case study room CS3 and reference room RF3 south-southwest facing (Figure 6.8). Temperature and RH were monitored in all six rooms for three years, and energy use was monitored in the case study rooms. Before the first year of the study, all rooms were draught proofed to make the active climate control more efficient: the windows were renovated, the doors were sealed, and dampers were closed and sealed.

Table 6.1. Case study and reference rooms and associated rotation of climate control measures.

Reference rooms		Case study rooms		Measure		
Number	Room	Number	Room	Year 1	Year 2	Year 3
RF1	Blå rummet	CS1	Grå rummet	DH	AV	CH
RF2	Bryssel	CS2	Florens	AV	CH	DH
RF3	Gröna sängkammaren	CS3	London	CH	DH	AV

Installations in a building that have remained untouched for hundreds of years required great caution. All measures must be resettable and be characterized by the precautionary principle. To minimize the risk for overheating and fire, conservation heating was installed with four low-temperature fire classified direct electric heaters with a total power of 800 W. A sorption dehumidifier was used as the sorption dehumidifier can run in low temperatures, even below zero, and as the dehumidified water is transported with the moist regeneration air to the outside via an air duct. This dehumidifier does not require no manual service to empty water containers, which can be impractical and even risky. The selected dehumidifier, *Fuktkontroll DA-250*, had a maximum power of 1400 W and dehumidifying capacity of 1,1 kg/h (@ 20 °C, 60% RH). The dry air from the dehumidifier and the adaptive ventilation system was supplied through vertically-directed nozzles, making sure that no historic objects were directly exposed to the dry airstream (Figure 6.9). The heaters and the dehumidifier were controlled with programmable hygrostats with the set points for RH approximately set according to mould growth control strategy – i.e., equation (71). A safety margin of d = 3% RH was used during the first year. In the second and third years a larger safety margin of d = 8% RH was used. The adaptive ventilation system consisted of a 110 W fan with a capacity of 300 m^3 per hour for the incoming air. The outgoing air was led through a valve mounted in the draught proofed chimney. The outdoor sensors were located next to the air intake duct and the indoor sensors were located in the middle of the room on a stand. The fan was controlled by the ratio between indoor and outdoor water vapour partial pressure as described in Chapter 5. In this setup, the fan was on when the ratio was larger than 1,1:

$$F_{p_w}\left(\frac{p_{wa}}{p_{wout}}\right) = \begin{cases} 1, \text{ for } \frac{p_{wa}}{p_{wout}} > 1{,}1 \\ 0, \text{ for } \frac{p_{wa}}{p_{wout}} < 1{,}1 \end{cases}. \tag{91}$$

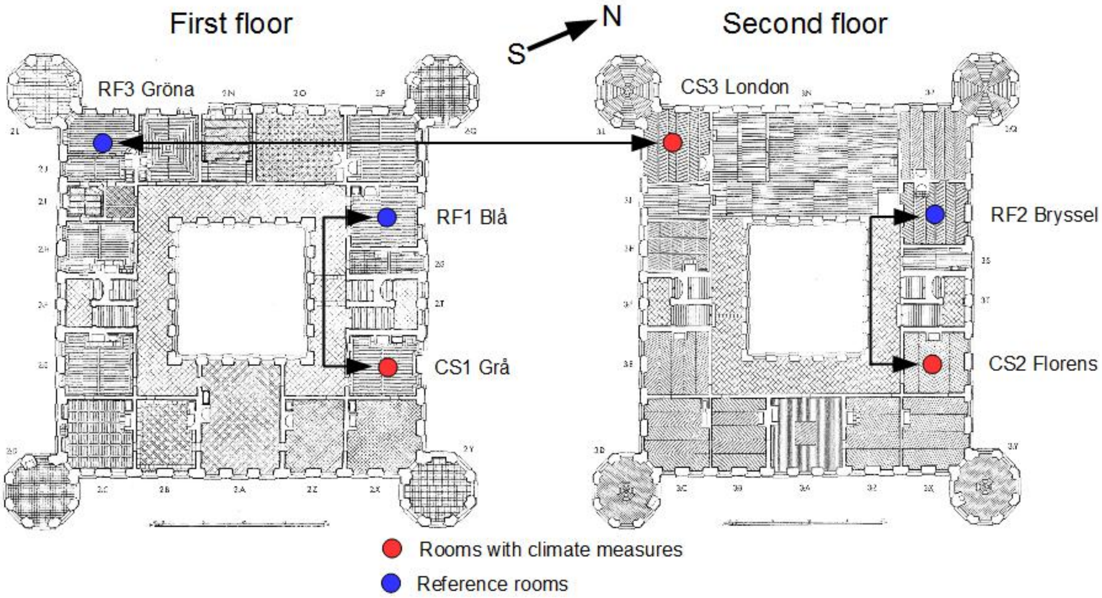

Figure 6.8. Rooms with measures and reference rooms in the study.

Figure 6.9. Left, dehumidifier in *Grå rummet* (Grey room). Middle, adaptive ventilation in the room *Blå rummet* (Blue room). Right, conservation heating in *London* room.

6.4 Results and analysis

Table 6.2 shows that the need for active control has been so low during all three years that there are only small differences between the rooms both between the case study rooms and between case study and reference rooms. The combination of a low demand for active control, existing differences in hygrothermal behaviour between the case study rooms, and variations in outdoor climate between the years makes it difficult to compare the different methods although some observations can be made.

After the first year, the indoor climate in CS1 had improved significantly even though the dehumidifier had not run for more than a few hours, most likely due to the draught proofing. It was decided to lower the control level by an additional 5% RH, which means that for year two and three a safety margin of 8% RH below LIM I was used (shown in the table in row $Mould_{LIM\ I\text{-}8}$). The draught proofing of the rooms had a positive effect on the case study rooms in terms of a more stable RH as indicated by the standard deviation calculated from the 30-day moving average of RH (SD30). For the reference rooms, the effect is less clear but these rooms were also more stable before draught proofing as can be seen in the statistics from the monitoring campaign in 2009-2010 referred to as the reference year in Table 6.2.

The energy use for all three control methods was low. Dehumidification used the lowest amount of energy – in total, 534 kWh for all three years. Conservation heating used 957 kWh and adaptive ventilation used 742 kWh. The load for adaptive ventilation has been more or less constant regardless of room and year, which is expected as the systems were controlled by the difference in indoor and outdoor climate and not risk of mould growth. The load for conservation heating and dehumidification was highest in CS3, which also was the leakiest room. Dehumidification and conservation heating successfully kept temperature and RH below the mould growth limit LIM I, except on one occasion during year one when the CH in room CS3 was unable to lower RH during a rapid weather change of warm and humid air. Adaptive ventilation has lowered the mixing ratio (MR) – i.e., mass of water vapour to mass of dry air – in comparison to the reference rooms and to the other case study rooms, but the mould risk has not been significantly lowered in comparison to the reference rooms; however, the mould risk was low in all rooms anyway. The SD30 fluctuations are significantly higher (25-30%) in the rooms where adaptive ventilation was installed.

Energy measurements showed that the conservation heating and dehumidification were active mainly during summer. This period with increased mould risk was studied more closely to assess the impact of the active control. Table 6.3 shows the data for July, August, and September for all three years. Year one had a beneficial outdoor climate during the three-month period, resulting in a low mould growth risk in all rooms and extremely low energy use in the case study rooms. There was a small mould risk in the reference rooms during year two, except in RF3, which always had a low mould risk due to heat gain either from sunlight or the heated rooms below. Dehumidification and conservation heating effectively reduce the mould risk during this period. Compared to the other methods, adaptive ventilation consistently resulted in the lowest MR but increases in RH fluctuations. The difference in MR between conservation heating and dehumidification is insignificant, which is consistent with the low energy use for dehumidification, only 116 kWh in total for the summer months. Adaptive ventilation used 182 kWh and conservation heating 342 kWh.

An important result of this case study is the effect of draught proofing. The two rooms CS1 and CS2 were well draught proofed but CS3 was adjacent to a tower room on one side and the castle's most leaky room on the other side, which was hard to draught proof. Comparing energy consumption per room for the whole three years shows that the two better draught proofed rooms CS1and CS2consumed in total 512 kWh and 585 kWh while the leakier room (CS3) consumed the double amount of energy (i.e., 1135 kWh) for the three years. This result points out importance of draught proofing when installing climate control measures in a historic building.

6.5 Discussion and Conclusions on mould growth control

This study introduces using isopleths for mould growth analysis to determine the safe set-points for microclimate control. Mould growth control was tested in Hangvar church simulations and in situ in a one-year Fide church case study. Both the simulations and in situ testing showed that using mould growth control to determine the safe set points for mould growth control of a dehumidifier is effective. In the simulated year, the energy saved compared to using fixed set point control was 57%. The in situ test showed the importance of the use of a safety margin to mitigate fast changes in indoor climate. Mould growth control was used and cross-compared in the three-year study in Skokloster Castle where conservation heating and dehumidification was controlled by the introduced set-point strategy. Comparing the three climate control measures in terms of energy efficiency and mould risk prevention, dehumidification consumed the least energy and was the most effective in reducing mould growth risk. Conservation heating is almost as good in reducing mould growth, but needed almost twice the amount of energy. Adaptive ventilation decreased mould risk and improved the climate in the rooms. However, there were occasionally some periods every second or third year where this measure was not sufficient. The energy consumption was low in-between dehumidifying and conservation heating.

Regarding stability, there is no significant difference between dehumidification and conservation heating as both showed very low fluctuations. Adaptive ventilation, however, resulted in increased short-term variations of RH, increasing the risk of mechanical damage. The data collected over the three summer months make it obvious that dehumidification effectively prevents mould growth and energy efficient during warm periods. The total amount of energy consumed during all three years is so low that the difference should not affect decision-making in the case study building. Draught proofing had a positive impact on energy efficiency and it also has had a beneficial effect on RH stability and mould risk. However, the indoor climate in Skokloster Castle is only just below the risk zone and active control is necessary to reach an acceptable risk level and to mitigate bad indoor climate during humid weather conditions.

Table 6.2. One year data from all rooms and all three years. Two thresholds are used to make a fine-grained assessment of the risk for mould growth. The reference year is from a monitoring campaign in 2009-2010.

	Case study rooms															
	Reference year				Year 1				Year 2				Year 3			
Room	CS1	CS2	CS3	Out	CS1	CS2	CS3	Out	CS1	CS2	CS3	Out	CS1	CS2	CS3	Out
Measure					DH	AV	CH		AV	CH	DH		CH	DH	AV	
Avg RH [%]	71	68	68	80	65	64	64	77	66	67	65	79	65	67	65	79,5
Avg T [°C]	8,0	8,5	8,6	6,8	10,5	10,0	11,3	8,0	10,0	10,3	11,0	8,1	10,2	9,6	10	7,2
Avg MR [g/kg]	5,4	5,2	5,2	5,5	5,6	5,3	5,6	5,4	5,4	5,6	5,7	5,6	5,4	5,5	5,3	5,3
SD	7,7	11,4	10,7	16,7	5,0	7,8	12,0	17,5	6,7	6,5	10,4	17,6	4,0	4,8	9,7	16,9
SD30	6,0	6,1	5,9	12,3	3,6	4,8	5,4	15,1	4,8	3,8	4,9	14,9	2,9	2,8	5,6	14,6
Runtime [h]					23	2264	539		2100	346	316		311	42	2382	
Energy [kWh]					32	249	431		231	277	443		249	59	262	
Mould $_{LIM\ I}$ [%]	3	3	3		0	0	1		0	0	0		0	0	1	
Mould $_{LIM\ I-8}$ [%]	32	11	14		4	2	20		9	2	1		0	0	10	
	Reference rooms															
Room	RF1	RF2	RF3		RF1	RF2	RF3		RF1	RF2	RF3		RF1	RF2	RF3	
Avg RH [%]	68	70	63		66	69	60		68	70	61		68	69	60	
Avg T [°C]	8,2	7,8	9,7		10,2	9,8	12,1		10,1	9,7	12,0		9,4	9,0	11,4	
Avg MR [g/kg]	5,3	5,2	5,3		5,5	5,5	5,6		5,6	5,7	5,7		5,4	5,4	5,4	
SD	5,5	8,8	7,0		5,3	10,0	9,3		5,3	9,7	8,9		3,8	8,0	7,3	
SD30	4,2	5,2	5,2		3,5	4,2	5,2		3,4	4,6	5,3		2,7	4,0	5,2	
Mould$_{LIM\ I}$ [%]	0	0	0		0	0	0		0	1	0		0	0	0	
Mould$_{LIM\ I-8}$ [%]	11	13	5		5	22	3		6	18	4		13	12	2	

Table 6.3. Data from July, August, and September for all rooms all three years.

	Case study rooms															
	Reference year				Year 1				Year 2				Year 3			
	CS1	CS2	CS3	Out	CS1	CS2	CS3	Out	CS1	CS2	CS3	Out	CS1	CS2	CS3	Out
Measure					DH	AV	CH		AV	CH	DH	-	CH	DH	AV	
Avg RH [%]	68	60	61	76	61	57	53	72	65	63	57	76	65	65	59	77
Avg T [°C]	18,6	20,1	20,0	15,5	18,9	19,1	20,7	15,7	18,5	19,8	21,0	16,7	18,7	18,8	19,6	15,6
Avg MR [g/kg]	9,2	8,8	8,9	8,2	8,4	7,9	8,1	7,8	8,8	9,2	9,1	8,9	8,8	8,8	8,4	8,4
SD30	4,5	4,0	4,7	16,8	3,7	4,2	4,4	18,2	3,7	2,0	3,5	16,9	2,1	2,1	4,2	15,9
Runtime [h]					2,2	636	3,8		454	140	51		283	30	563	
Energy [kWh]					3	70	3		50	112	71		227	42	62	
$Mould_{LIM\ I}$ [%]	1	0	0		0	0	0		0	0	0		0	0	0	
$Mould_{LIM\ I\text{-}8}$ [%]	51	2	5		1	0	0		18	0	0		0	0	6	
	Reference rooms															
	RF1	RF2	RF3		RF1	RF2	RF3		RF1	RF2	RF3		RF1	RF2	RF3	
Avg RH [%]	66	63	61		61	57	52		66	62	56		69	64	57	
Avg T [°C]	18,9	19,4	20,2		18,8	19,6	21,1		18,8	19,9	21,4		17,7	18,8	20,4	
Avg MR [g/kg]	9,1	8,9	9,1		8,4	8,2	8,2		9,1	9,2	9,0		8,7	8,7	8,9	
SD30	3,4	3,6	4,4		3,4	3,8	4,1		2,3	3,0	3,6		2,5	3,2	3,9	
$Mould_{LIM\ I}$ [%]	0	0	0		0	0	0		0	0	0		0	0	0	
$Mould_{LIM\ I\text{-}8}$ [%]	23	6	5		0	0	0		19	2	0		50	12	2	

7 Conclusions

This thesis addresses questions connected to climate control in massive historic buildings with the focus on how to control temperature and humidity. The research is motivated by the fact that many European cultural heritage objects – e.g., paintings, frescoes, sculptures, altars and organs – remain in historic buildings with no or limited indoor climate control. These massive historic buildings include castles, museums, monasteries and also churches, which form a major case study class considered for this thesis. In part, this thesis' motivation to develop non-invasive, low-cost, and energy efficient solutions for climate control in historic buildings is due to the lack of funding for the cultural heritage sector, or cleric institutions in case of the churches, together with heritage protection rules that often limit the possibility to accomplish installations of regular HVAC systems used in modern buildings. In particular, three methods were targeted: intermittent heating, adaptive ventilation, and humidity control to prevent mould growth.

Intermittent heating, a widely used climate control method in churches, is analysed in Chapter 4 by applying model-based techniques. From the system theory perspective, this analysis presents the major contribution of the thesis. Interestingly, this relatively simple structure model of the indoor climate that was proposed almost perfectly fits the measurements at three churches in Gotland, Sweden. This model was then utilized for synthesis of shaping the starting stage of the heating event to limit the change rate of relative humidity (RH). This was done to minimise the risk of mechanical damage to hygroscopic cultural heritage objects that were (e.g., wood, paper, and canvas) due to associated climate-induced moisture content gradient. At this stage, the control design method was validated by simulations. The experimental validation is then naturally a further step, which is left to the near-future research.

The subsequent part of the thesis presents results in rather applied directions. Existing indoor climate control methods – adaptive ventilation and humidity control – were analysed for the case study buildings with the objective to fill in the gaps in the state-of-the-art methods of climate control by applying extensive analysis on the gathered data. The aim was also to propose adjustments for the methods for indoor climate safety and energy efficiency. A significant contribution is also made for the implementation side, as it was necessary to design, install, and programme all the instrumentation, measurement, and control systems for the first case study tests.

Based on the measured data and gained experience, the adaptive ventilation, analysed mainly in Chapter 5 and partly in Chapter 6, was confirmed as a proper mitigation measure for buildings with internal sources of moisture. In particular, its applicability is mainly in the direction of mould growth reduction. On the other hand, this mitigation measure can increase the risk of mechanical damage due to enhanced fluctuations brought by the method. Elimination of these fluctuations is the main proposed adjustment of the method, discussed in more detail in the conclusion section of Chapter 5. The comparison of the three methods performed in Skokloster Castle (Chapter 6) revealed that when the historic building did not have considerable internal sources of moisture, the adaptive ventilation method has little effect on RH.

The last major field studied in Chapter 6 is an analysis of mould growth in interiors of historic buildings. The first contribution of this chapter, confirmed by both simulations and experiments, is that if the mould growth dependence on a combination of RH and temperature is taken into account when determining the RH set-point, considerable energy savings can be achieved, compared to the common RH control using a fixed set-point value. The second contribution of the chapter is case-study based cross-comparison of three control strategies in Skokloster Castle: adaptive ventilation, conservation heating, and direct dehumidification by sorption dehumidifier. Under the given conditions, drought-proofed interiors and no substantial internal source of moisture, the dehumidification by sorption dehumidifiers is the most effective method.

In summary, this thesis studied various methods and approaches to further develop indoor climate control by applying approaches of a model-based control, design, and implementation of novel control systems, including both instrumentation and software implementation aspects and analysis of the methods by applying recently proposed criteria and damage functions. The specific contributions to both fundamental and applied research are outlined in more detail below, separately for each of the objective stated in Chapter 3.

Objective 1: Propose a methodology for non-invasive temperature and humidity control of intermittent heating of massive construction historic buildings

This first objective is analysed and solved in Chapter 4 of the thesis. The main contribution is in performing the conceptual design of shaping the heating power at the beginning of the intermittent heating event in a massive historic building with heavy masonry walls. The motivation for this research is to avoid the indoor climate risk for cultural heritage objects of hygroscopic nature induced by fast RH change rate at the beginning of the heat-up event, if the full heating power was set at the beginning of the heat-up event. Following the emerging direction of applying model-based methods in the given cultural heritage field, simplified thermal and hygric analytical models of massive buildings were proposed. When forming the model structure, the linearity of the temperature responses with respect to square-root of time, caused by heat transfer within thick walls and associated with solution of the heat equation, had to be respected. In addition, the model needed to consider the accumulation nature of the interior air volume. First, balancing these phenomena (neglecting minor factors) required using a first-order nonlinear model to simulate air temperature response to the heating power step. The consequently proposed hygric model for simulating the air mixing ratio (MR) is of the same structure, due to a direct dependence of moisture evaporation from the walls is influenced by the temperature assuming the walls are saturated with moisture. For both the models, a two-step parameter identification procedure was proposed. First, the static (sensitivity) parameters are obtained directly from the linear parts of the responses, when visualised with square-root scaling of the time. The accumulation time constants are then obtained via signal integration. The proposed models and identification procedures were successfully validated on measured data at three churches in Gotland, Sweden (Fide, Hangvar, and Tingstäde churches). The models effectively approximated the initial response determined predominantly by indoor air accumulation, as well as subsequent square-root of time dependence governed by the heat transfer to the massive wall. Note that the limitation of these models is in that they can be applied to simulate step responses only.

The main contribution of Chapter 4 is then in proposing an algorithm for stepped shaping of the heating power at the starting stage of the heating event so that the RH hourly (or any other interval) change rate due to the heating is kept within a predefined range. This is done by applying the Magnus law to determine the RH from the temperature and MR of the air. Based on sensitivity analysis and simplified assumptions on temperature homogeneity in the wall during the starting stage of the heating event, the magnitudes of maximal heating power steps at hourly (or other) intervals are determined to respect the constraint on the RH change rate. In addition, a procedure to determine the overall heating time is proposed. The designed control procedure is then applied and validated on the models of all the three case study churches. For validation of the method, higher order dynamical models were proposed and parametrized from the available data, involving discretized heat equation. An almost ideal match with the results by the simplified models used to derive the control strategy shows that the stated simplifying assumptions were meaningful. Finally, implementation aspects of the proposed method were discussed. Note that preliminary results presented in Chapter 4 have been published in [1], and the final results are presented in [2], published in a top journal of the field. In both papers the doctoral candidate is the main author. In summary, objective 1 of the thesis was fulfilled.

Objective 2: Perform validation and analysis of adaptive ventilation method for relative humidity control in historic buildings

Objective 2, which focuses on analysis and design adjustments of adaptive ventilation, was met as described in Chapter 5 and Chapter 6. The motivation for the given research lies in the fact that even though the adaptive ventilation has been implemented as a mitigation measure in a number of test historic buildings, it has not been investigated sufficiently from the mould growth prevention, RH variability, algorithm, and technical implementation perspectives. These perspectives were analysed and solved in the thesis. The main contribution is an analysis and validation of the measure regarding humidity control, energy performance, and stability of the indoor climate. However, the study contributes via enhancing the know-how in the implementation aspects gained during a number of case study tests. In particular, a case study with adaptive ventilation as the only climate control measure was carried out in a historic farm building and the data collected were analysed to study the reduction of RH, mould risk, indoor climate fluctuations, and energy performance.

After the first study, it was apparent that when the outdoor air is drier than the indoor air, it is very likely that it is also colder. Hence, ventilating the interior with cold air is counterproductive as this would likely increase RH even though moisture is simultaneously removed from the building. A new solar energy augmented system that slightly heats the inlet air was developed and tested in a subsequent case study – a medieval church building. The sustainable strategy is to heat the inlet air only when there is accumulated solar energy available. The solution in this study was to export electricity to the grid during daytime and to import electricity from the grid when fan was running. If the system ran out of produced energy, the heaters were turned off. There is no doubt that adaptive ventilation lowers the humidity level. In the two case studies, the ventilation system transported out some 1600 kg and 1100 kg of water, respectively, during one year. The climate-induced risk for mould growth was acceptable except for some periods. Energy performance was also very good. An important aspect that will need to be addressed in the subsequent analysis is the increased variability of RH after application of adaptive ventilation. This can increase the risk of mechanical damage of cultural heritage objects of hygroscopic nature via transferring the RH variations to variation of moisture content and the associated gradients of stress within the material layers. The performed research shows that adaptive ventilation essentially lowers the number of hours of risk for mould growth on a yearly basis, but there is still an increased risk at some short periods when adaptive ventilation is not a sufficient measure. For these times, a backup strategy is to be applied such as using portable dehumidifiers.

In summary, the performed case study analysis confirmed that adaptive ventilation is a viable method, especially if the proposed adjustments are taken into account. Hence Objective 2 has been fulfilled. The results of performed research are presented in [3], [4], [5], and [6], where the doctoral candidate is either the main author or a key co-author.

Objective 3: Propose and validate adjustments of indoor climate control methods in historic interiors with the focus on the mould growth prevention

Although the mould growth analysis of adaptive ventilation method was performed previously in Chapter 5, its analysis forms the major scope of Chapter 6. The analysis of mould growth in interiors of historic buildings takes into account recently quantified mould growth intensity as a function of temperature, RH, and other factors. The quantified mould growth characteristic is then used to generate the RH set-point based on measured temperature. By applying this approach, significant energy savings can be achieved compared to RH to a constant set-point, which is often used in the cultural heritage sector as the primary indoor climate mitigation measure. This conclusion has been made based on both simulation and case study experiments. The simulation based validation was performed on a model of Hangvar Church (Gotland, Sweden), which was implemented in HAMbase tool in MATLAB and parametrized based on the measured data. Even when fixing the RH set-point to the rather high value of 75% of RH, the overall runtime of the dehumidifier was 72% higher compared to dehumidification with following RH set-point with respect to the mould growth characteristics. Applicability and benefits dehumidification with respect to mould growth were then confirmed via yearly experiment in Fide church (Gotland, Sweden).

As a final contribution, a wide case analysis in Skokloster Castle is presented. Of the three methods of mould growth targeting humidity control (adaptive ventilation, conservation heating, and direct dehumidification by sorption dehumidifier), direct dehumidification by sorption dehumidifier was best concerning the indoor climate quality and energy consumption. Note that this case study had no internal source of moisture as the test rooms were located on the first and second floor of the building. However, rather than a method, the drought tightness of the rooms performed before the first year of the study was a decisive factor in lowering the mould growth risk. However, the supportive use by an active measure proved crucial in eliminating the residual risks in the tested rooms. The results in this part of the thesis was published in [7, 8] and in the deliverable report of the 7FP EU project Climate for Culture [11]. Based on the results of the thorough data analysis, Objective 3 can be considered fulfilled.

8 Appendix

8.1 Psychrometrics

The relative humidity (RH), φ, is specified as the ratio between the actual water vapour pressure and the saturated vapour pressure at the given temperature:

$$\varphi = \frac{p_w}{p_{ws}} \cdot 100 \text{ (\%)}, \tag{92}$$

where $p_w$is the water vapour pressure and p_{ws} is the saturated water vapour pressure at the given temperature [96].

The saturated water vapour partial pressure is a function of temperature and can be calculated with the Magnus and Tetens empirical formula [83]:

$$p_{ws}(\vartheta) = p_{ws}(0) \cdot 10^{\frac{a\vartheta}{b+\vartheta}} \text{ (hPa)}, \tag{93}$$

where ϑ is temperature (°C), $p_{ws}(0) = 6{,}112$ (hPa) is the water vapour partial pressure at zero degrees centigrade, and $a = 7{,}65$ and $b = 243{,}12$ are empirically derived constants [83].

When calculating air humidity in HVAC systems, mixing ratio (MR) is useful and is specified as the mass of water vapour to the mass of dry air

$$X_a = \frac{m_w}{m_{da}} \text{ (kg/kg)}. \tag{94}$$

The SI-unit is kg per kg but often the more practical unit grams of water vapour per kg dry air is used. MR is the vertical axis in a psychrometric chart and can be calculated from relative humidity and temperature either from a psychrometric chart or according to equation (95) combined with equation (96) [97]:

$$X_a = 0.622 \frac{p_w}{p - p_w} \text{ (kg/kg)}. \tag{95}$$

The constant 0.622 is the ratio between the molar mass of water vapour and dry air, p is the atmospheric pressure which often is approximated with 1013 hPa, and $p_w$is the water vapor partial pressure, which can be calculated by re-formulating equation (92):

$$p_w = p_{ws} \cdot \frac{\varphi}{100} \text{ (hPa)} \tag{96}$$

As the difference between the atmospheric pressure and water vapour partial pressure, $p - p_w$, is approximately 1000 hPa, and equation (95) is often approximated with

$$X_a = 0{,}622 \frac{p_w}{1000}. \tag{97}$$

If equation (97) is combined with equation (96) and equation (93), the result is

$$X_a = 3{,}802 \cdot 10^{-5} \cdot \varphi \cdot 10^{\frac{a\vartheta}{b+\vartheta}} \text{ (kg/kg).} \tag{98}$$

Absolute humidity (AH) is the mass of water vapour in a certain volume of moist air V, i.e., the density of the water vapour (kg/m^3):

$$AH_a = \frac{m_w}{V} \quad \text{(kg/m}^3\text{),} \tag{99}$$

and can according to [18] be calculated using the following equation:

$$AH_a = \frac{1{,}344 \cdot 10^{-2}}{273{,}3+\vartheta} \cdot \varphi \cdot 10^{\frac{a\vartheta}{b+\vartheta}} \quad \text{(kg/m}^3\text{).} \tag{100}$$

8.2 Simulation model of Hangvar church

For comparative studies of mould growth control, a model of Hangvar church (Figure 4.2) has been developed and parametrised. The model was implemented in the MATLAB-Simulink based software HAMbase [93] developed by TUE (Figure 8.1).

The model consists of six zones with the following volumes:

Nave and chancel = 1000 m^3
Sacristy = 33 m^3
Attic above the nave = 376 m^3
Attic in tower the part = 353 m^3
Crawl space below the Nave = 35 m^3
Crawl space below the Sacristy = 2,5 m^3

A floor plan over Hangvar church can be seen in Figure 5.12.

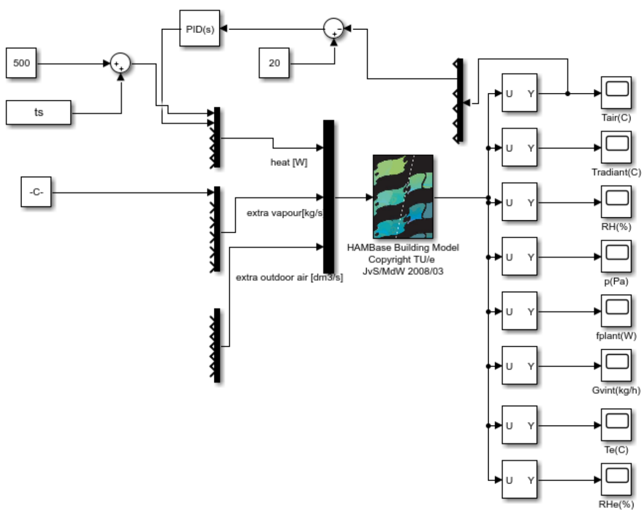

Figure 8.1. The HAMbase model in Simulink

In the model, properties of the construction components such as walls, windows, and doors are defined in an input file. The temperature in the sacristy was held constant at 20°C, as it is in the church. For simulation purpose, hourly energy data from the energy company were imported to the model to include the electrical heating and lighting at heat-up events at service. Meteorological data measured at a weather station managed by the Swedish Meteorological and Hydrological institute (SMHI) located about 18 kilometres from the church were used as outdoor data. The irradiation data were measured at Visby Airport, 29 km from the church.

During the test year, there are some differences between the simulations and measured data that most likely are caused by the distance between the church and the location of the weather stations (Figure 8.2 and 8.3). However, the dynamics and the averaged levels are captured in the model.

The HAMBase building model has a feature for adding extra water vapour into the modelled building, which can be used for simulations of dehumidification by adding negative vapour into the model. However, the capacity of a dehumidifier is strongly temperature dependent and has to be modelled for that. In the simulations for mould growth control, the capacity of a Munters ML 270 sorption dehumidifier was approximated by the model:

$$C(\vartheta) = -(0{,}9 + 0{,}06\,\vartheta)/3600 \ \ (\mathrm{kg\ s^{-1}})\,, \qquad (101)$$

based on the product sheet from the supplier.

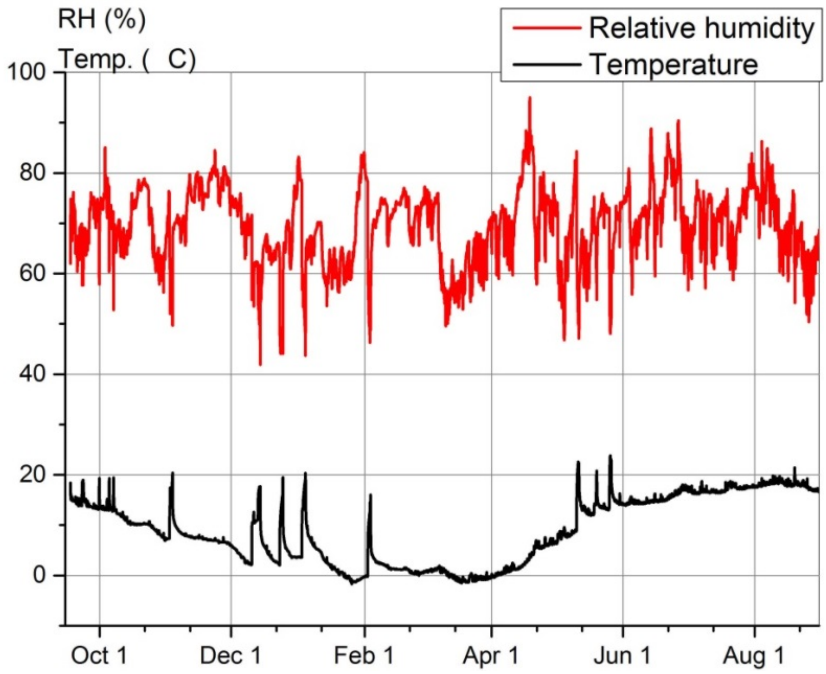

Figure 8.2. Measured temperature and relative humidity in Hangvar church.

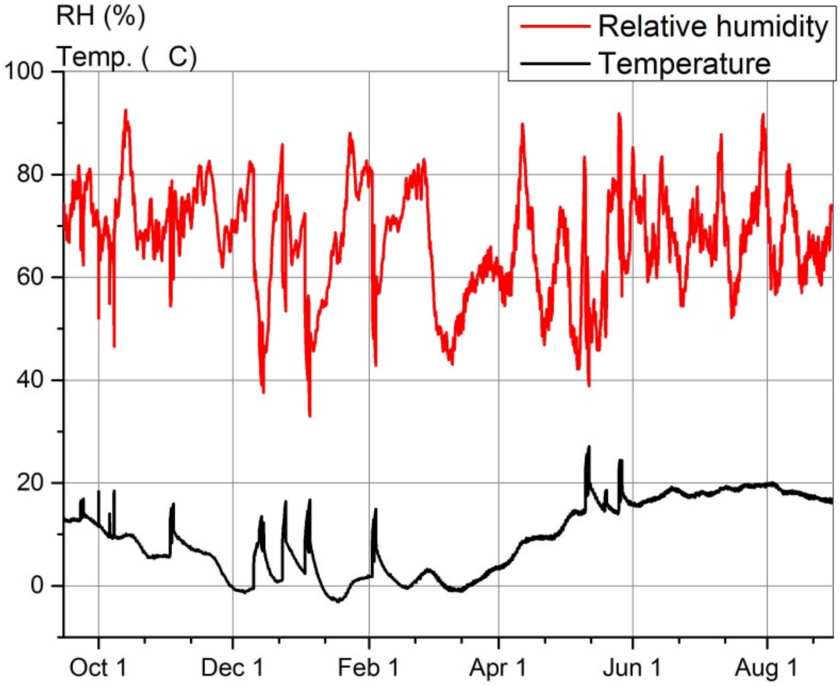

Figure 8.3. Simulated temperature and relative humidity in Hangvar church.

9 Bibliography

9.1 References with author contribution

[1] Wessberg M, Broström T, Vyhlidal T. A method to determine heating power and heat up time for intermittent heating of churches. Energy Procedia, vol. 132, Elsevier B.V.; 2017, p. 915–920. doi:10.1016/J.EGYPRO.2017.09.720.

[2] M. Wessberg, T. Vyhlídal, T. Broström, A model-based method to control temperature and humidity in intermittently heated massive historic buildings, Build. Environ. 2019,. doi:10.1016/J.BUILDENV.2019.03.024.

[3] Broström T, Hagentoft C-E, Wessberg M. Humidity Control in Historic Buildings through Adaptive Ventilation : a Case Study. NSB 2011 9th Nord. Symp. Build. Phys., 2011, p. 1–8.

[4] Larsen Klenz P, Wessberg M, Brostrom T. Adaptive ventilation for occasionally used churches. 3th Eur. Work. Cult. Herit. Preserv. EWCHP 2013, 2013, p. 55–62.

[5] Wessberg M, Larsen PK, Broström T. Solar energy augmented adaptive ventilation in historic buildings. NSB Nord. Symp. Build. Physic 2014, 2014, p. 648–655.

[6] Napp M, Wessberg M, Kalamees T, Broström T. Adaptive ventilation for climate control in a medieval church in cold climate. Int J Vent 2016;15:1–14. doi:10.1080/14733315.2016.1173289.

[7] Wessberg M, Leijonhufvud G, Broström T. An evaluation of three different methods for energy efficient indoor climate control in Skokloster Castle. In: de Bouw M, Dubois S, Dekeyser L, Vanhellemont Y, editors. Second Int. Conf. Energy Effic. Comf. Hist. Build., Flanders Heritage Agency; 2016, p. 144–150.

[8] Broström T, van Schijndel J, Wessberg M, Klenz Larsen P, et al. Energy efficient climate control in historic buildings. In: Leissner J, Kilian R, editors. Clim. Cult. Built Cult. Herit. times Clim. Chang. Cult. Final Rep., 2014, p. 29–32.

[9] Vyhlidal T, Zítek P, Camuffo D, Simeunovic G, Sladek O, Wessberg M. Relative humidity control in historical buildings Allowing the safe natural indoor climate fluctuations. 3rd Eur. Work. Cult. Herit. Preserv. EWCHP 2013, 2013, p. 77–84.

[10] Luciani A, Wessberg M, Broström T. The influence of air exchange on the stability of the indoor climate in Skokloster castle. E-Preservation Sci 2013;10:77–82.

[11] Brostrom T, Wessberg M, Vyhlidal T. Inverse damage function based RH and T set-point assessment. Clim Cult Deliv Rep D7.1.2, New Algorithms Optim Control Relat Humidity 2012:67–71.

9.2 Other References

[12] Zitek P, Vyhlidal T, Fiser J, Tornari V, Bernikola E, Tsigarida N. Diffusion-model-based risk assessment of moisture originated wood deterioration in historic buildings. Build Environ 2015;94:218–230. doi:10.1016/j.buildenv.2015.08.004.

[13] David Erhardt and Marion Mecklenburg, "Relative Humidity Reconsidered", *Preventive Conservation: Practice, Theory and Research*, Preprints of the Contributions to the Ottawa Congress, 12-16 September 1994, The International Institute for Conservation of Historic and Artistic Works, p. 32–38

[14] Jakieła S, Bratasz Ł, Kozłowski R. Numerical modelling of moisture movement and related stress field in lime wood subjected to changing climate conditions. Wood Sci Technol 2007;42:21–37. doi:10.1007/s00226-007-0138-5.

[15] Burström P, Nilvér K. Byggnadsmaterial: tillverkning, egenskaper och användning (3: e uppl.) Studentlitteratur 2018, p169–174.

[16] Mecklenburg Marion F, Tumosa CS, Erhardt D. Structural response of painted wood surfaces to changes in ambient relative humidity. In: Valérie Dorge FCH, editor. Paint. wood Hist. Conserv., Los Angeles, CA: The Getty Conservation Institute; 1998, p. 464–483.

[17] Mecklenburg Marion F. Determining the acceptable ranges of relative humidity and temperature in museums and galleries: Part 1, Structural Response to Relative Humidity. Smithsonian Museum Conservation Institute; 2007, p. 1–57.

[18] Camuffo D. Microclimate for Cultural Heritage : Conservation, Restoration, and Maintenance of Indoor and Outdoor Monuments. Vol. 2nd ed. Burlington: Elsevier Science 2014, p. 81–89.

[19] Łukomski M. Painted wood. What makes the paint crack? J Cult Herit 2012;13:S90–93. doi:10.1016/j.culher.2012.01.007.

[20] Erhardt D, Mecklenburg M F, Tumosa C S, McCormick-Goodhart M. Determination of allowable RH fluctuations. Newsl (Western Assoc Art Conserv) 1995;17:19–23

[21] Nordstrand Hanner C, Berggrén G, Hansson J, Stenback F. Kyrkans föremål: beskrivande lexikon. Göteborg: Göteborgs universitet; 2015, p 247.

[22] Bratasz Ł, Kozłowski R, Camuffo D, Pagan E. Impact of indoor heating on painted wood: Monitoring the altarpiece in the church of Santa Maria Maddalena in Rocca Pietore, Italy. Stud Conserv 2007;52:199–210.

[23] EN 15757. EN 15757, Conservation of Cultural Property – Specifications for temperature and relative humidity to limit climate-induced mechanical damage in organic hygroscopic materials. vol. 15757. European Committee for Standardization, Brussels; 2010.

[24] Wängdahl T. Inomhusklimat i ett statligt byggnadsminne. Linköpings Universitet, 2013, p 56.

[25] Adan OCG. On the fungal defacement of interior finishes. Eindhoven University of Technology, 1994, p. 27-40

[26] Mattsson J. Mögelsvamp i byggnader: förekomst, bedömning och åtgärder. Oslo: Mycoteam förlag; 2004, p. 13-34.

[27] Moon HJ, Augenbroe G. Assessing mold risks in buildings under uncertainty. Georgia Institute of Technology, 2005, p. 16-23.

[28] Sedlbauer K. Prediction of Mould Growth by Hygrothermal Calculation. J Build Phys 2002;25:321–336. doi:10.1177/0075424202025004093.

[29] Berk Z, Berk Z. Physical Properties of Food Materials. Food Process Eng. Technol., Elsevier; 2013, p. 1–27. doi:10.1016/B978-0-12-415923-5.00001-0.

[30] Hukka A. A mathematical model of mould growth on wooden material. Wood Sci Technol 2000;33:475–485.

[31] Johansson S, Wadsö L, Sandin K. Estimation of mould growth levels on rendered façades based on surface relative humidity and surface temperature measurements. Build Environ 2010;45:1153–1160. doi:10.1016/j.buildenv.2009.10.022.

[32] Ayerst G. The Effects of Moisture and Temperature on Growth and Spore Germination in some Fungi. J Stored Prod Res 1969;5:127–141. doi:10.1016/0022-474X(69)90055-1.

[33] Smith SL, Hill ST. Influence of temperature and water activity on germination and growth of Aspergillus restrictus and A. versicolor. Trans Br Mycol Soc 1982;79:558–560. doi:10.1016/S0007-1536(82)80058-2.

[34] Sedlbauer K. Prediction of mould fungus formation on the surface of and inside building components. Fraunhofer Institute for Building Physics 2001, p.75-141.

[35] Fanger P. Thermal comfort: Analysis and applications in environmental engineering. Danish Technical Press, Copenhagen, Denmark, 1970, p. 244.

[36] Legnér M. Kyrkan – ” en maskin att sitta i ”: Införandet av komfortteknik i medeltida kyrkor under 1900-talets första hälft. Bebyggelsehistorisk Tidskr 2012;63:1–17. In Swedish.

[37] Broström, Tor and Klenz Larsen, Poul Climate Control in Historic Buildings. Uppsala university, National Museum of Denmark 2015, p.51-52.

[38] Broström T. Uppvärmning i kyrkor Fukt och värmetekniska beräkningar för dimensionering och klimatstyrning. Kungliga Tekniska Högskolan, 1996, p.14-55, 92-116.

[39] Jacobsson F. Effektbehovet vid elektrisk uppvärmning av kyrkor samt uppvärmningsförsök i Gripsholms slott. Fritzes bokh.; 1926, p. 8-27.

[40] Henning T. Om intermittent uppvärmning av byggnader. Tek Tidskr Häfte 1936;9:146-154.

[41] Krischer O, Kast W. Zur Frage des Wärmebedarfs beim Anheizen selten beheizter Gebäude. Gesundheits-Ingenieur H., 1957, p. 321–52.

[42] Pfeil A. Kirchenheizung und Denkmalschutz: Wärmebedarf, Feuchtehaushalt, Heizungssysteme. Bauverlag; 1975.

[43] EN 15759-1:2011 Conservation of cultural property – Indoor climate – Part 1: Guidelines for heating churches, chapels and other places of worship 2011.

[44] Larsen Klenz P, Broström T, Vyhlídal T. Evaluation of different approaches of microlimate control. Clim Cult Deliv D7.1.1 2012,p. 6–51.

[45] Camuffo D, Pagan E, Rissanen S, Bratasz Ł, Kozłowski R, Camuffo M, et al. An advanced church heating system favourable to artworks: A contribution to European standardisation. J Cult Herit 2010;11:205–219. doi:10.1016/j.culher.2009.02.008.

[46] Nilsson H O, Broström T. Climate comfort measurements in Swedish churches equipped with new heating systems. 7th International Thermal Manikin and Modelling Meeting – University of Coimbra, 2008; p. 3–5.

[47] Brostrom T, Vyhlidal T, Simeunovic G, Klenz P, Zitek P. Evaluation of different approaches of microclimte control in cultural heritage buildings. In: Ashley-Smith J, Burmester A, Eibl M, editors. Clim. Collect. Stand. uncertainTies, Munich, 2013, p. 105–115.

[48] Bullock L. Environmental Control in National Trust Properties. J Archit Conserv 2009;15:83–98. doi:10.1080/13556207.2009.10785041.

[49] Larsen PK, Broström T. Climate control in historic buildings in Denmark. World Renewable. Energy Congr. 8-13 May, 2011, p. 2026–2033.

[50] Klenz Larsen P, Broström T. Climate Control in Historic Buildings. In: Kilian R, Vyhlidal T, Broström T, editors. World Renewable. Energy Congr. 8–13 May, Fraunhofer IRB Verlag; 2015, p. 77.

[51] Napp M, Kalamees T. Energy use and indoor climate of conservation heating, dehumidification and adaptive ventilation for the climate control of a mediaeval church in a cold climate. Energy Build 2015;108:61–71. doi:10.1016/j.enbuild.2015.08.013.

[52] Leijonhufvud G. Decision making on indoor climate control in historic buildings: knowledge, uncertainty and the science-practice gap. University of Gothenburg, 2016.

[53] Padfield T, Jensen P. Low energy climate control in museum stores. ICOM Comm. Conserv. 9th Trienn. Meet. Dresden, Ger. Democr. Republic, 26-31 August 1990 Prepr., 1990, p. 596–601.

[54] Larsen PK, Broström T. Climate control in cultural heritage buildings in Denmark. Dev. Clim. Control Hist. Build. Proc. from Int. Conf. "Climatization Hist. Build. state art", Linderhof Palace, December 2nd, 2010, 2011, p. 39–44.

[55] Zítek P, Vyhlídal T. Model-based moisture sorption stabilization in historical buildings. Build Environ 2009;44:1181–7. doi:10.1016/j.buildenv.2008.08.014.

[56] Henderson S. A basic concept of equilibrium moisture content. Agric Eng 1952;33:29–32.

[57] Zítek P, Vyhlídal T, Chyský J. Experience of Implementing Moisture Sorption Control in Historical Archives. Acta Polytech 2006;46:55–61.

[58] Vyhlídal T, Zítek P. Quasi-equal sorption humidity control. Clim Cult Deliv Rep D712, New Algorithms Optim Control Relat Humidity 2012:56–65.

[59] Böhm CB, Zehnder K, Bläuer-Böhm C, Zehnder K, Domeisen H, Arnold A. Climate control for the passive conservation of the Romanesque painted wooden ceiling in the church of Zillis (Switzerland). Stud Conserv 2001;46:251–268.

[60] Brockmann T. Langzeiterfahrungen mit dezentralen Kleinanlagen zur Feuchtegesteuerten Zwangslüftung. Klima und Klimastabilität Hist. Bauwerken, Wissenschaftlich-Techniche Arbeitsgemeinschaft für Bauwerkserhaltung e.V. Arbeitsgr. 6.11, 2010, p. 59–76.

[61] Reiss J, Kiessl K. Feuchtetechnicshe Untersuchung an Aussenwände der Torhalle Lorsch. Kunst Hessen Und Am Mittelrhein 1993;Heft 32133:91–98.

[62] Antretter F, Kosmann S, Kilian R, Holm A. Controlled Ventilation of Historic Buildings: Assessment of Impact on the Indoor Environment via Hygrothermal Building Simulation. In: de Freitas V, Delgado J, editors. Hygrothermal Behav. Build. Pathol. Durab., vol. 1: Springer Berlin Heidelberg; 2013, p. 93–111. doi:10.1007/978-3-642-31158-1.

[63] Hagentoft C-E, Kalagasidis AS. Mould growth control in cold attics through adaptive ventilation. Proc. 8th Nord. Symp. Build. Phys., 2008, p. 1237–1244.

[64] Hagentoft C, Kalagasidis A. Mold Growth Control in Cold Attics through Adaptive Ventilation. Validation by Field Measurements. 11th Int. Conf. Therm. Perform. Exter. Envel. Whole Build. Build. XI;, 2010, p. 1–8.

[65] Neuhaus E, Schellen H. Humidistat-controlled heating and ventilation systems to create preservation conditions in historic buildings in the Dutch climate. Proc. 9th Clima 2007 WellBeing Indoors, 2007, p. 2718–2728.

[66] Henze GP, Neumann C. Building simulation in building automation systems. In: Hensen JLM, Lamberts R, editors. Build. Perform. Simul. Des. Oper., Routledge; 2012, p. 402–440. doi:10.4324/9780203891612.

[67] Royer S, Thil S, Talbert T, Polit M. Black-box modeling of buildings thermal behavior using system identification. IFAC Proc. Vol., vol. 19, Elsevier; 2014, p. 10850–10855. doi:10.3182/20140824-6-ZA-1003.01519.

[68] Kramer R, van Schijndel J, Schellen H. Inverse modelling of simplified hygrothermal building models to predict and characterize indoor climates. Build Environ 2013;68:87–99. doi:10.1016/j.buildenv.2013.06.001.

[69] Kramer R, van Schijndel J, Schellen H. Simplified thermal and hygric building models: A literature review. Front Archit Res 2012;1:318–325. doi:10.1016/j.foar.2012.09.001.

[70] Wang S, Xu X. Simplified building model for transient thermal performance estimation using GA-based parameter identification. Int J Therm Sci 2006;45:419–432. doi:10.1016/j.ijthermalsci.2005.06.009.

[71] Ramallo-González AP, Eames ME, Coley DA. Lumped parameter models for building thermal modelling: An analytic approach to simplifying complex multi-layered constructions. Energy Build 2013;60:174–184. doi:10.1016/j.enbuild.2013.01.014.

[72] Bloomfield DP, Fisk DJ. The optimisation of intermittent heating. Build Environ 1977;12:43–55. doi:10.1016/0360-1323(77)90006-3.

[73] Xu B, Zhou S, Hu W. An intermittent heating strategy by predicting warm-up time for office buildings in Beijing. Energy Build 2017;155:35–42. doi:10.1016/j.enbuild.2017.08.062.

[74] Hazyuk I, Ghiaus C, Penhouet D. Optimal temperature control of intermittently heated buildings using Model Predictive Control: Part I – Building modeling. Build Environ 2012;51:379–87. doi:10.1016/j.buildenv.2011.11.009.

[75] Hazyuk I, Ghiaus C, Penhouet D. Optimal temperature control of intermittently heated buildings using Model Predictive Control: Part II – Control algorithm. Build Environ 2012;51:388–394. doi:10.1016/j.buildenv.2011.11.008.

[76] Stocker TF, Qin D, Plattner GK, Tignor MMB, Allen SK, Boschung J, et al. Climate change 2013 the physical science basis: Working Group I contribution to the fifth assessment report of the intergovernmental panel on climate change. vol. 9781107057. Cambridge: Cambridge University Press; 2013. doi:10.1017/CBO9781107415324.

[77] Kilian R, Broström T, Ashley-Smith J, Schellen HL, Martens M, Antretter F, et al. The Climate for Culture Method for Assessing Future Risks resulting from the Indoor Climate in Historic Buildings. 3rd Eur. Work. Cult. Heritaged Preserv. EWCHP 2013, 2013, p. 17–22.

[78] Smith GD. Numerical solution of partial differential equations: finite difference methods. Oxford University Press; 1985, p. 1-79.

[79] Hagentoft C-E. Introduction to Building Physics. Studentlitteratur; 2001,p. 202. doi:10.1002/bapi.200101660.

[80] Dawson HG. On the numerical value. Proc London Math Soc 1897;s1-29:519–522. doi:10.1112/plms/s1-29.1.519.

[81] Zítek P. Time delay control system design using functional state models. CTU Report vol. 2, No 1. Czech Technical University Publishing House Prague; 1998, p. 93.

[82] Schellen HL, van Schijndel AWM. Set point control for air heating in a church to minimize moisture related mechanical stress in wooden interior parts. Build Simul 2011;4:79–86. doi:10.1007/s12273-011-0026-7.

[83] Camuffo D. Thermodynamics for cultural heritage. In: Martini M, Milazzo M, Piacentini M, editors. Phys. Methods Archaeom., vol. 154, Amsterdam: IOS Press; 2004, p. 37–98.

[84] Van der Maas J, Maldonado E. A New Thermal Inertia Model Based on Effusivity. Int J Sol Energy 1997;19:131–160. doi:10.1080/01425919708914334.

[85] Polyak BT. Newton's method and its use in optimization. Eur J Oper Res 2007;181:1086–1096. doi:10.1016/J.EJOR.2005.06.076.

[86] Leissner J, Kilian R, Kotova L, Jacob D, Mikolajewicz U, Broström T, et al. Climate for Culture: assessing the impact of climate change on the future indoor climate in historic buildings using simulations. Herit Sci 2015;3:1–15. doi:10.1186/s40494-015-0067-9.

[87] Leissner J, Kilian R, editors. Climate for Culture: Built Cultural Heritage in times of Climate Change. Fraunhofer IRB Verlag; 2014. p. 97.

[88] Ashley-Smith J. Report on damage functions in relation to climate change. Clim Cult Deliv 42, Damage Risk Assessment, Econ Impact Mitig Strateg Sustain Preserv Sustain Preserv Cult Herit Times Clim Chang 2013:2–39.

[89] European Standard. EN 13829. Thermal Performance of Buildings—Determination of Air Permeability of Buildings—Fan Pressurization Method. 2001.

[90] Cooper EW, Etheridge DW, Smith SJ. Determining the adventitious leakage of buildings at low pressure. Part 2: Pulse technique. Build Serv Eng Res Technol 2007;28:81–96. doi:10.1177/0143624406072331.

[91] Martens MHJM. Climate risk assessment in museums. Eindhoven University of Technology, 2012.

[92] Schijndel AWM Van. Integrated Heat Air and Moisture Modeling and Simulation. Technische Universiteit Eindhoven, 2007, p. 220. doi:10.6100/IR622370.

[93] Zhang J, Hyunh A, Ye Q, Gong S. Culturebee – A Fully Wireless Monitoring and Control System for Protecting Cultural Heritage. 2011 IEEE 20th Int. Work. Enabling Technol. Infrastruct. Collab. Enterp., IEEE; 2011, p. 250–255. doi:10.1109/WETICE.2011.43.

[94] Avramidis S. Evaluation of “three-variable” models for the prediction of equilibrium moisture content in wood. Wood Sci Technol 1989;23:251–257.

[95] Broström T, Leijonhufvud G. The Indoor Climate in Skokloster Castle. In: Del Curto D, editor. Hist. Build. as museums Syst. Clim. Control Herit. Preserv., Nardini Editore; 2010, p. 84–93.

[96] American Society of Heating R and A-CE. 2017 ASHRAE® Handbook – Fundamentals (SI Edition). Knovel; 2017.

[97] Camuffo D, Fassina V, Havermans J (editors). Basic environmental mechanisms affecting cultural heritage: Understandingdeterioration mechanisms for conservation purposes. Cost Action D 42, Chem. Interact. between Cult. Artefacts indoor Environ., 2010, p. 176.

[98] A. Hayati, Natural Ventilation and Air Infiltration in Large Single Zone Buildings: Measurements and Modelling with Reference to Historical Churches, Gävle University Press , 2017. p. 44–46. https://www.diva-portal.org/smash/get/diva2:1117979/FULLTEXT01.pdf (accessed November 21, 2018).

[99] R.P.; Kramer, A.W.M.; Van Schijndel, H.L. Schellen, R. Kramer, H. Schellen, J. Van Schijndel, Should solar irradiance be included in inverse modelling?, n.d. p. 1–5. https://pure.tue.nl/ws/portalfiles/portal/3404415/391737108828248.pdf (accessed November 8, 2018).

[100] NT VVS 118, Nordtest method, local mean age of air - homogeneous emissions techniques. NORDTEST; 1997. p.1–7.